UBIQUITIN PROTEASOME PATHWAY, AUTOPHAGY AND A NOVEL THERAPEUTIC APPROACH TO PREVENT NEURODEGENERATION LINKED TO INFLAMMATION IN ALS

by

Natura Myeku

A dissertation submitted to the Graduate Faculty in Biology in partial fulfillment of the requirements for the degree of Doctor of Philosophy, The City University of New York

2011

This manuscript has been read and accepted by the Graduate Faculty in Biology in satisfaction of the dissertation requirement for the degree of Doctor of Philosophy

Date	Chair of Examining Committee Dr. MARIA FIGUEIREDO-PEREIRA
Date	Executive Officer Dr. LAUREL ECKHARDT
	Dr. JILL BARGONETTI, Hunter College
	Dr. LAUREL ECKHARDT, Hunter College
	Dr. GIOVANNI MANFREDI, Weill Cornell Medical College
	Dr. BOBBY THOMAS, Weill Cornell Medical College

Supervising Committee

THE CITY UNIVERSITY OF NEW YORK

Abstract

UBIQUITIN PROTEASOME PATHWAY, AUTOPHAGY AND A NOVEL THERAPEUTIC APPROACH TO PREVENT NEURODEGENERATION LINKED TO INFLAMMATION IN ALS

by

Natura Myeku

Advisor: Dr. Maria E. Figueiredo-Pereira

Neurodegenerative disorders such as Alzheimer's, Parkinson's and Huntington's diseases as well as amyotrophic lateral sclerosis (ALS), are a heterogeneous group of clinical disorders characterized by the selective loss of neurons in specific regions of the CNS. Despite their variability they have similar features including the accumulation of proteins that develop into inclusion bodies. Ubiquitinated proteins are major components of these inclusions suggesting that impaired proteasome activity and/or dysfunction of the ubiquitination pathway may be main players in this process. Emerging data reveal that autophagosomes are also components of inclusion

bodies, implicating autophagy in neurodegenerative disorders as well.

The research described in this thesis led to two discoveries:

1) The UPP, not autophagy, is the main pathway implicated in the degradation of soluble ubiquitinated proteins. Furthermore, proteasome impairment, and not autophagy dysfunction, causes the intracellular accumulation/aggregation of ubiquitinated proteins.

We demonstrate that proteasome impairment leads to accumulation of ubiquitinated proteins. Most importantly, inhibition of autophagy failed to cause ubiquitin protein accumulation. We also established that the soluble p62/sqstm1, a polyubiquitin shuttling factor, is associated with the proteasomes and not with autophagosomes. It is thought that p62/sqstm1 delivers polyubiquitinated proteins to proteasomes and/or autophagosomes for degradation. From a therapeutic point of view our data support the notion that pharmacological means to sustain or enhance proteasome activity and p62/sqstm1 levels could be an efficacious strategy to remove ubiquitinated proteins and prevent or delay the onset of neurodegeneration associated with protein aggregation.

2) The activity of the proteasome and the levels of p62/sqstm1 are significantly enhanced by dibutyryl-cAMP in spinal cord cultures.

We demonstrate that db-cAMP enhances the activity of the proteasome and p62/sqstm1 levels. Furthermore, pre-treatment of the neuronal cultures with db-cAMP mitigate cell toxicity induced by prostaglandin J2 (PGJ2). PGJ2 is an inflammatory mediator found to be elevated in post mortem slices of spinal cord motor neurons in ALS patients. Our data support the notion that enhancing of proteasome activity by the cAMP/PKA pathway provides an effective neuroprotective strategy against ALS and other neurodegenerative diseases associated with proteinaceous aggregates and signs of neuroinflammation.

In conclusion, our data support that impaired proteasome activity occupies the center stage in the development of neurodegenerative diseases. Enhancing proteasome activity can have therapeutic implications in drug development aiming at prevention and treatment of neurodegenerative disorders.

Acknowledgements

Foremost, I would like to express my sincere gratitude to my mentor, Dr. Maria Figueiredo-Pereira, for her continuous guidance, enthusiasm and motivation during the course of my PhD. Her devotion to my progress, empathy, work ethics and her vast knowledge has made my PhD work productive and stimulating. To me, Dr.P is a role model and a friend.

I would like to extend my gratitude to my thesis advisory committee, Dr. Jill Bargonetti, Dr. Laurel Eckhardt and Dr. Giovanni Manfredi for their contribution, insightful comments and hard questions.

I offer my deepest thanks and blessings to my family for their endless love and encouragement. To my parents, who have nurtured my inquisitive mind as a child and supported me in all my pursuits as an adult. To my late brother, to whom I dedicate all the work I do in life. To my sister, younger brother, niece and nephew who bring joy, laughter and happiness to me every day.

Natura Myeku

Table of Contents

List of Figures

List of Abbreviations

3MA 3-methyl adenine

Δ12-PGJ2 9-deoxy-delta 9,delta 12-13,14-prostaglandin J2

15d-PGJ2 15-deoxy-Δ12,14-prostaglandin J2

Δtau tau truncated at Asp421

AD Alzheimer's disease

ALS Amyotrophic lateral sclerosis

ALP autophagy/lysosome pathway

Atg autophagy-related

Baf bafilomycin A1

CMA chaperone-mediated autophagy

CQ chloroquine

CNS Central nervous system

COX-1 Cyclooxygenase-1

COX-2 Cyclooxygenase-2

CP Core particle

DAPI 4',6-Diamidino-2-Phenylindole

db-cAMP (Adenosine 3′, 5′-cyclic monophosphate dibutyryl sodium salt

DMEM Dulbecco's modified eagle's medium;

DMSO Dimethylsulfoxide

DTT Dithiothreitol

E1 ubiquitin activating enzyme

E2 ubiquitin conjugating enzyme

E3 ubiquitin ligase

E4 ubiquitin-chain elongating factor

ECL enhanced chemiluminescence;

Epx epoxomicin

Fk forskolin

FMK fluoromethyl ketone

HD Huntington's disease

GAPDH glyceraldehyde 3-phosphate dehydrogenase

LC3 light chain 3

LIR LC3-interacting region;

MEF mouse embryonic fibroblast;

MEM minimum essential medium;

mRNA messenger RNA

MTT 3-(4,5-dimethylthiazol-2-yl)-2,5-diphenyl tetrazolium bromide;

NF-κB nuclear factor-kappaB
PAGE polyacrylamide gel Electrophoresis

PARP poly (ADP-ribose) polymerase

PB1 phox-bem1

PBS phosphate buffer saline

PD Parkinson's disease

PE phosphatidylethanolamine

PDE4 Phosphodiesterase 4

Pen1 vector peptide Penetratin 1

PGD2 Prostaglandin D2

PGDS prostaglandin D2 synthases

PGE2 Prostaglandin E2

PGH2 Prostaglandin H2

PGJ2 Prostaglandin J2

PKA cAMP-dependent protein kinase

PLA proximity ligation assay

PPARγ Peroxisome Proliferator-activated receptor gamma

Rp Rolipram

RP Regulatory particle

Rpn regulatory particle non-ATPase subunit.

Rpt regulatory particle triple-A ATPase;

qRT-PCR quantitative reverse-transcription-polymerase chain reaction

SDS sodium dodecyl sulfate

P62/sqstm1 sequestosome1 (change order)

Suc-LLVY-AMC succinyl-Leu-Leu-Val-Tyr-7-amino-4-methylcoumarin

UBA ubiquitin-associated domain

UBL Ubiquitin-like domain

Ub-conjugate, ubiquitin conjugate

UCH Ubiquitin-carboxy terminal

UPP Ubiquitin/proteasome Pathway

CHAPTER I

INTRODUCTION

UBIQUITIN/PROTEASOME AND AUTOPHAGY/LYSOSOME PATHWAYS:

COMPARISON AND ROLE IN NEURODEGENERATION

Natura Myeku and Maria E. Figueiredo-Pereira

Department of Biological Sciences,

Hunter College of the City University of New York,

New York, New York 10065

FROM

Handbook of Neurochemistry and Molecular Neurobiology, pp. 513-528; Ed. Lajtha, Banik and Ray; Pub. Springer US, 2009

1.1. ABSTRACT

Neurodegenerative disorders, such as Alzheimer's, Parkinson's and Huntington's diseases as well as amyotrophic lateral sclerosis, are a heterogeneous group of clinical diseases that are characterized by the selective loss of neurons in specific regions of the CNS. Despite their variability, they have similar features including the accumulation of misfolded proteins that eventually develop into inclusion bodies. Whether these protein deposits are pathogenic or represent a coping mechanism to prolong survival of the affected neurons is a hotly debated issue. One important point to consider is that these protein deposits are indicative of a disease state as they are not prevalent in healthy cells. Ubiquitinated proteins are major components of these proteinaceous cytoplasmic or nuclear inclusions, suggesting that impaired proteasome activity and the ubiquitination machinery may be main players in this process. Emerging data revealed that autophagosomes are also components of inclusion bodies, implicating the autophagy/lysosome pathway in neurodegenerative disorders as well. Herein, we compare some of the most important characteristics of these two pathways for intracellular protein degradation and discuss their potential role in neurodegeneration.

When the proteasome is impaired, it is possible that autophagy may be the alternate pathway for clearing-out aggregated ubiquitinated proteins. The question emerges if this potential "survival" mechanism can be explored as a strategy to overcome the most common feature shared by various neurodegenerative disorders, i.e. protein aggregation manifested as inclusion bodies. One potential drawback is that degradation through autophagy seems to be a "bulky", non-specific process. A thorough knowledge of the mechanisms involved in the targeting of substrates to this pathway will provide clues to the putative specificity of this process so that its ectopic manipulation will target only the protein aggregates and not critical intracellular components.

1.2. UBIQUITIN PROTEASOME PATHWAY (UPP) AND AUTOPHAGY LYSOSOME PATHWAY (APL)

Many neurodegenerative disorders are associated with formation of protein aggregates, resulting ultimately in proteinaceous inclusions, such as Lewy bodies in Parkinson's disease and neurofibrillary tangles in Alzheimer's disease (118). While the composition of these abnormal inclusion bodies varies with the disorder, a general feature is that these aggregates contain

ubiquitinated proteins. Thus, although selective sets of neurons are affected in different neurodegenerative disorders, they are associated with an accumulation and aggregation of ubiquitinated proteins. In general, high levels of ubiquitinated proteins do not accumulate in healthy cells as they are rapidly degraded. The formation of these inclusion bodies is thus attributed to disturbed protein degradation (6).

Eukaryotic cells contain two major intracellular pathways for protein degradation: the ubiquitin/proteasome pathway (UPP) and the lysosome pathway. The UPP mainly degrades short-lived proteins such as cell cycle regulators and transcription factors, as well as misfolded proteins from the cytosol, nucleus and endoplasmic reticulum, while the lysosome degrades long lived proteins and cellular organelles. In mammalian cultured cells, 80-90% of protein degradation is carried-out by the UPP (109) while only 10-20% is attributable to lysosomes (53). Lysosomes are responsible for the turnover of extracellular proteins that enter cells by endocytosis and pinocytosis, as well as degradation of strictly intracellular proteins and organelles by autophagy. Three distinct types of autophagy have been described so far: microautophagy, chaperone-mediated autophagy (CMA) and macroautophagy (107).

Microautophagy is a constitutive form of autophagy better characterized in yeast (2). Its molecular details and functional importance in mammalian cells are largely unknown. CMA differs from the other two forms of autophagy because it does not require vesicular trafficking. Instead cytoplasmic proteins are delivered to the lysosome for degradation by a hsc 70-containing chaperone/co-chaperone complex. In addition, CMA is a selective form of lysosomal degradation, since it is restricted to the elimination of proteins that possess the penta peptide KFERQ in their sequence (123). Macroautophagy is inducible and is the best studied form of autophagy, so far (134). Our discussion herein will focus exclusively on this form of autophagy known as the autophagy/lysosome pathway or ALP.

The UPP and the ALP have been viewed as two distinct proteolytic pathways with no molecular links between them. However, this view was challenged by the finding of prominent ubiquitin-positive pathology evident in autophagy-deficient mice despite a functional UPP (64; 99). These studies strongly suggest that the ALP also participates in the degradation of ubiquitinated proteins. The challenge is to determine the impact of each of the two proteolytic pathways, i.e. the UPP and the ALP, in the accumulation/aggregation of ubiquitinated proteins as well

as in their removal under conditions that lead to neurodegeneration.

In this introduction we will compare some of the mechanisms involved in protein degradation by both pathways and discuss evidence supporting a cross-talk between them and their role in neurodegeneration. A better understanding of the relationship between these two major proteolytic systems may reveal new strategies to prevent or ameliorate the devastating effects of a decline in protein turnover and therefore contribute to treatment of neurodegenerative diseases associated with the accumulation and aggregation of ubiquitinated proteins.

1.3. COMPARISON BETWEEN THE UPP AND ALP

1.3.1. DEGRADATION SITES:

1.3.1.1. UPP: Through the UPP, intracellular proteins are degraded by a large multiprotein complex known as the 26S proteasome, which has a native molecular mass of ~2,000 kDa (26; 31). In eukaryotic cells, proteasomes are found in the cytoplasm both as free and ER-attached particles as well as in the nucleus (235). Translocation into the nucleus is mediated by nuclear localization signals found on proteasome subunits (α subunits) (13).

Degradation of polyubiquitinated proteins through the UPP is carried-out by the 26S proteasome, which includes the 20S core particle capped at one end or both by 19S regulatory particles or by a 19S particle at one end and an 11S particle at the other. It is well established that proteasome assembly to a functional 26S proteasome as well as the proteolytic operation of the proteasome, require substantial amounts of ATP (300-400 molecules per molecule of globular or unfolded substrate) (17), suggesting that ATP depletion in cells may affect proteasome function.

The 20S proteasome is composed of 28 subunits arranged in four heptameric-stacked rings forming a cylindrical structure with a hollow center in which proteolysis takes place (34). The barrel shaped 20S particle contains three internal chambers, but peptide hydrolysis occurs only in the middle one. The function of the two outer chambers remains to be elucidated, although they can hold one or two substrate molecules in storage, depending on substrate-size (196). It is not clear how the substrates move from the outer chambers to the middle chamber which contains the proteolytic active sites. This “enclosed” architecture, where the active sites are sheltered and face the inside of the proteolytic chamber, excludes degradation of proteins that come into contact with the outside of the 20S

proteasome. By itself, the 20S proteasome is autocatalytically inhibited, as the openings (one at each end) to the inside chambers are occluded (51). The pores open-up when the 20S proteasome associates with other particles such as the 19S and 11S regulatory particles (23). The former binds to polyubiquitinated proteins promoting their degradation, while the latter facilitates degradation of non-ubiquitinated short substrates. It has been suggested by *in vitro* studies, that unfolded hydrophobic substrates may also induce pore-opening if they come into contact with the 20S proteasome (117). Whether or not this is an *in vivo* event remains to be established.

1.3.1.2. ALP: Through the ALP, intracellular proteins are degraded by cathepsins that are proteases enclosed in the lysosome, an organelle surrounded by a phospholipid bilayer. The interior of the lysosome is maintained at an acidic pH (pH 5) by proton pumps embedded in the lysosomal membrane (127). Unlike the proteasome that lies unprotected within the cytoplasm and nucleus, cathepsins are sheltered by the lysosomal membrane and therefore there is no need for a complex architecture, such as the one exhibited by the proteasome. Accordingly, most cathepsins are monomeric (as an exception, cathepsin C is a tetramer), their

molecular weight ranges between 20 and 30 kDa, and the active sites on cathepsins reside in a cleft that is easily accessible to the substrates within the lysosome (127). Furthermore, cathepsins are optimally active at an acidic pH, a property that prevents them from degrading cytoplasmic proteins in the event that the lysosomal membrane falls apart and cathepsins are spilled into the neutral physiological pH of the cytoplasm. In addition, cathepsins are highly unstable at a neutral pH. Although peptide bond hydrolysis by cathepsins does not require ATP, their activity is indirectly dependent on ATP, because the proton pumps required to maintain an intralysosomal acidic pH are ATP-dependent.

1.3.2. DEGRADATION MECHANISMS:

1.3.2.1 UPP: The 20S proteasome hydrolyzes most peptide bonds at a neutral pH. The proteolytic activity of the 20S proteasome resides in three different beta subunits, each with distinct specificity exhibiting caspase-like, trypsin-like and chymotrypsin-like activities, respectively. The three proteolytically active β subunits (β1, β2 and β5) bear the active sites consisting of N-terminal threonines (52). These three subunits are first synthesized as inactive

precursors with a pro-peptide that, upon full incorporation of the subunits into 20S proteasomes, is autocatalytically removed to expose the active site Thr+1 (187). Substrate proteolysis by the proteasome involves both processive as well as endoproteolytic activities and does not always lead to the degradation of the substrate to small 8-9 amino acid fragments. In some cases, when certain domains of the protein substrate remain folded, the proteasome degrades only the unfolded segments. This process is essential for regulating the activity of certain transcription factors (176).

1.3.2.2. ALP: The more than 12 different kinds of cathepsins within lysosomes can, as a group, hydrolyze most peptide bonds on proteins. Cathepsins are distributed throughout the four protease classes. The majority of cathepsins are cysteine proteases (cathepsins B, C, H, K, L, S, and T). From the remaining cathepsins some are aspartyl proteases, such as cathepsins D and E, metalloproteases, such as cathepsin III, and serine proteases, such as cathepsin A, G and R. Cathepsins are synthesized as inactive zymogens and activation within the Golgi involves their proteolytic processing. The hierarchy for protein degradation by the diverse groups of cathepsins

is not always clear and their redundancy makes the function and necessity for each of these enzymes quite ambiguous (127).

1.3.3. SUBSTRATE TARGETING:

1.3.3.1. UPP: The targeting of proteins substrates for degradation by the UPP is a highly regulated process and, in most cases, requires their ubiquitination. Protein-ubiquitination involves: (1) the formation of a high energy thioester bond between Ub and a ubiquitin-activating enzyme (E1) in an ATP-dependent reaction; (2) a thioester bond between the activated ubiquitin and ubiquitin-conjugating enzymes (E2) is generated; (3) covalent attachment of the carboxyl terminal of ubiquitin, usually to the ε-amino group of a lysine on a protein substrate via an isopeptide bond mediated by ubiquitin ligases (E3); and (4) assembly of multiubiquitin chains by a family of ubiquitination factors (E4) which promote the elongation of the Ub-chains. Ubiquitin may also be transferred directly to proteins by ubiquitin-conjugating enzymes (E2) [reviewed in (74)].

Degradation of polyubiquitinated proteins is enhanced when more than one ubiquitin is attached to the target protein. The minimal signal for efficient degradation is a tetraubiquitin chain (214). Removal of two ubiquitins from

a tetraubiquitinated substrate by de-ubiquitinating enzymes can decrease substrate/26S proteasome affinity by approximately 100-fold, allowing the substrate to escape degradation. Longer chains do not increase substrate/26S proteasome affinity, but optimize their interaction time (213). The interaction of the polyubiquitin chain with the 26S proteasome involves hydrophobic patches on the surface of the tetraubiquitin chain, generated by Leu8, Ile44, and Val70 in each ubiquitin moiety, and two hydrophobic sequences with the motif LeuAlaLeuAlaLeu in the PA700 subunit S5a (241). Additional ubiquitin-binding subunits on the 26S proteasome exist since S5a is not an essential protein in yeast (240). The rate at which protein substrates of this pathway are degraded depends on the interplay between their de-ubiquitination and their unfolding (212).

1.3.3.2. ALP: Based on the current knowledge, targeting of protein substrates to degradation by the ALP seems to be a random process. However, ALP suppression or activation in animal cells is highly regulated. Autophagy appears to be constitutively active and is subject to suppression or further induction in response to extracellular stimuli, such as nutrient or growth factor-deprivation, stress or

pathogenic invasion, specific hormones and other factors (222). One target of these stimuli is mTOR (mammalian target of rapamycin), a large molecular weight kinase that is phosphorylated via the PI3 kinase/AKT-signaling pathway, and acts as a negative regulator of autophagy. Dephosphorylation of mTOR by nutrient deprivation or rapamycin leads to the induction of autophagy (92).

Two ubiquitin-like conjugation pathways, Atg12 and Atg8 directly regulate the formation of autophagosomes.

In the *Atg12 system*, the carboxyl-terminal Gly of Atg12 is activated by Atg7, an E1-like enzyme leading to the formation of a thioester intermediate (155). Atg12 is then transferred to Atg10, an E2-like enzyme, forming a second thioester intermediate. Finally the carboxyl-terminal Gly of Atg12 is covalently attached to Lys130 of Atg5, an acceptor molecule, via an isopeptide bond (136). The Atg12-Atg5 conjugate is present on the isolation membrane/phagophore and helps autophagosome expansion. Subsequently, the Atg12-Atg5 complex binds Atg16 non-covalently and the self-interaction of Atg16 promotes complex multimerization. This high molecular weight complex is distributed along the external lipid bilayer, thus helping the elongation process of the autophagosome (93; 177).

The *Atg8 system* is the second ubiquitin-like conjugation pathway. The mammalian orthologue of the yeast Atg8 is MAP-LC3 (microtubule-associated protein light chain), and is the only Atg protein to remain associated with fully-formed autophagosomes. MAP-LC3, thus serves as a specific marker for autophagy in mammalian cells (133; 156). The C-terminal region of MAP-LC3 is cleaved by the mammalian Atg4 cysteine protease. This processed form of nascent MAP-LC3 is known as LC3-I and has a Gly residue exposed at the C-terminus necessary for further activation of this protein by Atg7 (21; 157). An active LC3-I is then transiently transferred to a particular E2-like enzyme, Atg3, and finally LC3-I is transferred to the double membrane specifically to its acceptor molecule, phophatidylethanolamine (PE). This lipidated form of LC3 is known as LC3-II (91; 135). LC3-II is located on the autophagosome membrane on both sides of the lipid bilayer. Once the autophagosome is complete and is ready to fuse with the lysosome the Atg5-Atg12-Atg16 complex dissociates from the membrane, whereas Atg4 releases LC3-II from the external lipid bilayer into the cytoplasm by cleaving it off from the lipid molecule PE. Released LC3 can be reused for the biogenesis of new autophagosomes. Mature autophagosomes then swiftly fuse

with lysosomes where intralysosomal hydrolases are available for degradation.

1.3.4. SUBSTRATE IDENTIFICATION:

1.3.4.1. UPP: Three key characteristics are identified on proteins to be degraded by the UPP: (1)misfolding due to mutations or damaging events; (2)constitutively active ubiquitination signals; (3)post-translational modifications such as phosphorylation/dephosphorylation events or co-factor binding (234).

The unfolding of normal substrates precedes their degradation. This step is required to allow entry into the proteolytic chamber of the 20S proteasome through its narrow openings (211). Unfolding activities may be provided by ATPase subunits in the base of the 19S particle or by extraproteasomal chaperones.

1.3.4.2. ALP: As far as we know, this proteolytic pathway is considered to be a bulky, non-specific degradation process. ALP involves the sequestration of cytosolic regions containing proteins and organelles into double membrane vacuoles known as autophagosomes (63). Autophagosomes then rapidly fuse with lysosomes, which

provide all of the hydrolases required for degradation. Formation of the autophagosome is a *de novo* process and is one of the least understood steps of autophagosome biogenesis. In this process, a membrane of unknown origin, called phagophore, expands leading to autophagosome formation. As discussed above, (see "Substrate Targeting") Atg proteins play a role in phagophore formation as well as in causing it to expand into a double membrane sphere that will become an autophagosome (178).

1.3.5. SUBSTRATE DELIVERY- UPP & ALP:

Non-canonical chaperones were identified as molecules that deliver ubiquitinated proteins to the 26S proteasome. These shuttles for polyubiquitinated proteins contain an ubiquitin-like (UBL) domain at the N-terminus and at least one ubiquitin-associated (UBA) domain at the C-terminus (reviewed in (67; 120)). The UBL domain is known to interact with the 19S particle of the proteasome, in particular with the subunit S5a/Rpn10 (190). The UBA domain non-covalently binds polyubiquitin chains up to 300-times more tightly than mono-ubiquitin (reviewed in (174; 233)).

In the context of neurodegeneration, one of the UBL/UBA proteins that is best characterized as a delivery molecule for polyubiquitinated proteins is the sequestosome1, also

known as p62 (p62/sqstm1). This protein was first identified in human tissues by Shin and colleagues (166) and was found to be a stress inducible protein that contributes to the sequestration of polyubiquitinated proteins into aggregates (189). At its C-terminus p62/sqstm1 has a UBA domain that binds non-covalently to polyubiquitin chains. At its N-terminus, p62/sqstm1 has a PB1 domain, which is a protein-protein interaction domain. The PB1 domain assumes ubiquitin-like folding and can directly bind to the proteasome and also polymerize with other PB1-containing proteins including homo-polymerization (236). In this regard, p62/sqstm1 may play an important role as a scaffold and/or shuttle molecule sorting polyubiquitinated proteins and delivering them to the proteasome for degradation (228). Recent data reported that p62/sqstm1 binds directly to LC3 on the autophagosome membrane, via the LC3-interacting region (LIR), a 22 amino acid sequence. Thus, p62/sqstm1 seems to be specifically recruited to the autophagosome for degradation (164). By binding directly polyubiquitinated proteins via its C-terminal UBA domain, proteasomes via its N-terminal PB1 domain, and LC3 via its LIR domain, p62/sqstm1 may be shuttling polyubiquitinated proteins to an alternate degradation pathway, i.e. the ALP, when proteasomes are

impaired or overwhelmed. Due to its binding versatility, the p62/sqstm1 may play an important role as a scaffold and/or shuttle molecule storing polyubiquitinated proteins and delivering them to the UPP or ALP in a regulated manner.

1.4. ROLE OF THE UPP AND APL IN NEURODEGENERATION

Neurodegenerative disorders such as Alzheimer's disease (AD), Parkinson's disease (PD), Huntington's disease (HD) and amyotrophic lateral sclerosis (ALS) are characterized by selective loss of neurons in specific regions of the brain and usually manifest themselves in the later stages of life. The most common feature shared by these disorders is aberrant protein aggregation. Many of the proteins that cause these proteinopathies are dependent on the UPP for their degradation (180). However, proteasome function is impaired in the affected brain areas in patients with AD (86), PD (128), HD (194) and declines with age (85) as well as with oxidative stress (81). Collectively, these findings support the notion that UPP impairment is a risk factor in a variety of neurodegenerative disorders (139).

In the past, the ALP was not studied in the brain, since brain appears to be a protected tissue where nutrients can be delivered to it from other organs even under starvation conditions (22). Hence, induction of the ALP was not

thought to play a role in brain homeostasis. However, recent histological data from neuronal-specific Atg5 and Atg7 knock-out mice revealed the presence of neurodegenerative changes such as loss of cerebellar Purkinje cells and cerebral cortex neurons as well as the presence of ubiquitinated inclusions in many regions of the brain (62; 100). These data support a role for basal ALP in brain homeostasis. Furthermore, loss of ALP in the brain first leads to the accumulation of diffused abnormal proteins followed by the generation of inclusion bodies, which are hallmarks of numerous neurodegenerative diseases (61). In conclusion, both the UPP and the ALP seem to play important roles in the development of protein aggregates detected in neurodegenerative disorders, although the relationship between these two proteolytic pathways remains poorly defined.

Recent studies propose that when the UPP is not functioning properly, ALP seems to be a compensatory mechanism for intracellular protein degradation (159). In these studies overexpression of a microtubule-associated protein known to bind polyubiquitinated proteins, i.e. histone deacetylase 6 (HDAC6), was sufficient to rescue degeneration in an autophagy-dependent manner, in a *Drosophila* model of neurodegeneration. In this *Drosophila*

model the UPP was impaired by a temperature sensitive, dominant negative mutant of the β2 subunit of the 20S proteasome, which is responsible for the trypsin-like activity of the proteasome, or by expression of a toxic polyQ-expanded androgen receptor. HDAC6 overexpression seemed to accelerate the turnover of the mutant androgen receptor as well as of the high molecular weight aggregates that formed upon proteasome inhibition. Further studies by the same group (158) suggest that HDAC6 promotes the degradation of toxic proteins and mediates the potentially neuroprotective role of autophagy.

1.5. OVERALL CONCLUSIONS

We addressed the relationship between two proteolytic systems, the UPP and the ALP, which are relevant to the development of protein aggregates detected in a variety of neurodegenerative disorders. The postulated crosstalk between the two proteolytic pathways may inevitably be mediated by molecules, such as p62/sqstm1 and HDAC6, which may directly interact with these two systems. The following model is proposed:

Environmental and genetic insults may affect important cellular pathways involved in neuronal homeostasis, such as the ubiquitin/proteasome pathway, leading to the formation

of proteins aggregates. Under mild (non-lethal) conditions the cell will initiate a "pro-survival/repair" response, which may include, among others, increased expression of p62/sqstm1 and HDAC6. In addition, an alternate protein degradation pathway, i.e. autophagy, may be induced. These events indicate a cellular attempt to rescue and/or remove protein aggregates that, due to their bulky nature, are precluded from entering and being degraded by the proteasome. If the protein aggregates cannot be removed by these repair mechanisms and the proteasome is impaired as well, pro-death pathways, including apoptosis, may be activated most likely to remove the damaged cells. The resulting neuronal cell death may have devastating effects as, in the vast majority of cases, neurons lost to disease processes cannot be replaced. The ultimate result will be development and exacerbation of neurodegenerative disorders.

Overall, a better understanding of the relationship between the UPP and the ALP will be critical to the development of novel and more effective therapies that prevent and potentially rescue the pathological phenotypes of neurodegenerative disorders, such as AD, PD, HD and ALS, which are characterized by the accumulation of ubiquitinated proteins in a variety of inclusion bodies.

CHAPTER II

DYNAMICS OF THE DEGRADATION OF UBIQUITINATED PROTEINS BY PROTEASOMES AND AUTOPHAGY: ITS ASSOCIATION WITH SEQUESTOSOME 1/P62

Natura Myeku and Maria E. Figueiredo-Pereira

Department of Biological Sciences,

Hunter College of City University of New York,

New York, NY 10065

Journal of Biological Chemistry, under revision

2.1. ABSTRACT

Proteotoxicity resulting from accumulation of damaged/unwanted proteins contributes prominently to cellular aging and neurodegeneration. Proteasomal removal of these proteins upon covalent modification by polyubiquitination is a highly regulated process. Recent reports proposed a role for autophagy in clearance of diffuse ubiquitinated proteins delivered to autophagosomes by p62/sqstm1. Here, we compared the dynamics of the turnover of endogenous ubiquitinated proteins by proteasomes and autophagy by assessing the effect of their inhibitors. Autophagy inhibitors bafilomycin A1 and ammonium chloride failed to increase ubiquitinated protein levels. The proteasome inhibitor epoxomicin raised ubiquitinated protein levels at least three-fold higher than the lysosomotropic agent chloroquine. The same trend was observed when we compared SK-N-SH cells maintained under serum or serum-free conditions, as well as in WT and Atg5-/- mouse embryonic fibroblasts (MEFs). Notably, chloroquine inhibited both the 26S and 20S proteasomes in SK-N-SH cells and MEFs, although it required higher concentrations than epoxomicin. Furthermore, levels of p62/sqstm1 were significantly higher upon epoxomicin- than chloroquine-treatment. With epoxomicin, most of the soluble

p62/sqstm1 associates with proteasomes while non-soluble p62/sqstm1 is in aggregates that contain inactive proteasomes and autophagosomes. Up to 96 hour incubations with chloroquine failed to increase ubiquitinated protein levels in rat cortical neuronal cultures, while epoxomicin did. In conclusion, we clearly demonstrate that pharmacologic or genetic inhibition of autophagy fails to cause accumulation of ubiquitinated proteins unless the proteasome is affected. Finally, we provide strong evidence that p62/sqstm1 associates with proteasomes. Overall, the function of p62/sqstm1 in the proteasomal pathway and autophagy requires further elucidation.

2.2. INTRODUCTION

Chronic neurodegenerative disorders, such as Alzheimer's (AD) and Parkinson's (PD) diseases as well as amyotrophic lateral sclerosis (ALS), are a heterogeneous group of diseases characterized by selective loss of neurons in specific regions of the CNS. Despite their heterogeneity they have similar features including abnormal deposition of ubiquitinated protein aggregates in inclusion bodies within neurons in the respective affected areas of the CNS (reviewed in (125)). The ubiquitinated protein aggregates are thought to result from dysfunction of the

ubiquitin/proteasome pathway (UPP) or from structural changes in the protein substrates which prevent their degradation by the UPP (review in (28)). Emerging studies also implicate autophagy impairment in the formation of the ubiquitinated protein aggregates. Accordingly, two recent studies described prominent ubiquitin-positive aggregates in neurons of autophagy-deficient (Atg5-/- or Atg7-/-) mice (60; 98). Based on these results and on the finding that there was no apparent alteration in proteasome activity in the brains of autophagy deficient mice (97) it was suggested that autophagy acts continuously to dispose of diffuse ubiquitinated proteins in a house-keeping role (59; 94; 96).

Although the UPP and autophagy were thought to work in parallel, recent investigations suggest a functional link between the two proteolytic pathways (reviewed in (95)). The sequestosome 1/p62 (p62/sqstm1) could play an important role in mediating the link between the two pathways. Due to its ability to interact with polyubiquitin chains, p62/ sqstm1 was suggested to be a receptor that binds and delivers polyubiquitinated proteins to the two proteolytic pathways (199). P62/sqstm1 is a protein prone to aggregation and was first isolated in human tissues by Shin and colleagues (165). At its N-terminus, p62/sqstm1 has a

PB1 domain, which is a protein-protein interaction domain that assumes ubiquitin-like folding and can directly bind to proteasomes and other PB1-containing proteins including itself (236). Recently, p62/sqstm1 was shown to also interact with LC3, a protein that is an autophagosomal marker (163). P62/sqstm1 binds directly to LC3 via a 22 amino acid sequence, the LC3-interacting region (LIR) (162; 191). By binding to polyubiquitinated proteins via its C-terminal UBA domain, to proteasomes via its N-terminal PB1 domain, and to LC3-II via its LIR domain, p62/sqstm1 could direct polyubiquitinated proteins to the proteasome or to autophagy, when proteasomes are impaired or overwhelmed (161; 193). P62/sqstm1 may thus be a candidate for the missing link between the UPP and autophagy.

Here we compared the dynamics of the turnover of ubiquitinated proteins by proteasomes and autophagy by assessing the effect of pharmacologic inhibitors of each pathway on the accumulation of endogenous ubiquitinated proteins as well as on p62/sqstm1. We conclusively demonstrate that autophagy impairment does not cause the accumulation of ubiquitinated proteins. The minimal accumulation of ubiquitinated proteins observed upon chloroquine-treatment is due to weak proteasome inhibition by the lysosomotropic agent. Other autophagy inhibitors or

genetic impairment of autophagy in Atg5-/- MEFs did not cause the accumulation of ubiquitinated proteins. Furthermore, it is clear that p62/sqstm1 is associated with proteasomes. Its role in both proteolytic pathways, i.e. proteasomes and autophagy, requires further elucidation.

2.3. MATERIALS AND METHODS

2.3.1. Materials: Protease inhibitors: chloroquine, bafilomycin A1 and ammonium chloride were from Sigma (St. Louis, MO). Epoxomicin was from Peptides International Inc. (Louisville, KY). The substrate Suc-LLVY-AMC was from BACHEM Bioscience Inc. (King of Prussia, PA). Primary antibodies: rabbit polyclonal anti-ubiquitinated proteins (1:1,500, cat# Z0458) from Dako North America (Carpinteria, CA); mouse monoclonal anti-B-actin (1:10,000, cat# A-2228) and rabbit polyclonal anti-B-actin (1:10,000, cat# A-2066) were from Sigma (St. Louis, MO). Mouse monoclonal anti-α4 (1:500, cat# PW8120) and anti-Rpt6/S8 (1:1,000, cat#PW9265) and rabbit polyclonal anti-β5 (1:1,000, cat#PW8895) were from BIOMOL (Plymouth Meeting, PA). Rabbit polyclonal anti-p62/sqstm1 (1:1,000 cat# PM045) and anti-Atg5 (1:1000, cat#PM050), and mouse monoclonal anti-Atg16 (1:1,000 cat#M150-3) were from MBL International Corp. (Woburn, MA). For the glycerol gradient fractionation the mouse

monoclonal p62/sqstm1 (lck ligand) (1:500, cat#610833) was from BD Transduction Laboratories™ (San Jose, CA). Rabbit polyclonal anti-LC3 (1:1,000, cat# Nb 100-2220) was from Novus Biological (Littleton, CO). The *in vitro* synthesized K63-only and K48-only polyubiquitinated substrates were from Enzo Life Sciences Inc. (Farmingdale, NY). The respective secondary antibodies with HRP conjugate (1:10,000) were from Bio-Rad Laboratories (Hercules, CA).

2.3.2. Cells – Human neuroblastoma SK-N-SH cells are derived from peripheral tissue (19) and were obtained from ATCC. Under serum conditions, the cells were maintained at 37°C and 5% CO_2 in minimal essential media (MEM) with Eagle's salts containing 2mM L-glutamine, 1mM sodium pyruvate, 0.4% MEM vitamins, 0.4% MEM nonessential amino acids, 100 units/ml penicillin, 100µg/ml streptomycin and 5% normal fetal bovine serum. Under serum-free conditions, the cells were maintained as in serum conditions except that the media lacked non-essential amino acids and fetal bovine serum.

Wild type and Atg5-/- mouse embryonic fibroblast cell lines (MEFs) were obtained from RIKEN BRC (Japan) and cultured at 37°C and 5% CO_2 in DMEM with 100 units/ml penicillin, 100µg/ml streptomycin and 10% normal fetal bovine serum as described in (105). The Atg5-/- cell line

is deficient in Atg5 which is essential for autophagosome formation. Wild type and Atg5-/- MEFs were prepared from 13.5 day embryos and transformed with pEF321-T, an SV40 large T antigen expression vector to generate immortalized cell lines (104).

Rat cortical neuronal cultures were prepared from E18 embryos obtained from pregnant Sprague Dawley females following the methods described in (18). Cells were cultured at 37°C and 5% CO_2 in neurobasal media supplemented with B27 and 0.5mM L-glutamax. Cells were plated in 100-mm dishes precoated with 50µg/mL poly-D-lysine and at a density of 6 million cells per dish. Experiments were carried out following 8 days in culture.

2.3.3. Cell treatments - Cells were treated at 37°C for different times with vehicle (0.5% DMSO, control) or different concentrations of the protease inhibitors listed above. Drugs were added drop wise directly into the medium with a gentle swirl of the culture plate. At the end of the incubation, all cultures were washed twice with phosphate buffered saline (PBS) and processed for the different assays as described below. Cell washes removed unattached cells, therefore subsequent assays were performed on adherent cells only.

2.3.4. Cell viability - Cell survival was assessed with the 3-(4,5-dimethylthiazol-2-yl)-2,5-diphenyl tetrazolium bromide (MTT) assay as described in (141).

2.3.5. Western blotting – After treatment, cells were rinsed twice with PBS and harvested by gently scraping into hot (100°C) SDS buffer (0.01M Tris-EDTA, pH 7.5 and 1% SDS) to make sure all intracellular proteins were included. Samples were subjected to a 5-min boil at 100°C followed by a brief sonication. After determination of the protein concentration with the bicinchoninic acid assay kit (Pierce, Rockf., IL) the following was added to each sample: β-mercaptoethanol (358mM), bromophenol blue (0.005%), glycerol (20%), SDS (4%) in stacking gel buffer (0.1M Tris-Cl, pH 6.8). Following SDS-PAGE on 8% or 10% polyacrylamide gels, proteins were transferred to an Immobilon-P membrane (Millipore, Bedford, MA). The membranes were probed with the respective antibodies and antigens were visualized by a standard chemiluminescent horseradish peroxidase method with the ECL reagent. Semi-quantification of protein detection was done by image analysis with the ImageJ program (Rasband, W.S., ImageJ, U.S. NIH, Maryland, http://rsb.info.nih.gov/ij/, 1997-2006). Relative intensity (no units) is the ratio between

the value for each protein and the value for the respective loading control.

2.3.6. Peptidase activity of the proteasome – Total cell lysates were prepared on ice by homogenization in 0.01M Tris-EDTA, pH 7.5 buffer. The lysates were cleared by a 15-min centrifugation (19,000xg) at 4°C. The cleared samples were normalized for protein concentration determined with the bicinchoninic acid assay kit (Pierce, Rockf., IL). The chymotrypsin-like activity was assayed colorimetrically in 25μg of protein/sample with the substrate Suc-LLVY-AMC (400μM in DMSO) after 24h incubations at 37°C as described in (232).

2.3.7. Glycerol density gradient centrifugation – Cells were harvested in 25mM Tris-HCl, pH 7.5, 2mM ATP and 1mM DTT. Following homogenization and sonication the lysates were centrifuged (19,000xg for 15-min) at 4°C. The cleared supernatants (2 mg of protein/sample) were subjected to centrifugation (83,000xg for 24h) at 4°C in a Beckman SW41 rotor in a 10-40% glycerol gradient (fractions 13 to 1) made in the same lysis buffer. Following centrifugation 13 fractions (800μl each) were collected and analyzed. Aliquots (50μl) of each fraction were assayed for chymotrypsin-like activity with the substrate Suc-LLVY-AMC colorimetrically

after 24h incubations at 37°C as described in (231). Proteins were precipitated with acetone from 700μl of each fraction and subjected to Western blot analysis (10% gels). The membranes were probed with the respective antibodies and antigens were visualized by a standard chemiluminescent horseradish peroxidase method with the ECL reagent.

2.3.8. In-gel proteasome activity and detection – Upon treatment with vehicle (DMSO) or the respective drugs, cells were washed twice with PBS and were harvested with the following buffer A: 50mM Tris-HCl, pH 7.4, 5mM $MgCl_2$, 5mM ATP (grade 1; Sigma), 1mM DTT and 10% glycerol, which preserves 26S proteasome assembly (42). Following homogenization and centrifugation (19,000xg for 15-min) at 4°C the protein concentration of the cleared supernatants was determined with the Bradford assay (Bio-Rad Laboratories, Hercules, CA) and normalized with buffer A. The cleared supernatants (80μg protein/lane for proteasome activity and 40μg protein/lane for western blotting) were resolved by non-denaturing PAGE using a modification of the method described in (150). We used a gel consisting of three layers of equal amounts, from the bottom up, of 5%, 4% and 3% polyacrylamide with Rhinohide™ polyacrylamide strengthener (Molecular Probes). Bromophenol blue was added

to the protein samples prior to loading. Non-denaturing minigels were run at 150Volts for either three hours or 90-min. The gels were then incubated on a rocker for 10-min at 37°C with 15ml of 400µM Suc-LLVY-AMC in buffer B (buffer A modified to contain 1mM ATP). Proteasome bands were visualized upon exposure to UV light (360nm) and were photographed with a NIKON Cool Pix 8700 camera with a 3-4219 fluorescent green filter (Peca Products, Inc). Proteins on the native gels were transferred (110mA) for 2h onto PVDF membranes. Western blot analyses were then carried-out sequentially for detection of the 20S and 26S proteasomes with anti-β5 and anti-Rpt6/S8 subunit antibodies. The anti-β5 antibody reacts with a core particle subunit, therefore detects both the 26S and 20S proteasomes. The anti-Rpt6/S8 antibody reacts with a regulatory particle subunit thus only detecting 26S proteasomes. Antigens were visualized by a chemiluminescent horseradish peroxidase method with the ECL reagent. Aliquots of the samples were also boiled for 5-min in Laemmli buffer and loaded onto 10% gels (40µg of protein/lane) for western blot analysis following SDS-PAGE.

2.3.9. Filter trap assay - Cells were washed twice with PBS and harvested with RIPA buffer [20mM Tris-HCl pH 7.5; 137mM NaCl; 1mM EGTA; 10% glycerol (v/v), 1mM sodium

orthovanadate; 1mM phenylmethylsulfonyl fluoride; 1mM β-glycerophosphate; 2.5mM sodium pyrophosphate; 50mM sodium fluoride; 1% Nonidet P40 and protease inhibitor cocktail]. Following homogenization, lysates were centrifuged at 4°C (for 15-min at 19,000xg). Cell pellets were resuspended by sonication in harvesting buffer containing 2% SDS; 100µg protein/sample were trapped by filtration through a pre-wet Trans-Blot nitrocellulose membrane 0.2µm (Bio-Rad Laboratories, Hercules, CA) adapted to a 96-well dot blot apparatus from Bio-Rad Laboratories, (Hercules, CA) as described in (229). Due to the 0.2 µm pore size of this membrane only aggregated proteins are retained while the soluble ones pass through the pores of the membrane. To detect aggregates, the membranes were probed with the anti-p62/sqstm1 or the anti-ubiquitinated protein antibodies.

2.3.10. *In situ* Proximity Ligation Assay (PLA): After treatment SK-N-SH cells were washed twice with PBS and fixed in 4% paraformaldehyde for 15-min at room temperature. The PLA assay was performed as described previously in (202) and with the Duolink PLA detection kit 613 from Axxora, LLC, San Diego, CA. Slides were mounted with Vectashield medium containing DAPI (Vector Laboratories, Inc., Burlingame, CA). Cell staining was

visualized with an UltraViewVoX Spinning Disk Confocal microscope (Perkin Elmer, Waltham, MA).

2.3.11. Statistical analysis - statistical significance was estimated using one-way ANOVA (Tukey-Kramer multiple comparison test) with the Instat 2.0, Graphpad Software (San Diego, Ca).

2.4. RESULTS

2.4.1. Chloroquine, ammonium chloride and bafilomycin A1 as autophagy inhibitors – To investigate the link between autophagy and degradation of ubiquitinated proteins, SK-N-SH cells were treated with three different autophagy inhibitors, namely choloroquine (CQ, 100μM), ammonium chloride (NH_4Cl, 10mM) and bafilomycin A1 (Baf, 200nM) at concentrations reported in the literature to inhibit autophagy. We compared the effects of the three drugs on cell viability and autophagy inhibition. In parallel studies, we treated cells with epoxomicin (Epox, 25nM), an irreversible proteasome inhibitor. **Fig. 1A** shows that at the concentrations tested bafilomycin A1 was the most toxic of the drugs tested.

Autophagy inhibition was assessed by accumulation of the autophagosome marker LC3-II, which is accepted as an overall indicator of autophagy impairment. LC3-II levels

were most prominent after chloroquine treatment (123-fold increase) as indicated by the strong LC3-II band on the western blots **(Fig. 1B).** In bafilomycin A1-treated cells LC3-II levels (32-fold increase) were lower than in chloroquine-treated cells and ammonium chloride and epoxomicin treatment failed to induce LC3-II accumulation **(Fig. 1B).** These data show that among the three autophagy inhibitors tested, chloroquine most effectively raised LC3-II levels. Proteasome inhibition by epoxomicin had no inhibitory effect on autophagy.

2.4.2. Epoxomicin and to a lesser extent chloroquine increased p62/sqstm1 and ubiquitinated protein levels but the two other autophagy inhibitors did not – P62/sqstm1 was suggested to be specifically degraded by autophagy (101; 160) and its levels were proposed to increase in response to autophagy inhibition (20). We compared how the four proteolytic inhibitors listed above affected p62/sqstm1 as well ubiquitinated protein levels. It is clear that from the four drugs tested, epoxomicin most effectively increased p62/sqstm1 **(9-fold, Fig. 1C)** and ubiquitinated protein **(three-fold, Fig. 1D)** levels in SK-N-SH cells. Chloroquine caused a detectable increase in p62/sqstm1 (six-fold), albeit to a lesser extent than epoxomicin.

Ammonium chloride and bafilomycin A did not increase p62/sqstm1 levels. Another autophagy inhibitor, 3-MA failed to increase the levels of ubiquitinated proteins, p62/sqstm1 and LC3-II (*not shown*). Upon treatment with chloroquine we observed a 1.7-fold increase in ubiquitinated proteins. Actin levels were not increased by any of the treatments **(Fig. 1E).**

To further investigate the cross-talk between the UPP and autophagy we decided to focus our studies on chloroquine and epoxomicin, since ammonium chloride and bafilomycin A1 failed to increase p62/sqstm1 and ubiquitinated protein levels and the latter inhibitor was highly cytotoxic.

2.4.3. We compared the effects of inhibiting each pathway alone with inhibiting both pathways together (Fig. 2). - Similar results were obtained in cells maintained under serum or serum free conditions (*the latter not shown*). P62/sqstm1 levels were raised four-fold over control by epoxomicin ($p<0.01$) but only two-fold by chloroquine ($p>0.05$, *not significant*) **(Fig. 2 A and D).** In cells treated with both inhibitors, p62/sqstm1 levels were higher than in cells treated with epoxomicin alone but the difference was not statistically significant *($p>0.05$).* As

expected, LC3-II levels were increased only in cells treated with chloroquine as proteasome inhibition does not block autophagy function. Chloroquine alone raised LC3-II levels two-fold **(*p<0.01,* Fig. 2B and D)**. LC3-II levels were similar in cells treated with chloroquine alone or in combination with epoxomicin (*p>0.05*). The levels of LC3-I and of the α4 subunit of the 20S proteasome did not show any significant changes **(Fig. 2 B, C and D)**. Together these data clearly demonstrate that proteasome inhibition most efficiently increases p62/sqstm1 levels when compared to autophagy impairment, the latter ascertained by accumulation of LC3-II in cells treated with chloroquine.

2.4.4. Both epoxomicin and chloroquine inhibit Suc-LLVY-AMC hydrolysis – Inhibition of lysosomal function was recently shown to reduce proteasome activity (172), therefore we compared the effect of epoxomicin and chloroquine on the cleavage of Suc-LLVY-AMC, a short substrate used to measure proteasome activity. Similar results were obtained under serum and serum-free conditions (*the latter not shown)*. As shown in **Fig. 2G**, Suc-LLVY-AMC hydrolysis measured in total lysates was blocked by at least 80% in cells treated with epoxomicin or chloroquine alone or combined.

Despite a similar decline in Suc-LLVY-AMC hydrolysis observed in cells treated with each or both drugs, the levels of ubiquitinated proteins were quite different. Treatment with epoxomicin caused a ~three-fold rise in ubiquitinated protein levels ($p<0.01$) compared to a much smaller increase (1.8-fold, $p>0.05$) in cells treated with chloroquine **(Fig. 2E and F)**. Combined treatment with epoxomicin and chloroquine enhanced ubiquitinated protein levels by four-fold, which was significantly different from the values observed under epoxomicin alone **($p<0.01$, Fig. 2E and F)**. Ubiquitin protein aggregates were detected with the filter trap assay in cells treated with epoxomicin by itself or in combination with chloroquine **(Fig. 2H)**. Actin levels were not changed upon proteasome or/and autophagy inhibition **(Fig. 2E)**.

These data clearly demonstrate that measuring Suc-LLVY-AMC hydrolysis using total cell lysates does not accurately reflect proteasome activity. This is not surprising, since it is well established that the substrate Suc-LLVY-AMC is cleaved not only by the proteasome (205) but also by other chymotrypsin-like proteases as well as by calpains (183). In addition, it is clear that the overall levels of ubiquitinated proteins in chloroquine-treated cells are very low. This includes K48- and K63-linked chains as both

are detected with the poly-Ub antibody from DAKO (Carpinteria, CA) used in these studies **(Fig. 2E, *left panel*)**. This is relevant to autophagy because K63-linked chains were postulated to selectively facilitate the clearance of ubiquitinated proteins via the autophagic pathway (209).

2.4.5. Chloroquine inhibits proteasome activity albeit to a lesser extent than epoxomicin – The decline in Suc-LLVY-AMC hydrolysis together with the accumulation of ubiquitinated proteins observed in cells treated with chloroquine could reflect proteasome inhibition by the lysosomotropic agent. To test this hypothesis, total extracts from cells treated with chloroquine under serum or serum free conditions (*the latter not shown*) were fractionated by glycerol density gradient centrifugation. We also evaluated control and epoxomicin-treated cells. Fractions were analyzed for Suc-LLVY-AMC hydrolysis which reflects the chymotrypsin-like activity.

Compared to controls, the chymotrypsin-like activity of chloroquine-treated cells was significantly reduced **(Fig. 3A)** in the fractions corresponding to the elution of both forms of the proteasome: fractions 7-8 (*peak for 26S*) and fractions 9-10 (*20S*); compare chloroquine treatment

(*circles*) with control (*squares*). Almost no Suc-LLVY-AMC hydrolysis was detected in cells treated with epoxomicin (*crosses close to the X-axis*).

To confirm the proteasome elution pattern, aliquots from each fraction were subjected to western blot analysis with the anti-α4 antibody that reacts with a subunit of the 20S core particle, and with the anti-Rpt6/S8 antibody that reacts with an ATPase subunit of the 19S particle **(Fig. 3 B, C and D, *rows 1 & 2*)**. Immunodetection of the α4 and Rpt6/S8 subunits confirmed a similar elution pattern under all treatment conditions. From these experiments we can conclude that a 24h treatment with 100μM chloroquine inhibits both the 20S and 26S forms of the proteasome although not as effectively as 25nM epoxomicin.

2.4.6. P62/sqstm1 associates with 26S proteasomes and not with autophagosome-related proteins upon fractionation of total cells lysates by glycerol gradient centrifugation – Western blot analyses of the glycerol gradient fractions were probed for p62/sqstm1 and for three of the proteins related to autophagosomes: Atg5, Atg16 and LC3. As expected, under control conditions no p62/sqstm1 was detected **(Fig. 3B, *row 3*)**. Autophagosome-related proteins co-eluted with the 20S proteasome and also in lighter

fractions **(Fig. 3B, *rows 4, 5 & 6*)**. The lighter elution of the autophagosome-related proteins could reflect autophagosome buoyant density conferred by its lipid membrane. A similar elution pattern was observed in cells treated with chloroquine **(Fig. 3C, *rows 4, 5 & 6*)** and epoxomicin **(Fig. 3D, *rows 4, 5 & 6*)**. As a loading control we also probed the blots for actin **(Fig. 3B, C and D, *row 7*)**. In accordance with our previous results **(Fig. 1 and 2)**, significant lower levels of p62/sqstm1 were detected in cells treated with chloroquine **(Fig. 3C, *row 3*)** than with epoxomicin **(Fig. 3D, *row 3*)**. Most of the p62/sqstm1 co-eluted with the 26S proteasome, except for a "putative" aggregated form detected in the heaviest fraction (fraction #1) observed in cells treated with chloroquine or epoxomicin. These results clearly demonstrate that "soluble" p62/sqstm1 has a higher affinity for 26S proteasomes than for autophagosome-related proteins.

2.4.7. Corroboration that chloroquine inhibits the proteasome - To confirm that chloroquine inhibits the proteasome we assessed its activity with the in-gel assay using the Suc-LLVY-AMC substrate as described under "Experimental Procedures". The in-gel assay for measuring proteasome activity has the advantage of differentiating

between the two forms of the 26S proteasome (one capped and two capped) as well as the 20S proteasome. Cells were treated for 24h without (0, control) or with three concentrations of chloroquine (100μM, 150μM or 200μM). An equal amount of protein (80μg) from the cleared cell lysates was loaded onto each lane of the native gels.

These studies clearly demonstrate a concentration-dependent decline in proteasome activity **(Fig. 4A, *left panel*)**. Semi-quantification of the bands detected in **Fig. 4A** show a significant (*mostly p<0.01*) decline in proteasome activity **(Fig. 4B)** in both 26S forms (*upper graph: two capped, white bars; one capped, black bars*) as well as in 20S proteasomes (*bottom graph*).

Immunoblot analyses of the native gels with the anti-β5 **(Fig. 4A, *two middle panels*)** as well as with the anti-Rpt6/S8 **(Fig. 4A, *right panel*)** antibodies revealed a substantial concentration-dependent decline in the levels of 26S proteasomes **(Fig. 4C, *semi-quantification*)**. On the contrary, the levels of 20S proteasome increased slightly **(Fig. 4A, *two middle panels;* Fig. 4C, *semi-quantification*)**. The total levels of β5 subunit did not vary while Rpt6/S8 was slightly decreased by treatment with the highest (200μM) chloroquine concentration **(Fig. 4D, *rows 1 & 2*)**. These findings suggest that the decrease in proteasome

activity observed in cells treated with chloroquine is linked to a parallel decline in 26S proteasome assembly. As expected LC3-II was detected only in cells treated with chloroquine **(Fig. 4D, *row 3*).** Actin levels were unaltered **(Fig. 4D, *row 4*).**

2.4.8. Proteasomal association with p62/sqstm1 upon epoxomicin or chloroquine treatment – P62/sqstm1 levels are almost undetectable under basal conditions. To increase p62/sqstm1 levels we treated cells with epoxomicin or chloroquine, to investigate the association of p62/sqstm1with proteasomes and/or LC3 as an indicator for autophagosomes. Not surprisingly, proteasome inhibition assessed by the in gel-assay was much stronger in cells treated with 25nM epoxomicin than with 100µM chloroquine **(Fig. 5A, *left panel*).** Immunoblot analyses of the native gels with the anti-β5 **(Fig. 5A, *middle panel*)** as well as with the anti-Rpt6/S8 **(Fig. 5A, *right panel*)** antibodies revealed a decrease in 26S proteasomes and a slight increase in 20S proteasomes upon treatment with chloroquine. In cells treated with epoxomicin, such changes were not obvious because besides the conventional 26S and 20S proteasome bands, additional bands were detected with both antibodies **(Fig. 5A).** These additional bands most

likely correspond to increased amounts of proteasome precursor complexes and intermediates shown to occur in cells upon proteasome inhibition (129).

To identify LC3 that is associated with autophagosomes, native gels where run for a much shorter time (90-min instead of three hours) just until the dye front reached the bottom of the gels **(Fig. 5B)**. The in-gel assay revealed proteasome activity only **(Fig. 5B, *left panel*)**, but western blotting with the anti-LC3 antibody detected LC3 indicative of autophagosomes on the bottom half of the gel **(Fig. 5B, *right panel*)**. Under native conditions there is no separation between LC3-I and LC3-II, only "total" LC3 is detected in two bands that could represent different autophagosome populations, just like three proteasome bands are observed under native conditions. The levels of "total" LC3 do not change probably because often when LC3-I decreases LC3-II increases. In epoxomicin-treated cells, which are the conditions in our experiments under which p62/sqstm1 levels are the highest, p62/sqstm1 staining was observed exclusively in association with the proteasome **(Fig. 5B, *middle panel*)**. In chloroquine-treated cells almost no p62/sqstm1 was associated with proteasomes or LC3-associated with autophagosomes **(Fig. 5B, *middle panel*)**.

To determine the fate of ubiquitinated proteins and p62/sqstm1 upon chloroquine-treatment cells were harvested in the same buffer used for running native gels. For these native gels, cells are harvested in a buffer that preserves 26S proteasome assembly (see "Experimental Procedures") and after homogenization two fractions are generated upon centrifugation: the cleared supernatant, which is run on the native gel, and a pellet containing insoluble particles that is usually discarded. For SDS-PAGE both fractions, the cleared supernatant and the pellet, were analyzed followed by western blotting to detect ubiquitinated proteins, p62/sqstm1, proteasomes (anti-β5 and anti-Rpt6/S8) and autophagosomes (anti-LC3) **(Fig. 5C, *semi-quantification* in 5D)**. For loading control the blots were probed for actin **(Fig 5C, *row 5*)**. In addition, aggregates in the pellet fractions were assessed by the filter trap assay **(Fig. 5E)** and Suc-LLVY-AMC hydrolysis was measured in the supernatant and pellet fractions **(Fig. 5F)**.

Under control conditions, ubiquitinated proteins and proteasomes were detected mostly in the soluble fraction **(Fig. 5C, *upper panel as well as rows 1 and 2,* and 5D)**. LC3-I was distributed evenly between the two fractions **(Fig. 5C, *row 4,* and D)**. LC3-II and p62/sqstm1 levels were very low in both fractions **(Fig. 5C and 5D)**.

In cells treated with chloroquine, ubiquitinated proteins were more abundant in the pellet fraction **(Fig. 5C, *upper panel* and Fig. 5D)**. Proteasome levels were still higher in the soluble fraction **(Fig. 5C, *rows 1 and 2,* and 5D)**. LC3-I was slightly more abundant in the pellet **(Fig. 5C, *row 4,* and 5D)**. Most of LC3-II and p62/sqstm1 were found in the pellet **(Fig. 5C, *rows 4 and 3*, Fig. 5D)**.

In epoxomicin-treated cells, ubiquitinated proteins, proteasomes and LC3-I were evenly distributed between the two fractions **(Fig. 5C, *upper panel as well as rows 1, 2 and 4;* also Fig. 5D)**. Notably, the β5 subunit displayed a higher molecular weight, possibly because epoxomicin (MW = 554.7) is covalently bound to it. LC3-I levels were higher than in controls supporting the view that LC3-I is a proteasome substrate (46). P62/sqstm1 was 1.6-fold more abundant in the pellet than in the supernatant **(Fig. 5C, *row 3* and Fig. 5D)**. LC3-II was almost undetectable in the supernatant, but low levels were present in the pellet **(Fig. 5C, *row 4*)**.

In chloroquine- as well as in epoxomicin-treated cells the pellet fraction contains aggregates with p62/sqstm1 **(Fig. 5E)**. Under all conditions, proteasome activity assessed with Suc-LLVY-AMC was very low in the pellet fraction **(Fig. 5F)**.

Overall, these findings establish that when the proteasome is inhibited by epoxomicin and p62/sqstm1 levels are high, p62/sqstm1 is distributed among two fractions: the soluble (supernatant) fraction found to be associated with proteasomes and the aggregated (pellet) fraction that also contains inactive proteasomes and autophagosome proteins. Upon autophagy inhibition induced by chloroquine, most of the p62/sqstm1 co-localizes with autophagosomes in the pellet fraction.

2.4.9. Validation that p62/sqstm1 associates with the proteasome – We used a *P*roximity *L*igation *A*ssay (PLA) for detecting *in situ* whether p62/sqstm1 interacts with the proteasome. In this assay a pair of oligonucleotide-labeled secondary antibodies (PLA probes) generates an individual fluorescent signal when bound to the primary antibodies in close proximity (43; 201; 230). The PLA assay allows for the *in situ* detection of individual, endogenous, interacting protein pairs in cells. We found that p62/sqstm1 and the proteasome interact *in situ* even under basal conditions (Ct, control), when p62/sqstm1 levels are low **(Fig. 6A)**. In cells treated with chloroquine (CQ, 100μM) the interaction signal was mostly perinuclear **(Fig. 6B)**. In the epoxomicin-treated cells (Epx, 25nM) the signal

was distributed throughout the cell **(Fig 6C)**. The same pattern was obtained with the anti-Rpt6/S8 **(Fig. 6)** or anti-α4 (*not shown*) proteasome antibodies. Under lower magnification (*not shown*), most cells in each condition exhibited a signal pattern similar to the one shown in each figure panel. Omission of each or both of the primary antibodies produced no signal (*not shown*). These results further substantiate that these two molecules, i.e. p62/sqstm1 and proteasomes are associated within cells.

2.4.10. Chloroquine inhibits proteasome activity in wild type and Atg5-/- MEFs – To establish if proteasome inhibition by chloroquine was observed in other cell lines besides the human neuroblastoma SK-N-SH cells, we tested the effects of the lysosomotropic agent on wild type (WT) and autophagy deficient (Atg5-/-) MEFs. Contrary to what was observed with SK-N-SH cells **(Fig. 2G)**, chloroquine at 100μM and 200μM failed to inhibit Suc-LLVY-AMC hydrolysis measured with total cell lysates obtained from WT (*white bars*) and Atg5-/- (*black bars*) MEFs **(Fig. 7A)**. In addition, inhibition of Suc-LLVY-AMC hydrolysis by epoxomicin was found to be significantly less effective in MEFs **(Fig. 7A)** than in SK-N-SH cells **(Fig. 2G)**. The proteasome inhibitor at 25nM reduced Suc-LLVY-AMC hydrolysis in SK-N-SH cells by

almost 90% **(Fig. 2G),** while even at a concentration as high as 150nM only 23% inhibition was observed in WT (*white bars*) and Atg5-/- (*black bars*) MEFs **(Fig. 7A).**

Based on these surprising results, we decided to assess proteasome activity in MEFs by the in-gel assay **(Fig. 7B and C).** Just like in SK-N-SH cells **(Fig. 4A),** it is clear that chloroquine inhibits proteasome activity and impairs its assembly in a concentration-dependent manner in WT **(Fig. 7B, *three left panels*)** and Atg5-/- **(Fig. 7B, *three right panels*)** MEFs. For loading control the blots were probed for actin **(Fig 7B).** When assessed by the in-gel assay, epoxomicin effectively inhibited proteasome activity in WT **(Fig. 7C, *left panel*)** and Atg5-/- **(Fig. 7C, *right panel*)** MEFs. These findings support the view that chloroquine inhibits proteasome activity in cell lines other than SK-N-SH cells, although it is significantly less potent than epoxomicin. In addition, MEFs contain other proteases besides the proteasome that effectively cleave the substrate Suc-LLVY-AMC and their activity is not reduced by chloroquine or epoxomicin. The nature of these proteases remains to be established. That the Atg5-/- is indeed defective in autophagy is demonstrated in **Fig. 7D,** as upon chloroquine treatment LC3-II was only detected in WT and not in the Atg5-/- MEFs.

2.4.11. No increases in ubiquitinated proteins and p62/sqstm1 are observed in Atg5-/- MEFs unless they are treated with epoxomicin – Genetically impairing autophagy as in Atg5-/- MEFs did not cause an increase in ubiquitinated proteins or p62/sqstm1. As shown in **Fig. 8,** control or chloroquine-treated WT (*white bars*) and Atg5-/- (*black bars*) MEFs exhibited similar levels of ubiquitinated proteins **(Fig. 8A and 8E)** and p62/sqstm1 **(Fig. 8B and 8E).** As expected, the levels of ubiquitinated proteins and p62/sqstm1 where only significantly higher (*at least* $p<0.05$) in epoxomicin-treated MEFs **(Fig. 8A, B & E).** LC3-II was detected in WT but not in Atg5-/- MEFs **(Fig. 8C and E)** and the proteasome α4 subunit was unaltered under all conditions **(Fig. 8D).**

2.4.12. Chloroquine does not increase the levels of ubiquitinated proteins in rat primary cortical neuronal cultures – We also investigated the effect of pharmacologically inhibiting autophagy with chloroquine on rat primary cortical neuronal cultures. As shown in Figures **9A and 9D,** chloroquine failed to increase ubiquitinated protein levels upon incubations up to 96h. We used lower drug concentrations than with SK-N-SH cells or MEFs because we incubated the cells for longer times and the higher

concentrations were cytotoxic. That autophagy was inhibited is demonstrated by the increase in LC3-II observed in cells treated with chloroquine **(Fig. 9B and 9D)**. On the other hand, epoxomicin clearly increased the levels of ubiquitinated proteins even after 24h of incubation with concentrations as low as 5nM. No changes were detected in β-tubulin **(Fig. 9C)**.

2.5. DISCUSSION

Proteotoxicity resulting from accumulation of damaged/unwanted proteins contributes prominently to cellular aging and age-associated neurodegeneration. Removal of these proteins upon their covalent polyubiquitination occurs via proteasomal degradation. There is a controversy on whether autophagy also turns over diffuse polyubiquitinated proteins upon their delivery by p62/sqstm1. Here we examined the dynamics of each of these pathways on the turnover of ubiquitinated proteins by comparing the effect of pharmacologic inhibitors of each pathway and genetic inhibition of autophagy on the accumulation of ubiquitinated proteins as well as on p62/sqstm1.

Initially, we compared the effect of the proteasome inhibitor epoxomicin with three autophagy inhibitors:

chloroquine, ammonium chloride and bafilomycin A1. Chloroquine and ammonium chloride are weak bases that become protonated and accumulate inside lysosomes raising the pH thus inactivating lysosomal hydrolases (31). The change in pH also causes accumulation of autophagosomes in cells by inhibiting the fusion of autophagosomes with lysosomes (32). Chloroquine is a more effective inhibitor than ammonium chloride thus requiring a 100-fold lower concentration (33). In some studies, concentrations of ammonium chloride as high as 100mM are required to observe LC3-II accumulation (34). It is thus not surprising that we did not observe LC3-II accumulation with 10mM ammonium chloride. Bafilomycin A1 is a potent and specific inhibitor of vacuolar H+-ATPase and prevents maturation of autophagic vacuoles by inhibiting fusion between autophagosomes and lysosomes (35). The increase in ubiquitinated proteins in epoxomicin-treated SK-N-SH cells was considerably higher than in cells treated with chloroquine. The same trend was observed in epoxomicin- and chloroquine-treated SK-N-SH cells maintained under serum or serum-free conditions, in rat primary cortical neuronal cultures, as well as in WT and Atg5-/- MEFs, the latter exhibiting genetically inhibited autophagy. That autophagy was impaired by chloroquine was confirmed by the high LC3-II levels

observed in all chloroquine-treated cells except in Atg5-/- MEFs, which are autophagy deficient and thus LC3-II was not detected. K63-linked ubiquitination was suggested to selectively facilitate clearance of ubiquitinated proteins by autophagy (26). The low levels of ubiquitinated proteins detected upon chloroquine treatment were not caused by a lack of reactivity of the DAKO antibody used in our studies with K63-ubiquitinated proteins. We demonstrate that the antibody has a similar affinity for K48- and K63-ubiquitinated substrates. Together these results clearly indicate that autophagy impairment *per se* fails to cause accumulation of ubiquitinated proteins except in cells treated with chloroquine, where ubiquitinated protein amounts are low compared to epoxomicin.

We considered if the limited accumulation of ubiquitinated proteins observed under chloroquine-treatment could be due to proteasomal inhibition, so we compared the effect of chloroquine and epoxomicin on proteasome activity. The lysosomotropic agent inhibited 26S and 20S proteasomal activities assessed in total lysates as well as by glycerol density fractionation and the in-gel assay, albeit to a lesser extent than epoxomicin. The decrease in 26S proteasome activity was partially due to its disassembly and was observed in SK-N-SH cells as well as in

WT and Atg5-/- MEFs. No overall changes in the levels of individual proteasome subunits were observed upon chloroquine treatment. Another study with human neuroblastoma cells confirmed that chloroquine inhibited proteasome activity measured in total cell lysates (23). Notably, chloroquine was shown to inhibit 20S proteasomes by binding to regions between the α and β subunits 20Å away from the proteolytic sites (36), supporting the view that chloroquine belongs to a new class of proteasome inhibitors that do not bind to its active sites.

It is likely that an ~50% proteasome inhibition as observed upon chloroquine treatment, only causes a weak accumulation of ubiquitinated proteins because under homeostatic conditions there is a surplus of proteasome activity in cells. Only when most of the proteasome activity is inhibited, as in the case of epoxomicin treatment, the accumulation of ubiquitinated proteins is detectable. A similar phenomenon was observed in yeast and flies. Yeast cells continue to grow when 70-80% of their proteasome activity is inhibited by peptide aldehydes or β-lactone (37) confirming that under homeostatic conditions the capacity of the proteasome in yeast exceeds the required activity. Thus, a 20-30% proteasome capacity is sufficient for yeast cell survival and growth under

homeostatic conditions. Similarly, feeding young flies sublethal concentrations of the proteasome inhibitor PSI had no apparent effect on survival or the levels of polyubiquitinated proteins (38). On the other hand, in old flies the disassembled state of the 26S proteasome severely diminishes its activity, therefore rendering old flies exceptionally sensitive to proteasome inhibitors.

Besides proteasomal dysfunction observed with the pharmacological inhibition of autophagy, proteasome impairment was also detected in autophagy deficient transgenic mice resulting from genetically inactivated autophagy. Accordingly, reduced proteasome activity was observed in brain cortical extracts of cathepsin D deficient mice (39). However, in transgenic mice lacking Atg7 (Atg7-/-) exclusively in neurons no apparent proteasomal dysfunction was detected in the brain (4). Both studies report ubiquitin-positive neuronal inclusions despite the observed incidence (39) or absence (4) of proteasome impairment. The discrepancy in the outcome of proteasome activity reported in these two studies could be due to different genetic approaches. While in the first study cathepsin D deficiency was targeted to all cells (40), in the second study atg7 knockout was specific to neurons in the CNS (4). In the latter study, it is possible

that proteasome activity was impaired in the neurons exhibiting ubiquitin-positive neuronal inclusions but not in the ubiquitin-negative neurons or glia. Since total brain proteasome activity was assessed in the Atg7-/- mice, the observed rise in glia numbers could cause a parallel rise in proteasome activity thus masking any potential decrease occurring in neurons with high levels of ubiquitinated proteins.

In conclusion, it is clear that the limited accumulation of ubiquitinated proteins observed under autophagy impairment results from weak proteasome inhibition by the lysosomotropic agents themselves or by proteasome overload. A recent study demonstrated that genetically inactivated autophagy compromises the UPP, increases the levels of proteasome substrates as well as the accumulation of aggregation-prone proteins (41). Thus caution needs to be exercised when using autophagy-incompetent cells to conclude that autophagy acts continuously in a housekeeping role to dispose of diffuse ubiquitinated proteins, because in these cells the turnover of UPP substrates is compromised (41). Recent studies demonstrated that aggresomes containing polyglutamine aggregates associate with UPP components and cytoplasmic chaperones but were never co-localized with autophagosomes or lysosomes,

further supporting proteasomal-mediated turnover of these proteins (42).

Epoxomicin and chloroquine affected MEFs differently from SK-N-SH cells. Both drugs inhibited proteasome activity assessed by the in-gel assay in MEFs and SK-N-SH cells. Chloroquine impaired autophagy in WT MEFs as indicated by LC3-II accumulation; the latter was not detected in Atg5-/- MEFs confirming that they are deficient in autophagy. However, hydrolysis of the chymotrypsin-like substrate Suc-LLVY-AMC by total MEF lysates was insensitive to chloroquine inhibition and at least four-fold less sensitive to epoxomicin inhibition, when compared to SK-N-SH cells. Since Suc-LLVY-AMC is cleaved not only by the proteasome (24) but also by other chymotrypsin-like proteases as well as by calpains (25), we postulate that MEFs have enzymes that cleave this substrate and that are insensitive to epoxomicin and/or chloroquine. These enzymes are present in WT as well as in Atg5-/- MEFs. Notably, a recent paper identified an Atg5/Atg7-independent autophagy in MEFs (43;44). This alternate form of autophagy was detected in several types of mammalian embryonic organs such as brain, liver and heart. It plays a role in mitochondrial clearing during erythrocyte maturation and is

inhibited by bafilomycin A1, but its sensitivity to chloroquine was not tested.

The 26S proteasome itself has an inherent capacity to bind polyubiquitinated proteins through at least two of its subunits, i.e. Rpn 10/S5a (45) and Rpn 13 (46). In addition, several protein families recognize and bind polyubiquitinated proteins and proteasomes, functioning as shuttling factors. Together the proteasome receptors and the shuttling factors seem to function as ubiquitin chain-length sensors that shape the ubiquitin signal in terms of chain length and linkage type (47). P62/sqstm1 could be one of these shuttling factors. We demonstrate that under proteasome inhibition there is a robust increase in p62/sqstm1 levels in comparison to autophagy inhibition, which raises p62/sqstm1 levels to a much lower level. Furthermore, proteasome inhibition in cells leads to a clear association between endogenous soluble p62/sqstm1 and proteasomes, established by three different methods (glycerol gradient fractionation, in-gel assay and proximity association assay). We showed this association without having to overexpress any proteins, a process that perturbs the natural interactome balance (48). P62/sqstm1 was also found with inactive proteasomes and LC3-II in protein aggregates upon proteasome or autophagy inhibition.

P62/sqstm1 is a scaffold protein that encodes multiple binding domains for proteins involved in the UPP, autophagy, signaling such as through NFκB, extrinsic apoptotic pathway and tumorigenesis [reviewed in (49)]. By mediating/interacting with so many different pathways, p62/sqstm1 seems to play a critical role in cellular life and death decisions.

Our studies do not rule out that chaperone-mediated autophagy (CMA) is activated when proteasomes are blocked. CMA is independent of vesicle formation or membrane invagination, thus does not require LC3-II, and also has its own delivery system not mediated by p62/sqstm1 [reviewed in (50;51)]. CMA clients are directly targeted to lysosomes for degradation by the chaperone Hsc70, which recognizes the motif KFERQ present in approximately 30% of cytoplasmic proteins. The relation between CMA activation and proteasome impairment remains to be established.

In conclusion, our studies convincingly demonstrate that autophagy impairment does not cause accumulation of ubiquitinated proteins unless the proteasome is affected. Low levels of ubiquitinated proteins detected upon autophagy impairment result from weak proteasome inhibition by lysosomotropic agents or by impaired flux through the proteasome due to substrate excess. Finally, great care

needs to be exercised when attempting to infer that p62/sqstm1 is a selective autophagy cargo receptor because it interacts with many client molecules including the proteasome thus playing a function in a variety of pathways including the UPP and autophagy. The roles of p62/sqstm1 in cellular function require further investigation.

CHAPTER III

cAMP ENHANCES 26S PROTEASOME ACTIVITY, P62/SEQUESTOSOME1 LEVELS AND SURVIVAL OF RAT SPINAL CORD NEURONAL CULTURES

Natura Myeku and Maria E. Figueiredo-Pereira

Department of Biological Sciences,

Hunter College of City University of New York,

New York, New York 10065

Submitted to Molecular Neurodegeneration, a BioMed Central Journal, January 2011

3.1. ABSTRACT

Two pathologic features of motor neurons in patients with amyotrophic lateral sclerosis (ALS) are proteasome impairment and accumulation/aggregation of ubiquitinated proteins in abnormal inclusions. In addition, neuroinflammation is associated with the death of motor neurons in ALS. There is a notion that the abnormal protein aggregates play an important role in triggering inflammation in ALS. We reasoned that enhancing proteasome activity in neurons would be of the utmost therapeutic value to avoid/attenuate the accumulation/aggregation of ubiquitinated proteins and mitigate chronic ALS neuroinflammation.

As far as we know this is the first demonstration that 26S proteasome activity as well as the levels of p62/sequestosome1 (p62/sqstm1), a shuttling protein for polyubiquitinated proteins, are stimulated in primary neuronal cell cultures by cAMP. We report that incubating rat E18 spinal cord neuronal cultures with dibutyryl-cAMP (db-cAMP) increases 26S proteasome activity by ~two-fold and p62/sqstm1 levels by ~four-fold. We tested if db-cAMP prevented proteasome impairment caused by treatment with the bioactive and neurotoxic product of inflammation prostaglandin J2 (PGJ2). Prostaglandins of the J2 series

are particularly relevant to ALS degeneration because their levels are higher in spinal cord motor neurons of sporadic ALS patients than in control individuals. Therefore it is likely that PGJ2 levels rise considerably under pathological conditions associated with ALS-neuroinflammation. Pre-treatment with db-cAMP prevented to a certain extent the significant decline in proteasome activity induced by PGJ2. However, proteasome activity in the neuronal cultures was still lower upon db-cAMP/PGJ2 treatment than under control conditions. The failure of total protection by db-cAMP was attributed to the down-regulating effect of PGJ2 on proteasome subunits (Rpt6 and β5) and on the catalytic subunit of protein kinase A (PKA-subCα). This reduction in PKA-subCα levels significantly diminished db-cAMP activation of PKA, the latter known to enhance proteasome activity. Notably, db-cAMP mitigated PGJ2-induced neurotoxicity and loss of cell viability.

These studies suggest that optimizing cAMP-enhancement of proteasome activity and p62/sqstm1 levels could offer an effective therapeutic approach to prevent neurotoxicity linked to proteasome impairment and inflammation in ALS-neurodegeneration.

3.2. INTRODUCTION

The ubiquitin/proteasome pathway (UPP) is a major intracellular pathway that degrades proteins in a highly complex and tightly regulated manner (reviewed in (50; 147)). The UPP plays a critical role in cellular processes including oxidative stress, inflammation and apoptosis, all of which are related to abnormal protein deposition and cell death in neurodegeneration (reviewed in (16)). UPP impairment is implicated in the pathogenesis of many neurodegenerative disorders, including amyotrophic lateral sclerosis (ALS), characterized by abnormal neuronal inclusions containing ubiquitinated proteins (reviewed in (7)). One of the factors associated with the inability to eliminate ubiquitinated proteins in these disorders, is proteasome impairment caused by aging, mitochondrial dysfunction, oxidative stress, inflammation and other conditions (reviewed in (221)). Compared to astrocytes, neurons are particularly sensitive to the toxic effects of proteasome inhibition (32). Enhancing proteasome activity in neurons is thus of therapeutic interest to avoid/attenuate the accumulation/aggregation of ubiquitinated proteins common to most chronic neurodegenerative disorders (reviewed in (76)).

In ALS, two of the pathological features in motor neurons are proteasome impairment and protein aggregation (reviewed in (29)). Proteasome impairment was found to occur in motor neurons of transgenic mouse models suggesting that it contributes to disease progression (27). Furthermore, a well defined correlation was identified between the speed of protein aggregation and the rate of disease progression in ALS patients (171). The accumulation/aggregation of ubiquitinated proteins observed in ALS could be one of the factors that triggers neuroinflammation (reviewed in (49)). Inflammation is associated with the death of motor neurons in ALS. For example, microglia activation was observed in the ALS affected areas and increased expression of pro-inflammatory mediators is an early event in ALS mouse models (reviewed in (24; 48)). Cyclooxygenase-2 (COX-2), an enzyme that is involved in inflammatory cascades as well as in normal neuronal activities, is significantly elevated in the spinal cord of ALS patients and ALS mouse models (4; 88). Cyclooxygenase inhibition with non-steroidal anti-inflammatory drugs preserves motor neurons in ALS transgenic mouse models (36; 87; 169). Although these studies support the notion that COX-2 is involved in ALS

its contribution to the neurodegenerative process remains poorly defined.

To develop therapeutic strategies that more effectively cope with the role of COX-2 in ALS neuronal pathology it is essential to identify mechanisms induced by COX-2 products. Cyclooxygenases produce an array of prostaglandins (121). Physiological concentrations of prostaglandins in body fluids are in the pico-nanomolar range (45), but their levels rise considerably under pathological conditions such as hyperthermia, infection and inflammation, reaching the micromolar range at the site of damage (47; 73). Prostaglandins E2 (PGE2) and D2 (PGD2) are abundantly produced in the CNS (35; 154). Recent data indicate that PGE2 is mainly produced in the spinal cord by COX-1, and that COX-1 ablation fails to attenuate neurodegeneration in an ALS mouse model (5). PGD2, the major CNS prostaglandin (1; 153; 173), is unstable and is metabolized by non-enzymatic dehydration into bioactive prostaglandin J2 (PGJ2) and its metabolites, Δ12-PGJ2 and 15d-PGJ2 (198; 206; 217). Notably, the levels of 15d-PGJ2, were found to be elevated in spinal cord motor neurons of ALS patients (103; 246). It is thus likely that PGJ2 levels rise considerably under pathological conditions associated with ALS-neuroinflammation. The effects of PGJ2 on the UPP and

protein aggregation are thus particularly relevant to ALS neurodegeneration and neuroinflammation. PGJ2 impairs proteasome activity (78; 149), deubiquitinating enzymes (111; 142) and induces accumulation (102) and aggregation (112) of ubiquitinated proteins in neuronal cells. Moreover, we established that prostaglandins of the J2 series were the most neurotoxic of the prostanoids that we tested, which also included PGA1, D2 and E2 (110).

We reasoned that enhancing the activity of the 26S proteasome and optimizing the delivery of its ubiquitinated substrates to accelerate their degradation would be an ideal strategy to improve the removal of ubiquitinated proteins and prevent their aggregation. In the studies described herein, we discovered that the activity of the 26S proteasome and the levels of a ubiquitin-conjugate shuttling protein, p62/sequestosome1 (p62/sqstm1), are both significantly enhanced by dibutyryl-cAMP (db-cAMP) in rat spinal cord neuronal cultures. The db-cAMP effect was mimicked by treatment with forskolin in conjunction with rolipram. Db-cAMP-treatment also diminished neurotoxicity and the reduction in cell viability induced by PGJ2, but not to a full extent. We conclude that the action of db-cAMP in stimulating 26S proteasome activity and up-regulating p62/sqstm1 is a reason for further evaluation of

the cAMP/PKA signaling pathway as a beneficial therapeutic approach in neurodegenerative diseases associated with protein aggregation.

3.3. MATERIALS AND METHODS

3.3.1. Materials - Prostaglandin J2 and Rolipram were from Cayman Chemical (Ann Arbor, MI, USA). Adenosine 3′, 5′-cyclic monophosphate dibutyryl sodium salt (db-cAMP) was from Calbiochem/EMD Bioscience (Gibbstown, NJ). Forskolin and 3-(4,5-Dimethylthiazol-2-yl)-2,5-diphenyl-tetrazolium bromide (MTT) were from Sigma-Aldrich (St. Louis, MO). The substrate Suc-LLVY-AMC was from BACHEM Bioscience Inc. (King of Prussia, PA). Antibodies: rabbit polyclonal anti-ubiquitinated proteins (1:1,500, cat# Z0458) from Dako North America (Carpinteria, CA); mouse monoclonal anti-Rpt6/S8 (1:1,000, cat# PW9265) and rabbit polyclonal anti-β5 (1:1,000, cat# PW8895) were from BIOMOL (Plymouth Meeting, PA); rabbit polyclonal anti-p62/sqstm1 (1:1,000 cat# PM045) was from MBL International Corp. (Woburn, MA); mouse monoclonal anti-neurofilament H (non-phosphorylated; SMI32) (1:1,000, cat# SMI32R) and anti β-tubulin III (1:5,000, cat# MMS-435P) were from Covance (Princeton, New Jersey); rabbit polyclonal anti-PKA C-α (1:1,000, cat# 4782) was from Cell Signaling Technology (Danvers, MA). The

respective secondary antibodies with HRP conjugate (1:10,000) were from Bio-Rad Laboratories (Hercules, CA). Goat anti-mouse and anti-rabbit Alexa-488 and Alexa-568 coupled secondary antibodies for immunofluorescence were from Invitrogen (1:500, cat# A11029 and A11036, respectively).

3.3.2. Cell cultures – Dissociated cultures of Sprague Dawley rat embryonic (E18) spinal cords were prepared and maintained for 48h as described in (72) with some modifications. The isolated spinal cords free of meninges and dorsal root ganglia were digested with papain (2 mg/ml from Worthington Biochemical Corp., Lakewood, NJ) in Hibernate E without calcium (BrainBits LLC., Springfield, IL) at 37°C for 30min in a humidified atmosphere containing 5% CO_2. After removal of the enzymatic solution the tissues were gently dissociated in NbActiv4 media (BrainBits LLC., Springfield, IL) using a one ml pipettor with a sterile blue plastic tip. The dissociated tissues were centrifuged at 300Xg for 5min. The pellet was resuspended in NBActiv4 media without antibiotics and plated on Lab-Tek™ II - CC2™ chamber slides (Nalgene Nunc International, Rochester, NY) pre-coated with 100µg/µL poly-D-lysine (Sigma-Aldrich). Cultures were incubated at 37°C in a humidified atmosphere containing 5% CO_2.

3.3.3. Organotypic spinal cord slices – The organotypic slices were prepared from Sprague Dawley rat embryonic (E18) spinal cords and maintained as described in (80) with some modifications. The lumbar area of the spinal cord was isolated and sliced into 350µm slices with a McIlwain Tissue Chopper (Bannockburn, IL). Slices were carefully placed in Millicell CM semi permeable culture inserts (Millipore, Billerica, MA) at a density of 4-5 slices per well. The inserts were placed in 35mm cell culture dishes containing 1.2ml of NbActiv4 media and incubated at 37°C in a humidified atmosphere containing 5% CO_2. Slices were allowed to recover for 7 days prior to treatment for 24h with the indicated drugs. Media without antibiotic was changed twice a week.

3.3.4. Culture Treatments - Both cultures (dissociated cells and organotypic slices) were treated for 24h with DMSO or water (control) or with different drugs: PGJ2, forskolin and rolipram in DMSO, or db-cAMP in ultra pure filtered water added directly to the NbActiv4 media. The final DMSO concentration in the medium was 0.5%. At the end of the incubation, all cultures were washed twice with phosphate buffered saline (PBS) and processed for the different assays as described below.

3.3.5. Cell Viability Assay - Cells were plated at a density of $2.5X10^5$ cells per well on Lab-Tek™ II - CC2™ 4-well chamber slides under various conditions for 24h. Cell viability was assessed with the 3-(4,5-dimethylthiazol-2-yl)-2,5-diphenyl tetrazolium bromide (MTT) assay as described in [84]. This assay assesses mitochondrial viability.

3.3.6. Cell Toxicity Assay - Cells were plated at a density of $2.5X10^5$ cells per well on Lab-Tek™ II - CC2™ 4-well chamber slides under various conditions for 24h. Cell toxicity was assessed with a bioluminescent cytotoxicity assay using the aCella-TOX kit following manufacturer's specifications (Cell Technology Inc. Mountain View, CA). This assay assesses cell toxicity based on the release of GAPDH from dying cells.

3.3.7. Western Blotting – Western blot analysis was carried out following SDS-PAGE. Cells were plated at a density of $1.5X10^6$ cells per well on Lab-Tek™ II - CC2™ 1-well chamber slides. After treatment, cells were rinsed twice with PBS and harvested by gently scraping into ice-cold lysis buffer [20mM Tris-HCl, pH 7.5, 137mM NaCl, 1mM EGTA, 2.5mM $Na_4P_2O_7$,1mM β-glycerophosphate, 50mM NaF, 1mM phenylmethylsulfonyl fluoride, 1% NP40, 1mM Na_3VO_4, 1% glycerol and protease inhibitor cocktail (Sigma-Aldrich St

Louis, MO)]. Following lysis (30min) and centrifugation (14,000xg for 10min) at 4°C the protein concentration of the cleared supernatants was determined (BCA kit, Pierce, Rockf., IL). Normalized samples were boiled for 5min in Laemmli buffer and loaded onto 10% gels (30-40µg of protein/lane). Following electrophoresis, proteins were transferred onto an Immobilon-P membrane (Millipore, Bedford, MA, USA). The membrane was probed with the respective antibodies and antigens were visualized by a standard chemiluminescent horseradish peroxidase method with the ECL reagent. Semi-quantitative analysis of protein detection was done by image analysis with the ImageJ program (Rasband, W.S., ImageJ,U.S. NIH, Maryland, http://rsb.info.nih.gov/ij/, 1997-2006). Relative intensity (no units) is the ratio between the value for each protein and the value for βIII-tubulin (loading control)

3.3.8. In-Gel Proteasome Activity and Detection - Cells were plated at a density of $1.5X10^6$ cells per well on Lab-Tek™ II - CC2™ 1-well chamber slides. Upon treatment with vehicle (control, DMSO or water) or the respective drugs, cells were washed twice with PBS and harvested for the in-gel assay as described in (148) with 80µg protein/lane loaded for proteasome activity and 40µg protein/lane loaded for western blotting. The native gels were run at 125V for

90min. The in-gel proteasome activity was detected by incubating the native gel on a rocker for 10min at 37°C with 15ml of 400µM Suc-LLVY-AMC followed by exposure to UV light (360nm) and photographed with a NIKON Cool Pix 8700 camera with a 3-4219 fluorescent green filter (Peca Products, Inc). Proteins on the native gels were transferred (110mA) for 2h onto PVDF membranes. Immunoblotting was then carried-out sequentially for detection of the 20S and 26S proteasomes with anti-β5 and anti-Rpt6/S8 subunit antibodies. The anti-β5 antibody reacts with a core particle subunit, therefore detects both the 26S and 20S proteasomes. The anti-Rpt6/S8 antibody reacts with a regulatory particle subunit thus only detecting 26S proteasomes. Antigens were visualized by a chemiluminescent horseradish peroxidase method with the ECL reagent. For loading control, aliquots of the samples were also boiled for 5min in Laemmli buffer and loaded onto 10% gels (40µg of protein/lane) for immunoblotting with anti-βIII-tubulin.

3.3.9. PKA assay - PKA activity was determined with a nonradioactive assay kit (Assay Designs Ann Arbor, MI). Cells were plated at a density of $1.5X10^6$ on Lab-Tek™ II - CC2™ 1-well chamber slides. After treatment cells were rinsed twice with PBS and harvested as for western blotting without boiling. PKA activity was determined with 0.15µg of

protein per well following manufacturer's specifications. Absorbance was measured at 450nm with a PowerWave HT Spectrophotometer. Relative kinase activity for each sample was determined according to the kit instructions.

3.3.10. Immunofluorescence - Cells were plated at a density of $1.5X10^5$ cells per well on Lab-Tek™ II - CC2™ 4-well chamber slides. Spinal cord slices were grown on Millicell CM semi permeable culture inserts. After treatment, cell cultures and slices were rinsed with PBS, fixed for 30min with 4% paraformaldehyde in PBS, blocked/permeabilized with 2.5% BSA, 5% normal goat serum, and 0.3% Triton X-100 for 1h in PBS and incubated with the primary antibodies listed in each figure. Slides with dissociated cells were mounted with ProLong® Gold antifade mounting reagent with DAPI (Invitrogen). Cell staining was visualized with an UltraViewVoX Spinning Disk Confocal microscope (Perkin Elmer, Waltham, MA). Organotypic slices were carefully placed on glass slides and mounted with Vectashield medium (Vector Laboratories, Inc., Burlingame, CA). Cell staining was visualized with an Axio Imager M2 microscope (Carl Zeiss Micro Imaging, Inc. Thornwood, NY).

3.3.11. Quantitative Reverse Transcription-PCR Analysis (qRT-PCR) - Total RNA was isolated with the RNAeasy Mini Kit from Qiagen, Inc. (Valencia, CA) according to

manufacturer's specifications. RNA was evaluated for quantity and integrity by taking OD measurements at 260/280nm and agarose gel electrophoresis. 10ng of RNA were reverse transcribed using the DyNAmo™ cDNA Synthesis kit (Finnzymes Inc. Woburn, MA). PCR primers were purchased from Applied Biosystems (Foster City, CA). The PCR primers to amplify the following rat cDNAs were: for the proteasome subunits Rpt6 [PSMC5 (Rn00579821_m1)] and β5 [PSMB5 (Rn01488741_m1)], for PKA subunit Cα [PRKACA (Rn01432302_m1)], for p62/sqstm1 [SQSTM1 (Rn00709977_m1)], for ubiquitin B [UBB (Rn03062801_gH)] and ubiquitin C [UBC (Rn01789812_g1)], and for GAPDH [GAPDH (Rn01775763_g1)] which was used to normalize. Quantitative real-time PCR was carried out in 384-well plates containing in each well 5µl of TaqMan Universal PCR Master Mix (Applied Biosystems, Foster City, CA), 0.5µl of each primer, 2.5µl of RNase-free water and 2µl of the reverse transcribed reaction in a LightCycler 480 ® for Real-Time PCR System (Roche Diagnostics Corp., Indianapolis, IN). As suggested by the manufacturer, thermal cycling conditions comprised of an initial denaturation step of 10min at 95°C followed by 45 cycles of: 10sec at 95°C, 30sec 60°C and a cooling step of 10sec at 40°C. Cycle threshold (C_T) values for each gene in each sample were obtained using a LightCycler 480 Software.

Differences in C_T values between the genes of interest and the reference gene (ΔC_T) were calculated as follows: $2^{-[\Delta Ct\ (treated) - \Delta Ct\ (DMSO)]}$, where $\Delta C_T = C_T$ (gene of interest) - C_T (*gapdh*).

3.3.12. Statistical analysis - Statistical significance was estimated using one-way ANOVA (Tukey-Kramer multiple comparison test) with the Instat 2.0, Graphpad Software (San Diego, Ca).

3.4 RESULTS

3.4.1. Db-cAMP enhances the activity of 26S and 20S proteasomes in rat E18 spinal cord neuronal cultures – We previously demonstrated that 20S proteasome subunits are phosphorylated by a cAMP protein kinase (PKA) tightly associated with the complex (167). Furthermore, *in vitro* and *in vivo* studies with non-neuronal cells reported that forskolin (an activator of adenylate cyclase that increases cAMP and activates PKA) or isoproterenol (a β-adrenergic receptor agonist) treatment activates PKA which in turn modulates proteasome activity (9; 244; 248). To attempt to stimulate proteasome activity in rat E18 spinal cord neuronal cultures we treated them with $N^6,O^{2'}$-dibutyryl-cAMP (1mM, sodium salt, db-cAMP). Db-cAMP is a cell permeable analog of cAMP that is significantly less susceptible to

hydrolysis by phosphodiesterases (131). Proteasomal chymotrypsin-like activity was measured with the substrate Suc-LLVY-AMC by the in-gel native gel assay. In this assay the native gel is overlayed with the proteasome substrate and a signal is detected only where the substrate is cleaved by the proteasome. Free 19S particles are not detected, in accordance with a report in yeast showing that the 19S and its subcomplexes are undetectable as free particles (12). As seen in **Fig. 10A (*left panel*, quantified in Fig. 10B)**, treating cells with 1mM db-cAMP approximately doubled the activity of the 26S and 20S proteasomes compared to control conditions. Likewise, forskolin (100μM, Fk) in conjunction with rolipram (10μM, Rp), a cell permeable phosphodiesterase (PDE4) inhibitor, significantly enhanced proteasome activity.

To determine if the increase in proteasome activity was accompanied by an elevation in proteasome levels we performed western blot analyses with anti-Rpt6 and anti-β5 antibodies **(*middle and right panels*, Fig 10A, quantified in Fig. 10C)**. Rpt6/S8 is and ATPase subunit of the 19S regulatory particle and β5 is a subunit of the core (20S) proteasome particle thus a component of both 26S and 20S proteasomes. Treatment with db-cAMP, but not with forskolin/rolipram, increased 26S and 20S proteasome levels

although not to a statistical significant level except for two-capped 26S proteasomes *(p<0.05)*. Taken together these findings establish that the elevation in proteasome activity was due in part to a parallel elevation in proteasome levels.

3.4.2. **Db-cAMP does not prevent effictively the inhibitory effect of PGJ2 on the 26S proteasome –** We previously demonstrated that PGJ2 treatment of human neuroblastoma SK-N-SH cells inhibited 26S proteasome activity by causing its disassembly (151; 227). We now show that PGJ2 treatment of rat E18 spinal cord neuronal cultures significantly decreased *(p≤0.05)* the activity of both forms of the 26S proteasome (two cap and one cap), while the activity of the 20S proteasome was elevated *(p<0.001)* (**Fig 11 A, *left panel*, compare lanes 1 and 2, quantified in Fig. 11B)**. This result indicates that PGJ2-treatment triggered proteasome disassembly in the primary neuronal cultures as well.

Notably, db-cAMP mitigated to some extent the PGJ2 inhibitory effect. As seen in **Fig. 11A** (*left panel*, compare lanes 2 and 3), 26S proteasome activity is higher in cells treated with db-cAMP/PGJ2 than in cells treated with PGJ2 alone. Although 26S proteasome activity in cells treated

with db-cAMP/PGJ2 is still lower than in control, the difference is no longer statistically significant **(*p>0.05*, Fig. 11B)**. Forskolin/rolipram pre-treatment exacerbated the PGJ2 inhibitory effect on the 26S proteasome **(Fig. 11A, lane 4, quantified in Fig. 11B)**.

Western blot analyses of the native gels probed with anti-Rpt6 and anti-β5 antibodies revealed that, compared to control, the levels of the 26S proteasome were significantly decreased under all conditions that included PGJ2-treatment **(Fig. 11A, *middle and right panels*, compare lane 1 with lanes 2 – 4)**. The levels of the 20S proteasome were unaltered upon PGJ2-treatment but increased, albeit to non-significant levels, in cells treated with db-cAMP or forskolin/rolipram in conjunction with PGJ2. Overall, these results indicate that db-cAMP alone enhances proteasome activity but in combination with PGJ2 does not effectively prevent the decrease of proteasome activity in the primary neuronal cultures.

3.4.3. **PGJ2 prevents the increase in the levels of the Rpt6 proteasome subunit, p62/sequestosome1, PKA subunit Cα and PKA activity induced by db-cAMP** – We show that one of the mechanisms by which db-cAMP enhances proteasome activity is by modulating proteasome subunit levels.

Treatment of rat E18 spinal cord neuronal cultures with db-cAMP significantly increased the protein **(*p<0.05*, Fig. 12)** and mRNA levels **(*p<0.001*, Fig. 13)** of Rpt6, one of the subunits of the 19S regulatory particle. The levels of β5, another proteasome subunit that is a component of the 20S core particle, is elevated only at the mRNA level **(*p<0.001*, Fig. 13)**. Forskolin/rolipram treatment mimic the db-cAMP effect on proteasome subunits **(Fig. 12, protein and Fig. 13, mRNA)**.

The scaffold protein p62/sequestosome1 (p62/sqstm1) shuttles polyubiquitinated proteins to the proteasome for degradation and is being considered as a therapeutic target and/or biomarker for neurodegenerative diseases including ALS (192; 237). As far as we know this is the first report showing that both db-cAMP and forskolin/rolipram enhance the levels of p62/sqstm1 at the protein **(four-fold, *p<0.001*, Fig. 12)** and mRNA levels **(two-fold, *p<0.05*, Fig. 13)**. Rpt6 and p62/sqstm1 levels thus appear to be regulated by cAMP in a coordinated and parallel manner.

To address mechanisms by which PGJ2 abrogates the enhancement of proteasome activity induced by db-cAMP or forskolin/rolipram we investigated if there were changes in subunit levels. As shown in **Fig. 12** and **Fig. 13**, indeed PGJ2 abolished the db-cAMP or forskolin/rolipram-dependent

increase in Rpt6 levels. PGJ2 also cancelled the raise in p62/sqstm1 protein levels **(Fig. 12)**, although the mRNA levels remained elevated **(Fig. 13)**. Notably, PGJ2 caused a robust down-regulation of the catalytic subunit Cα of PKA at the protein **(Fig. 12)** and mRNA **(Fig. 13)** levels. This latter result translated into a significant decrease *(p<0.001)* in PKA activity when the rat primary neuronal cultures were treated with db-cAMP and PGJ2 compared to db-cAMP alone **(Fig. 14)**.

Overall these data indicate that depletion of proteasome and PKA subunits as well as the decline in PKA activity could all contribute to the reduction in proteasome activity observed upon PGJ2-treatment. According to *in vitro* and *in vivo* studies with non-neuronal cells it is well established that PKA-dependent phosphorylation of the proteasome enhances its activity (11; 243; 247).

3.4.4. **Db-cAMP mitigates moderatly the accumulation of ubiquitinated proteins induced by PGJ2** - Incubations with the product of inflammation PGJ2 increased the levels of endogenous ubiquitinated proteins in rat E18 spinal cord neuronal cultures to ~four-fold above control **(Fig. 15A, *top panel*, quantified in Fig. 15B)**. Additionaly, pre-incubations with db-cAMP or forskolin/rolipram moderately

prevented the PGJ2-dependent increase in ubiquitinated proteins **(Fig. 15A, *top panel*, quantified in Fig. 15B).** This is in accordance with our previous finding demonstrating that the inhibitory effect of PGJ2 treatment on proteasome activity is lessened to some extent by db-cAMP or forskolin/rolipram **(Fig. 11).**

We noticed that db-cAMP or forskolin/rolipram treatment alone elevated the intracellular levels of ubiquitinated proteins albeit to a non-significant level. This increase in ubiquitinated proteins was not due to proteasome impairment, as both treatments enhance proteasome activity. We reasoned that the levels of ubiquitin itself could be elevated. Indeed, db-cAMP increased the mRNA levels of the *ubB* gene *($p<0.05$)* which could contribute to the slight increase in ubiquitinated proteins upon treatment with the nucleotide **(Fig. 15C).** Furthermore, PGJ2 in combination with db-cAMP or forskolin/rolipram raised the mRNA levels of both stress inducible ubiquitin genes, i.e. *ubB* and *ubC* to highly significant levels *($p<0.001$).* Both genes *ubB* and *ubC* were shown to be essential for stress tolerance (181; 182).

3.4.5. Db-cAMP or forskolin/rolipram diminish PGJ2 cytotoxicity and its reduction of cell viability - We

previously showed that prostaglandins of the J2 series were the most neurotoxic of the prostanoids that we tested, which also included PGA1, D2 and E2 (113). We now demonstrate that pre-treatment with db-cAMP or forskolin/rolipram significantly mitigates the cytotoxic effect of PGJ2 assessed by the release of GAPDH from dying cells **(*p<0.001*, Fig. 16A)**. Furthermore, both pre-treatments significantly diminished the loss of viability of the primary neuronal cultures upon PGJ2 treatment **(*p≤0.05*, Fig. 16B)**.

3.4.6. Db-cAMP does not alter neurite fragmentation and aggregation of ubiquitinated proteins induced by PGJ2 – We analyzed the effects of PGJ2 on rat E18 spinal cord neuronal cultures and organotypic slices by immunofluorescence. In control (0.5% DMSO, 24h) or db-cAMP (1mM, 24h) treated neuronal cultures, staining for non-phosphorylated neurofilament heavy chain (*green*) displayed a uniform distribution extending from the nuclear envelope out to the periphery of the cell body and neurites **(Fig. 17A and B)**. Low levels of ubiquitinated proteins (*red*) were detected exhibiting a diffuse distribution throughout the cell body. The nucleus was stained blue with DAPI. Upon treatment with 20μM PGJ2 for 24h, neurofilament

immunoreactivity in the cell body was similar to control conditions but displayed a thin and fragmented distribution along the neurites **(Fig. 17C, *white arrows*)**. Ubiquitin immunoreactivity depicted small protein aggregates with a perinuclear distribution **(Fig.17C)**. Pre-treatment with db-cAMP failed to alter the PGJ2 effects on neurofilament and ubiquitinated protein distribution in the spinal cord neuronal cultures **(Fig. 17D)**.

The effects of PGJ2 on neurofilament distribution of motor neurons in lumbar spinal cord organotypic slices were similar to those observed for the neuronal cultures. In control and db-cAMP (1mM, 24h) treated slices, motor neurons displayed light neurofilament staining in the cell bodies and strong staining in the thick neurites **(Fig. 18A and B, higher magnification in E and F)**. Upon treatment with 20μM PGJ2 for 24h, neurofilament staining was redistributed, concentrating mostly in the cell body with thinning and fragmentation within the neurites **(Fig. 18C, higher magnification in G)**. The effect of PGJ2 on neurofilaments was not abolished by pre-treatment with db-cAMP **(Fig. 18D, higher magnification in H)**.

Overall, these data show that neurofilament and ubiquitinated protein distribution in spinal cord neurons is altered by PGJ2 and that pre-treatment with db-cAMP

failed to protect the neurons from the morphological damage induced by PGJ2.

3.5. DISCUSSION

We demonstrate here for the first time that in spinal cord neuronal cultures db-cAMP enhances the activity of 26S proteasomes. This effect was mimicked albeit to a lesser extent, by forskolin in conjunction with rolipram. The increase in proteasome activity induced by db-cAMP was accompanied by an elevation in the levels of the 26S proteasome holoenzyme. The 26S proteasome includes a 19S regulatory particle and a 20S core particle (review in (89)). At the subunit level, db-cAMP raised the protein levels of Rpt6, a subunit of the proteasome 19S regulatory particle, but not that of the β5 subunit, which is a constitutive component of the proteasome 20S core particle. These results suggest an independent regulation of proteasome 19S and 20S subunit pools in the primary neuronal cultures. A similar PKA-mediated enhancement in 26S proteasome activity involving differential regulation of proteasome 19S and 20S subunits was observed in isoproterenol-induced cardiac hyperthrophy in mice (38). In contrast, PKA-mediated stimulation of 26S proteasome activity did not include an increase in proteasome subunit

levels following the intracoronary administration of isoproterenol or forskolin or ischemic pre-conditioning in the canine heart (10). The reason for this discrepancy is not clear. The composition of the proteasome 19S particle was modified in mouse embryonic fibroblasts by environmental toxins such as arsenite (204) and the 20S core particle was altered in human cell lines by γ-interferon (71). These changes included upregulation of a 26S proteasome stabilizing factor known as AIRAP (arsenite-inducible RNA-associated protein) (203), and of three subunits of the 20S proteasome that harbor its active sites (70). In yeast, 26S proteasome composition can also be altered by different conditions. Accordingly, ubiquitin deficiency in yeast induces upregulation of the 19S-associated deubiquitinating enzyme Ubp6, thus sparing ubiquitin from proteasomal degradation (58). It is clear that to meet varying cellular requirements proteasome genes are subjected to a tight regulation that includes selective induction of individual subunits. Alternatively, a concerted regulation of all known proteasome genes occurs when the proteasome is inhibited (reviewed in (57)). In yeast, the transcription factor Rpn4 regulates the expression of all proteasome subunits through a negative feedback loop essential for cell survival under stress

conditions (225). The negative feedback includes induction of all proteasome genes by Rpn4 and its rapid degradation by the assembled proteasome. A homolog of Rpn4 has yet to be identified in mammalian cells, but proteasome subunit levels are also regulated by a negative feedback mechanism that allows for compensation upon proteasome inhibition (130). In mammalian cells, the transcription factors NF-κB (39) and Nrf2 (106) were implicated in regulating proteasome subunit expression although the details of this regulation are poorly defined.

Enhancement of 26S proteasome activity by treatment with db-cAMP observed in our studies with primary neuronal cultures or reported by others in myocardium upon PKA stimulation with different agents (8; 37), involves increases in the protein levels and/or phosphorylation of particular proteasome subunits, as well as an enrichment in the 26S assembled holoenzyme. The transcription factor(s) mediating the PKA-dependent upregulation of proteasome subunits have not been identified. Nevertheless, a recent study suggests that the cAMP-response element binding protein (CREB) could regulate the expression of some of the components of the UPP (195). Accordingly, transcriptional activation of CREB increased the rate of degradation of the protein regulator of calcinurin 1(RCNA1) and this increase

was blocked by proteasome inhibitors. RCNA1 is a protein that is highly expressed in the brains of Down Syndrome and Alzheimer's disease patients (44). It is tempting to speculate that CREB may function to directly or indirectly regulate proteasome subunit levels through a negative feedback loop in a manner similar to Rpn4 in yeast. CREB is degraded by the proteasome in a phosphorylation- and ubiquitination-dependent manner (30; 210). In addition to a putative transcriptional-mediated regulation of proteasome subunit levels by PKA, both *in vitro* and *in vivo* studies demonstrated that PKA regulates proteasome activity through the phosphorylation of proteasome regulatory and core subunits (119; 215; 242). The latter studies show that subunit phosphorylation can directly enhance proteasome activity and/or promote proteasome assembly.

Besides increasing protein levels of the proteasome subunit Rpt6, we established that db-cAMP treatment effectively raised the levels of p62/sqstm1 by approximately four-fold in the primary neuronal cultures. As far as we know this is the first report showing that p62/sqstm1 levels are regulated by cAMP. This is important because, due to oxidative damage to its promoter, there is an age-correlated decrease in p62/sqstm1 levels which is also apparent in neurodegenerative disorders such as

Alzheimer's and Parkinson's diseases (41). Furthermore, some bone disorders are caused by mutations in p62/sqstm1 (69; 108) and its absence induces neuronal cell death (145; 175). Elevating p62/sqstm1 levels could thus be of therapeutic value for both bone and neurodegenerative disorders. Recently, p62/sqstm1 was implicated in controlling excessive inflammatory responses in activated macrophages (90) and in protection from acoustic stress (208). The overall impact of p62/sqstm1 on cell survival is not surprising because it is a scaffold protein capable of integrating kinase-activated and ubiquitin-mediated survival signals (140).

Based on its capacity to enhance 26S proteasome activity and p62/sqstm1 levels we tested if db-cAMP protected the primary neuronal cultures against PGJ2-toxicity. Indeed, pre-treatment with db-cAMP mitigated PGJ2-toxicity although the protection was not complete. One of the reasons for this short fall could be that PGJ2 diminishes the db-cAMP-dependent increases in 26S proteasome activity as well as in proteasome subunit and p62/sqstm1 protein levels. Similarly, PGJ2-treatment caused down-regulation of the PKA catalytic subunit Cα accompanied by a reduction in PKA activity. We previously showed by temporal microarray analysis of neuronal cells that PGJ2 triggers a "repair"

response that includes decreased expression of cell growth/maintenance genes and increased expression of heat shock, protein folding, stress response, detoxification and cysteine metabolism genes (226). The former effect, i.e. down-regulation of cell growth/maintenance genes,could be responsible for the reduction in PKA subunits leading to lower PKA activity and in turn, to proteasome and p62/sqstm1 depletion in cells treated with a combination of db-cAMP and PGJ2 compared to db-cAMP alone. PGJ2-induced decreases in PKA levels and activity could contribute to PGJ2 toxicity, since PKA activation is generally associated with neuroprotection (reviewed in (200)).

As proteasome levels and activity are significant lower in cells treated with db-cAMP and PGJ2 than in cells treated with db-cAMP alone, it is not surprising that ubiquitinated protein conjugates are more abundant under the former conditions. Protein degradation by the UPP can be regulated by how much ubiquitin is available, as shown in human myeloma cell lines and NIH3T3 cells (122). In these cell lines, raising the expression of the ubiquitin gene *ubC* increased the rate of degradation of the oncogenic transcription factor c-MAF by the proteasome; the raise in *ubC* expression also elevated overall ubiquitinated protein conjugates and decreased cell viability. In our studies

with the primary neuronal cultures treated with db-cAMP and PGJ2, we observed up-regulation of two ubiquitin genes *ubB* and *ubC* accompanied by an elevation in Ub-conjugates as well as an increase in cytotoxicity and loss of cell viability, when compared to cells treated with db-cAMP alone. Furthermore, a two-fold increase in the expression of *ubC* was observed in the motor cortex and anterior horn region of cervical spinal cord of ALS patients compared to controls; ubiquitinated filamentous inclusions were also detected in the same neuronal populations of ALS patients (68). Ubiquitin homeostasis is tightly regulated and depletion of free ubiquitin by accumulation of ubiquitin-protein conjugates under stress conditions is compensated by *de novo* ubiquitin synthesis (55). The induction of polyubiquitin gene expression observed in our studies and in the brain and spinal cord of ALS patients indicates that the particular neuronal populations are under stress. Interestingly, in *Aplysia* the nervous tissue contains 20-times more free ubiquitin and six-times more proteasomes than muscles (25). If such differential distribution is conserved in mammalian tissues is not known; we speculate that this variation in tissue distribution of ubiquitin and proteasome levels could be a factor in the propensity of neurons to exhibit accumulation and aggregation of

ubiquitin conjugates under stress conditions involving proteasome impairment.

We detected protein aggregation upon PGJ2-treatment in the spinal cord neuronal cultures as well in neurons of spinal cord organotypic slices. Pre-treatment with db-cAMP did not prevent aggregate formation in both cultures, most likely because the oligonucleotide did not fully abolish the proteasome inhibition induced by PGJ2. One of the major pathological features in ALS is the presence of inclusion bodies with ubiquitin positive deposits in the lower motor neurons of the spinal cord and brainstem (124). Whether these protein deposits are pathogenic or represent a coping mechanism to prolong survival of the affected neurons is a hotly debated question. One important point is that these protein deposits are indicative of a disease process as they are not prevalent in healthy cells. A recent study that analyzed the aggregation propensity of different SOD1 mutations established that aggregation of the mutant protein is a key factor in ALS progression thus supporting the neurotoxic effect of protein aggregation (170). In addition, it was proposed that motor neurons in familial ALS are selectively vulnerable to neurodegeneration because they contain higher levels of SOD1 than the surrounding cells (224). This notion is based on the finding that

aggregation of proteins is directly proportional to their concentration (223). It is thus plausible that in familial as well as in sporadic ALS, there is a "toxic" gain of function for aberrant proteins manifested by the increase in their levels attributable, among other factors, to proteasome impairment (3; 56; 82).

Impairment of intracellular proteolytic systems such as the UPP and autophagy is a common feature of most chronic neurodegenerative disorders such as ALS, and is recognized as playing a major role in disease pathogenesis. While the major function of the UPP is to remove soluble, short lived, normal as well as misfolded proteins, autophagy substrates include long lived proteins as well as toxic oligomeric complexes and damaged organelles. From a therapeutic point of view, the UPP is an ideal early target to prevent/treat these chronic neurodegenerative disorders to avoid protein aggregation and the onset of cell death pathways leading to neuronal demise (15; 77). Our data presented here indicate that enhancement of 26S proteasome activity and up-regulation of p62/sqstm1 could be important neuroprotective events downstream of PKA activation. Our studies support the notion that enhancing proteasome and p62/sqstm1 function to effectively reduce aberrant protein levels by exploring the PKA pathway could offer a very

effective therapeutic strategy for ALS and other chronic neurodegenerative disorders associated with proteinaceous aggregates.

CHAPTER IV

PROTEASOME-CASPASE-CATHEPSIN SEQUENCE LEADING TO TAU PATHOLOGY INDUCED BY PROSTAGLANDIN J2 IN NEURONAL CELLS

Lisette T. Arnaud, Natura Myeku and Maria E. Figueiredo-Pereira

Department of Biological Sciences,

Hunter College of City University of New York

New York, NY 10065

FROM

Natura Myeku carried out Caspase 2 Activity Assay and Caspase 3 knockdown by siRNA

Journal of Neurochemistry 2009 vol 110(1) pages: 328–342

4.1. ABSTRACT

Neurofibrillary tangles (NFT) are a hallmark of Alzheimer's disease. The major neurofibrillary tangle component is tau that is truncated at Asp421 (Δtau), hyperphosphorylated and aggregates into insoluble paired helical filaments. Alzheimer's disease brains also exhibit signs of inflammation manifested by activated astrocytes and microglia, which produce cytotoxic agents among them prostaglandins. We show that prostaglandin (PG) J2, an endogenous product of inflammation, induces caspase-mediated cleavage of tau, generating Δtau, an aggregation prone form known to seed tau aggregation prior to neurofibrillary tangle formation. The initial event observed upon PGJ2-treatment of human neuroblastoma SK-N-SH cells was the build-up of ubiquitinated proteins indicating an early disruption of the ubiquitin-proteasome pathway. Apoptosis kicked in later, manifested by caspase activation and caspase-mediated cleavage of tau at Asp421 and poly (ADPribose) polymerase. Furthermore, cathepsin inhibition stabilized Δtau suggesting its lysosomal clearance. Upon PGJ2-treatment tau accumulated in a large perinuclear aggregate. In rat E18 cortical neuronal cultures PGJ2-treatment also generated Δtau detected in dystrophic neurites. Levels of Δtau were diminished by caspase 3

knockdown using siRNA. PGD2, the precursor of PGJ2, produced some Δtau. PGE2 generated none.

Our data suggest a potential sequence of events triggered by the neurotoxic product of inflammation PGJ2 leading to tau pathology. The accumulation of Ub proteins is an early response. If cells fail to overcome the toxic effects induced by PGJ2, including accumulation of Ub proteins, apoptosis kicks in triggering caspase activation and tau cleavage, the clearance of which by cathepsins could be compromised culminating in tau pathology. Our studies are the first to provide a mechanistic link between inflammation and tau pathology.

4.2. INTRODUCTION

Inflammation is implicated in Alzheimer's disease (AD) (126). A recent study with P301S mutant human tau transgenic mice established that hippocampal synaptic pathology and microgliosis could be the earliest manifestations of neurodegeneration related to tauopathies (239). Prominent microglial activation was shown to precede tangle formation and immunosuppression of young P301S Tg mice diminished tau pathology and increased lifespan. It was proposed that neuroinflammation is linked to early progression of tauopathies (238).

Activated microglia and astrocytes produce a variety of agents, among them prostaglandins (132). The major prostaglandin produced in the CNS is prostaglandin D2 (PGD2) (146);(152). PGD2 levels were found to be significantly increased in the frontal cortex of AD patients compared to age matched controls (79). PGD2 is produced by two distinct types of prostaglandin D2 synthases (PGDS): (1) the lipocalin enzyme (L-PGDS) and (2) the hematopoietic enzyme (H-PGDS) (218). In addition, PGD2 binds to G protein-coupled seven transmembrane receptors, DP1 and DP2 (219), which are robustly expressed in the hippocampus and cerebral cortex (116). In AD patients and in Tg2576 mice, a well established AD model, the levels of H-PGDS and DP1 were found to be selectively up-regulated in microglia and astrocytes within senile plaques (138). Based on these results it was suggested that PGD2 acts as a mediator of plaque associated inflammation in the AD brain (137). Similarly, L-PGDS which is one of the most abundant CSF proteins produced in the brain, was localized in amyloid plaques in both AD patients and Tg2576 mice (84). Secreted L-PGDS in the CSF has a dual function: it increases CSF-PGD2 levels (186) and also acts as a lipophilic-ligand carrier (220). L-PGDS was found to bind Aβ monomers and prevent Aβ aggregation, suggesting that L-PGDS

is a major Aβ chaperone and disruption of this function could be related to the onset and progression of AD (83).

PGD2 exerts both neuroprotective and neurotoxic effects through its binding to DP1 and DP2 receptors, respectively (115). PGD2 is very short lived and readily undergoes in vivo and in vitro non-enzymatic dehydration to generate the biologically active cyclopentenone J2 prostaglandins, which include PGJ2, Δ12-PGJ2 and 15-deoxy-Δ12,14-PGJ2 (15d-PGJ2) (197).

Unlike most other classes of prostaglandins, cyclopentenone prostaglandins like PGJ2 have a cyclopentenone ring with reactive α,β-unsaturated carbonyl groups that form covalent Michael adducts with nucleophiles such as free sulfhydryls in cysteine residues of glutathione and cellular proteins (207). Just like serine, threonine and tyrosine phosphorylation is crucial for various signal transduction pathways, it has become recently clear that a highly conserved redox reaction involving cysteine thiols in proteins provides post-translational means for regulating redox signaling (184). S-nitrosylation of cysteine thiols by nitric oxide was first discovered, followed by the more recently revealed S-alkylation by electrophiles (electron deficient carbon centers). Electrophile binding by endogenous metabolites

[such as PGJ2] is currently regarded as playing a crucial role in determining whether neurons will live or die (185).

We focused on PGJ2 because it is potently neurotoxic and a highly reactive product of inflammation. A recent review suggested that "formation of cyclopentenone eicosanoids [such as PGJ2] in the brain may represent a novel pathogenic mechanism that contributes to many neurodegenerative conditions" (144). Because of their high reactivity with thiol-containing intracellular compounds like glutathione or thiol-containing proteins via Michael addition, any attempt to measure PGJ2 levels in human tissues or fluids will be highly inaccurate and will not reflect its biological activity (216). Similar to PGJ2, nitric oxide has a half life of just a few seconds, and yet it is well accepted as a major signaling molecule in neurons and in the immune system (143). The same can be said for PGJ2, i.e. that it is a major signaling molecule/oxidative stress agent.

Here we address the effect of the highly reactive lipid electrophile PGJ2 on tau cleavage in human neuroblastoma SK-N-SH cells as well as in rat primary cortical cultures. Our results demonstrate that products of inflammation such as PGJ2 have a bifunctional effect on intracellular protein turnover. They impair the ubiquitin-proteasome pathway

leading to the abnormal build-up of ubiquitinated proteins and activate caspase-mediated proteolysis responsible for generating Δtau that could serve as a seed for cytotoxic protein aggregation. This dual effect on intracellular protein turnover, i.e. proteasome impairment and caspase activation, set off by the product of inflammation could be a major factor in the progression of AD neurodegeneration.

4.3. MATERIALS AND METHODS

4.3.1. Treatment with caspase 3 siRNA – We used a highly efficient non-toxic siRNA delivery approach in which the siRNAs are linked to the vector peptide Penetratin 1 (Pen 1) as described in (33). Rat E18 cortical neuronal cultures were plated at a density of $9X10^5$ cells in two ml of media per well in a six-well plate and cultured for three days. The cultures were then treated with 80nM of Pen1-caspase 3-siRNA or Pen1-scrambled-siRNA for 6h prior to treatment with vehicle (control) or PGJ2 for an additional 16h before harvesting. The siRNAs were a gift from Dr. C. Troy (Columbia University, NY, NY). The sequence for the siCasp3 was AGC CGA AAC UCU UCA UCA U (GenBank accession number BC038825, initiation at base 111, target bases 569-589) and for the scramble siRNA was CCU CAU GAA AGC ACU CAU U.

4.3.2 Western Blotting - Western blot analysis was

carried out by SDS-PAGE on 10% polyacrylamide gels. After treatment cells were rinsed twice with PBS and were harvested by gently scraping into ice-cold homogenization buffer [20mM Tris-HCl, pH 7.5, 137mM NaCl, 1mM EGTA, 2.5mM $Na_4P_2O_7$, 1mM b-glycerophosphate, 50mM NaF, 1mM PMSF, 1%NP40,1mM Na_3VO_4 , 1% glycerol and protease inhibitor cocktail (Sigma-Aldrich)]. Samples were boiled for 5m in Laemmli buffer and loaded onto gels (18-50mg of protein/lane). Following electrophoresis, proteins were transferred to an Immobilon-P membrane (Millipore, Bedford, MA). The membrane was probed with the respective antibodies and antigens were visualized by a standard chemiluminescent horseradish peroxidase method with the ECL reagent. As a control for protein loading the Western blots were probed for actin [mouse monoclonal anti-actin (1:2500, clone AC-20) from Sigma-Aldrich] or βIIItubulin. Semi-quantitative analysis of protein detection was done by image analysis with the ImageJ program (Rasband, W.S., ImageJ,U.S. NIH, Maryland, http://rsb.info.nih.gov/ij/, 1997-2006). Relative intensity (no units) is the ratio between the value for each protein and the value for actin.

4.3.3 Caspase activity assays – Caspase screening assays (for caspases 2, 3, 8 and 9) and caspase 3 assays were carried out with ApoAlert caspase kits (plates) from

ClonTech (Mountain View, CA). As ClonTech does not carry an assay exclusively for caspase 2, the time course for Caspase 2 activation was established with a caspase 2 kit from Biovision (Mountain View, CA) following manufacturer's specifications. Natura: you did the caspase 2 assay, correct?

4.4. RESULTS

4.4.1. PGJ2-treatment activates caspases which in turn mediate tau cleavage – Since Δtau coincided with the onset of apoptosis detected by PARP cleavage, we investigated if PGJ2 activates intracellular caspases. Initially, we run a caspase screening assay and established that treatment of SK-N-SH cells with 20mM PGJ2 for 16h, significantly (*p≤0.014*, T test) activated all caspases tested, i.e. initiator caspases (CASP2, CASP8 and CASP9) as well as the effector caspase 3, albeit different levels of activation were observed **(Fig. 19A)**. Not surprisingly, Caspase 3 showed the greatest activation (~20-fold) upon PGJ2-treatment, since it is an effector caspase. Following 8h of treatment with 20mM PGJ2, caspase 3 activity was significantly higher than in control (*p<0.001*, *asterisks*) and reached a peak (24-fold increase) by 16h post-treatment **(Fig. 19B)**. The peak in caspase 3 activity coincides with

the peak in PARP cleavage, a known substrate for this caspase, and the Δtau peak supporting the view that tau is also a substrate for caspase 3, as addressed in the discussion. Caspase 2 activation followed a time course similar to caspase 3, albeit its peak activation only reached a 2.5-fold increase observed after 16h of incubation with 20μM PGJ2 **(Fig. 19C).**

4.4.2. Caspase 3 knockdown by siRNA decreases the levels of PGJ2-induced tau cleavage. Caspase 3 siRNA (casp3 siRNA) clearly decreased the levels of pro-caspase 3 in both control and PGJ2-treated cells **(Fig. 20A, compare lanes 3 and 4 with 1 and 2).** In addition, casp3 siRNA caused a decline in the levels of Δtau as well as cleaved caspase 3 (ΔCasp3) as shown in Fig. **20B and C,** respectively. A scrambled siRNA failed to lower the levels of pro-caspase 3 and Δtau **(Fig. 20G and H)** as well as ΔCasp3 (not shown). These data provide strong support for a caspase 3 role in tau cleavage induced by PGJ2-treatment.

4.5. DISCUSSION

PGJ2 modulates tau cleavage (Asp421) through caspase mediated proteolysis - Our study provides the first evidence that a product of inflammation, PGJ2, modulates

tau cleavage at Asp421 through caspase-mediated proteolysis in neuronal cells. This is important in view of the fact that studies from other groups indicate that caspase-cleavage of tau at Asp421 is an early event in AD tangle pathology (179);(54). We also demonstrate for the first time that PGJ2-treatment induces tau cleavage at Asp421 (Δtau) which coincides with the onset of apoptosis indicated by caspase activation as well as by the concurrence of tau and PARP cleavage. Only caspase inhibitors attenuated Δtau levels induced by PGJ2-treatment. Caspase 3 knock down by siRNA also decreases Δtau levels in PGJ2-treated cells. Neither calpain nor cathepsin inhibitors diminished Δtau levels. Our data also indicate that Δtau must be cleared by lysosomal proteases, since cathepsin inhibition by pepstatin or by high concentrations (20μM) of caspase inhibitors that also affect cathepsins (188), caused an increase in Δtau levels induced by PGJ2-treatment. Together these studies provide a mechanistic link between a product of inflammation and tau pathology

CHAPTER V

MODELS AND CONCLUSIONS

MODEL 1

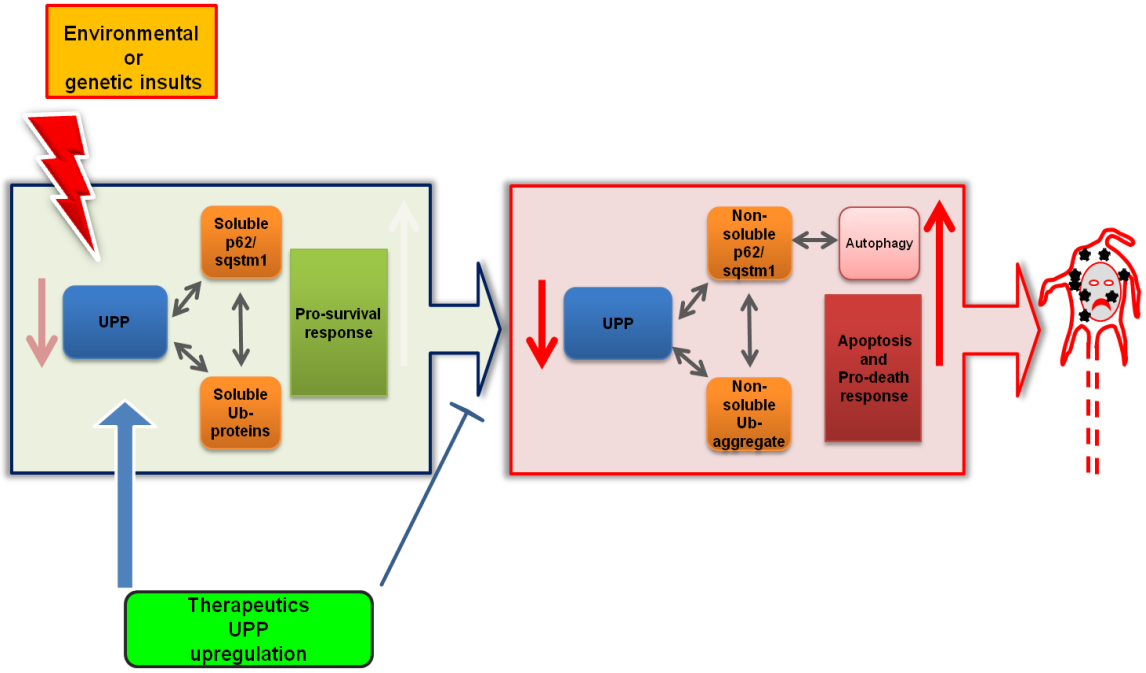
Environmental or genetic insults
UPP
Soluble p62/ sqstm1
Soluble Ub-proteins
Pro-survival response
UPP
Non-soluble p62/ sqstm1
Autophagy
Non-soluble Ub-aggregate
Apoptosis and Pro-death response
Therapeutics UPP upregulation

MODEL 2

A

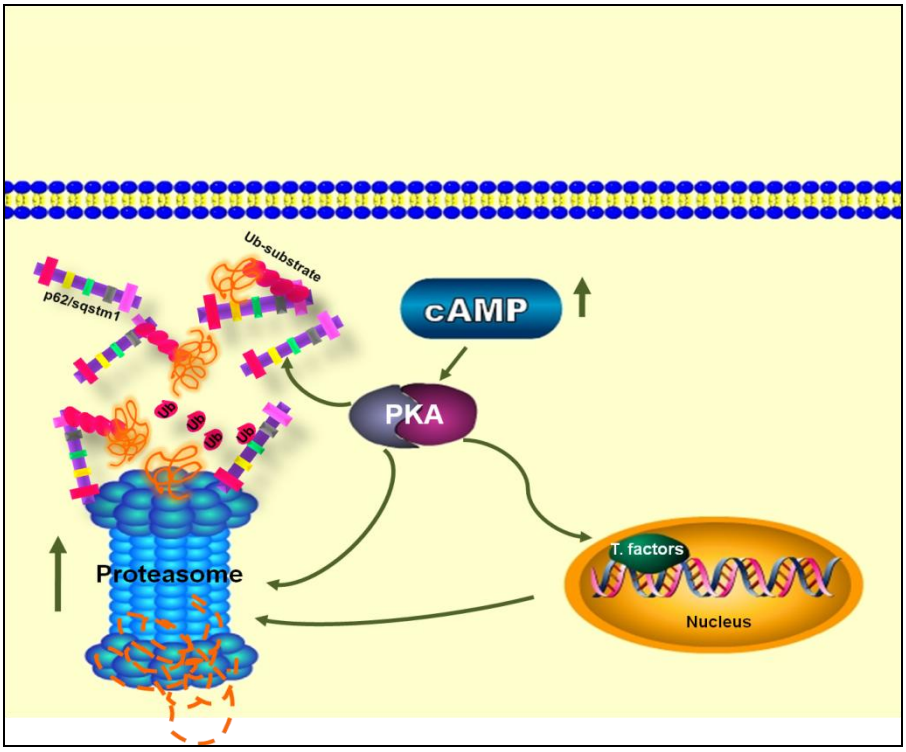
Ub-substrate
p62/sqstm1
cAMP
PKA
Ub
Ub
Ub
Ub
Proteasome
T. factors
Nucleus

B

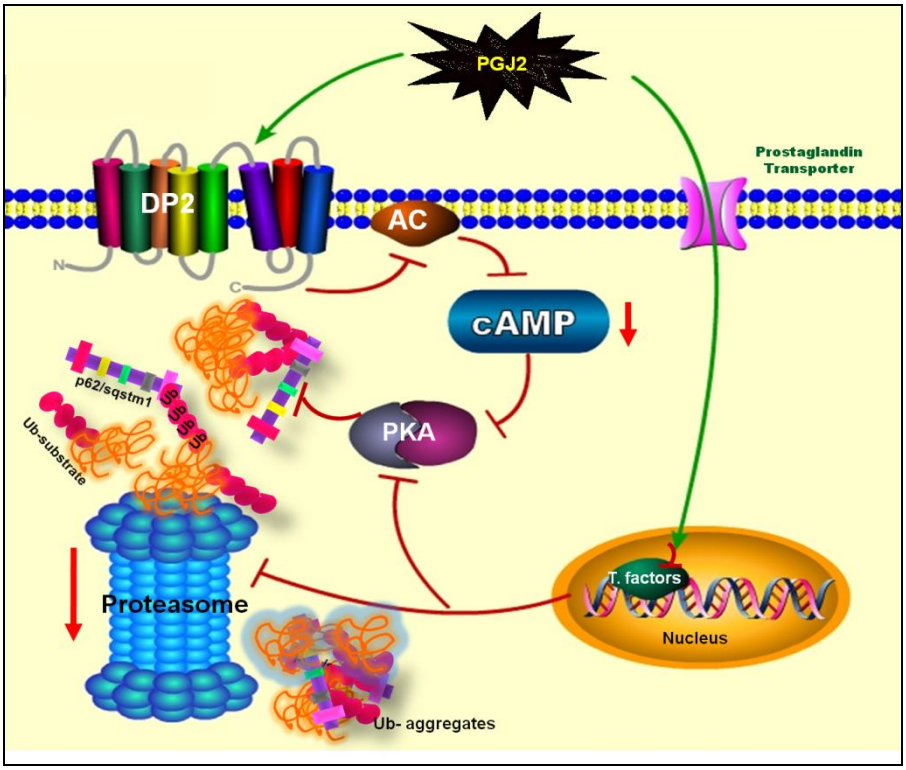
PGJ2
Prostaglandin
Transporter
DP2
AC
N
C
cAMP
p62/sqstm1
Ub
Ub
Ub
Ub
Ub-substrate
PKA
Proteasome
T. factors
Nucleus
Ub- aggregates

Our overall hypothesis is that over the life time environmental and genetic insults down-regulate proteasome activity leading to gradual accumulation of misfolded and ubiquitinated proteins (see Model 1). Post-mitotic aging neurons are incapable of diluting the cytotoxic effects of abnormal protein accumulation. Instead, they up-regulate a pro-survival/repair response, which among others includes increased levels of p62/sqstm1. This cytosolic protein contains multiple domains serving as a scaffold in a variety of cell signaling pathways. Because of its binding capacity to ubiquitinated substrates on one end and to the 26S proteasome on the opposing end, the immediate pro-survival role of p62/sqstm1 in protein homeostasis seems to be to facilitate degradation of soluble ubiquitinated substrates by delivering them to the proteasome.

If the capacity of the pro-survival response is overwhelmed, formation of insoluble protein aggregates is inevitable. Because of their bulky nature, aggregates are precluded from being degraded by the proteasome, therefore p62/sqstm1 could acquire an adaptive function which is to promote protein aggregation into inclusion bodies. The biological importance of aggregates is not clear, however, it could be the latest attempt of the cell to prevent cytotoxicity related to protein accumulation. In a final

effort to clear these toxic aggregates, p62/sqstm1 binds directly to LC3, an autophagosome-related protein, to sequester and deliver aggregates for autophagic clearance and therefore, autophagy plays an important role in clearing out protein aggregates that are precluded from proteasomal degradation. In addition, activation of pro-death pathways, including apoptosis may well be under way which can lead to eminent neuronal death.

From a therapeutic stand point, enhancing proteasome activity and the levels of p62/sqstm1 are ideal strategies to arrest or slow down accumulation of ubiquitinated and/or misfolded proteins. Alternatively, inducing autophagic function to clear ubiquitinated aggregates has also been proposed. However, prolonged massive up-regulation of autophagy could lower steady state levels of mitochondria and decrease oxidative phosphorylation (reviewed in(14)).

Drugs that increase cAMP levels can be used as a novel strategy to treat age-related neurodegenerative disorders characterized by proteasome impairment and accumulation of ubiquitinated aggregates. Elevation of proteasome activity induced by cAMP can be mediated by increases in subunit levels and/or through subunit phosphorylation by PKA, an effector molecule for cAMP (see Model 2A). Concomitantly, p62/sqstm1 levels are elevated, acting in a concerted

fashion with the proteasome to clear ubiquitinated substrates. As a result, ubiquitinated protein build up is reduced accompanied by a decrease in cell toxicity.

Failure to promptly remove ubiquitinated aggregates can also trigger neuroinflammation and prostaglandin production within neurons and glial cells (see Model 2B). Neurotoxic prostaglandins, such as PGJ2, act in a paracrine and autocrine fashion, eliciting its effect in a receptor-dependent and -independent manner, thereby perturbing important cellular pathways involved in neuronal homeostasis including the ubiquitin/proteasome and cAMP/PKA pathways.

The effects of prostaglandins of the J2 series are mediated through the DP2 receptor which is coupled to adenylate cyclase via G_i proteins evoking inhibition of cAMP production (reviewed in (75; 168)), as well as through an active transport system (reviewed in (66)). Once inside the cell, an additional mechanism allows transport of the prostaglandin J2 into the nucleus, where it affects gene transcription (reviewed in (65)). In our studies described here, we demonstrate that PGJ2 down-regulates the levels of one of the catalytic subunits of protein kinase A (PKA-subCα) as well as proteasome subunits (Rpt6 and β5). In addition, others showed DP2-mediated depletion of cAMP with

a decrease in PKA activity and cell survival (114). We propose that all of these PGJ2 effects are important contributors to formation of protein aggregates and progression of chronic neurodegenerative diseases that are associated with inflammation.

Our data clearly demonstrate that the UPP and not autophagy is implicated in clearance of ubiquitinated proteins in neurons. The function of the polyubiquitin shuttling factor p62/sqstm1 remains to be clarified. However, our studies support the notion that p62/sqstm1 is closely associated with the proteasome and plays an important role in the delivery of ubiquitinated substrates for proteasomal degradation. Furthermore, we demonstrate for the first time that treating cells with db-cAMP enhances proteasome activity and p62/sqstm1 levels in rat E18 spinal cord neuronal cultures. These data further implicate p62/sqstm1 as a facilitator of protein degradation by the proteasome.

In our studies we observed that cAMP did not completely prevent PGJ2-induced proteasome impairment and cell toxicity, most likely due to the down-regulating effect of PGJ2 on proteasome subunits (Rpt6 and β5) and on the catalytic subunit of protein kinase A (PKA-subCα).

It is critical to develop strategies to improve proteasome activity and p62/sqstm1 levels to prevent protein aggregation. Protein aggregates can trigger inflammation, and also trap various “survival” proteins, such as molecular chaperones, proteasomes, autophagosomes and p62/sqstm1. Once trapped in the aggregates these “survival” factors are no longer able to reverse the neuronal damage, causing the activation of the pro-death response and neuronal death.

CHAPTER VI

FUTURE DIRECTIONS

Maintenance of protein homeostasis presents a critical task for post mitotic neuronal cells. Over their life time, these cells develop a loss of quality control and a gain of protein deposition indicating proteasome impairment. Therefore, developing therapeutic strategies that aim at upregulating proteasome activity can be a very effective strategy to treat or delay chronic neurodegenerative diseases associated with protein aggregation.

We propose that future studies should focus on:

1) Knockdown of PKA catalytic subunit α by siRNA.

Our data indicate that enhancement of proteasome activity is mediated through the cAMP/PKA pathway. Others showed that PKA regulates proteasome activity through phosphorylation of its subunits (245). To test if PKA affects proteasome activity, we will use the siRNA approach for the PKA catalytic subunit α. We anticipate that the knockdown of PKA subunit will decrease proteasome activity; hence, cAMP treatment will not have an up-regulatory effect on proteasome activity and levels. The data will support our finding that cAMP/PKA pathway can modulate proteasome activity, and can be considered as a therapeutic strategy to prevent protein accumulation due to decrease in proteasome actvity.

2) Investigation of UPP ligases such as: CHIP and parkin as downstream targets of cAMP/PKA that can affect proteasomal degradation.

Our data demonstrate that db-cAMP treatment of spinal cord neuronal cultures enhances proteasome activity/levels as well as p62/sqstm1 levels, the latter is known to shuttle ubiquitinated proteins for degradation to the proteasome, thus, facilitates degradation of proteins by the proteasome. We hypothesize that other proteins that promote protein degradation by the proteasome such as ubiquitin ligases may be up-regulated under db-cAMP treatment. To test this hypothesis we will investigate the levels of CHIP (carboxyl terminus of Hsp70-interacting protein) and parkin, which are ubiquitin ligases that induce ubiquitylation and degradation of its substrates. The results will further substantiate our hypothesis that elavation of proteasome activity leads to a parallel increse in the levels/activity of proteins that promote protein degradation by the proteasome, and act in a concerted fashion with proteasomes to degrade ubiqutinated substartes.

3) Elucidation of the mechanisms by which p62/sqstm1 improves degradation of ubiquitinated proteins by the

proteasome.

We established that proteasome inhibition causes a more robust increase in p62/sqstm1 levels than autophagy impairment. Furthermore, we demonstrated a clear association between p62/sqstm1 and the 26S proteasome. Finally, we determined that cAMP induces a coordinated elevation in proteasome activity and p62/sqstm1 levels.

These results strongly support the notion that p62/sqstm1 shuttles ubiquitinated proteins to the proteasome for degradation, and collaborates with the proteasome in protein clearance. Loss of p62/sqstm1 function or a decrease in its expression could thus lead to inefficient protein degradation in already vulnerable aging neurons.

To confirm this hypothesis, it would be interesting to assess p62/sqstm1 expression levels in postmortem brain and spinal cord tissues of patients diagnosed with neurodegenerative diseases compare to control individuals. Furthermore, it would be important to investigate the effect of p62/sqstm1 down-regulation by RNA interference on proteasome activity in neuronal cells.

Our expectations are that p62/sqstm1 expression levels decrease over time. The depletion in 62/sqstm1 levels was suggested to correlate with oxidative damage to the p62

promoter, which is common in neurodegenerative disorders (40). We anticipate that depletion of p62/sqstm1 can contribute to the decline in clearance of ubiquitinated proteins by the proteasome and in cell viability. Further elucidation of the role of p62/sqstm1 in proteasomal degradation could lead to the development of pharmacological means to enhance p62/sqstm1 function and delay neurodegeneration linked to protein aggregation.

7.3. OVERALL CONCLUSION

In our view, further characterization and optimization of the mechanisms by which the cAMP/PKA pathway enhances proteasome activity and p62/sqstm1 levels are critical to the development of a therapeutic approach to prevent and slow down the progression of neurodegenerative diseases that are associated with the abnormal accumulation and aggregation of ubiquitinated proteins.

Additionally, autophagy plays an important role in clearing out protein aggregates. Therefore, autophagic induction is also considered a promising therapeutic target for treatment of age-related disorders.

It is equally important to characterize and optimize the mechanisms by which neurotoxic products of inflammation damage neuronal cells. Treatment with PGJ2, as we show in

our present and previous studies, recapitulates many of the pathological processes relevant to neurodegeneration. Abolishing the neurotoxicity induced by inflammatory mediators such as PGJ2 is likely to be another effective therapeutic strategy to treat/prevent neurodegeneration.

CHAPTER VII

FIGURES

Figure 1 (next page) – Comparison between the effects of proteasome and autophagy inhibitors on cytotoxicity as well as on LC3-I and LC3-II, p62/sqstm1 and ubiquitinated protein levels in SK-N-SH cells. (A) Cell viability was assessed with the MTT assay. Data represent the mean ± s.e. from at least eight determinations. The viability for each condition was compared to the viability of cells treated with vehicle only (control, 100%). The *asterisk* (*) identifies the values that are significantly different (*p<0.001*) from the control. Western blot analyses (8% and 10% gels) to detect LC3-I and LC3-II **(B)**, p62/sqstm1 **(C)**, ubiquitinated proteins **(D)** and actin as loading control **(E)** in total extracts of human SK-N-SH neuroblastoma cells (40 µg of protein/lane). Cells were treated with the different inhibitors for 24h. Molecular mass markers in kDa are shown on the right. Similar results were obtained in duplicate experiments. Epox, epoxomicin; CQ, chloroquine; NH4Cl, ammonium chloride; Baf, bafilomycin A1.

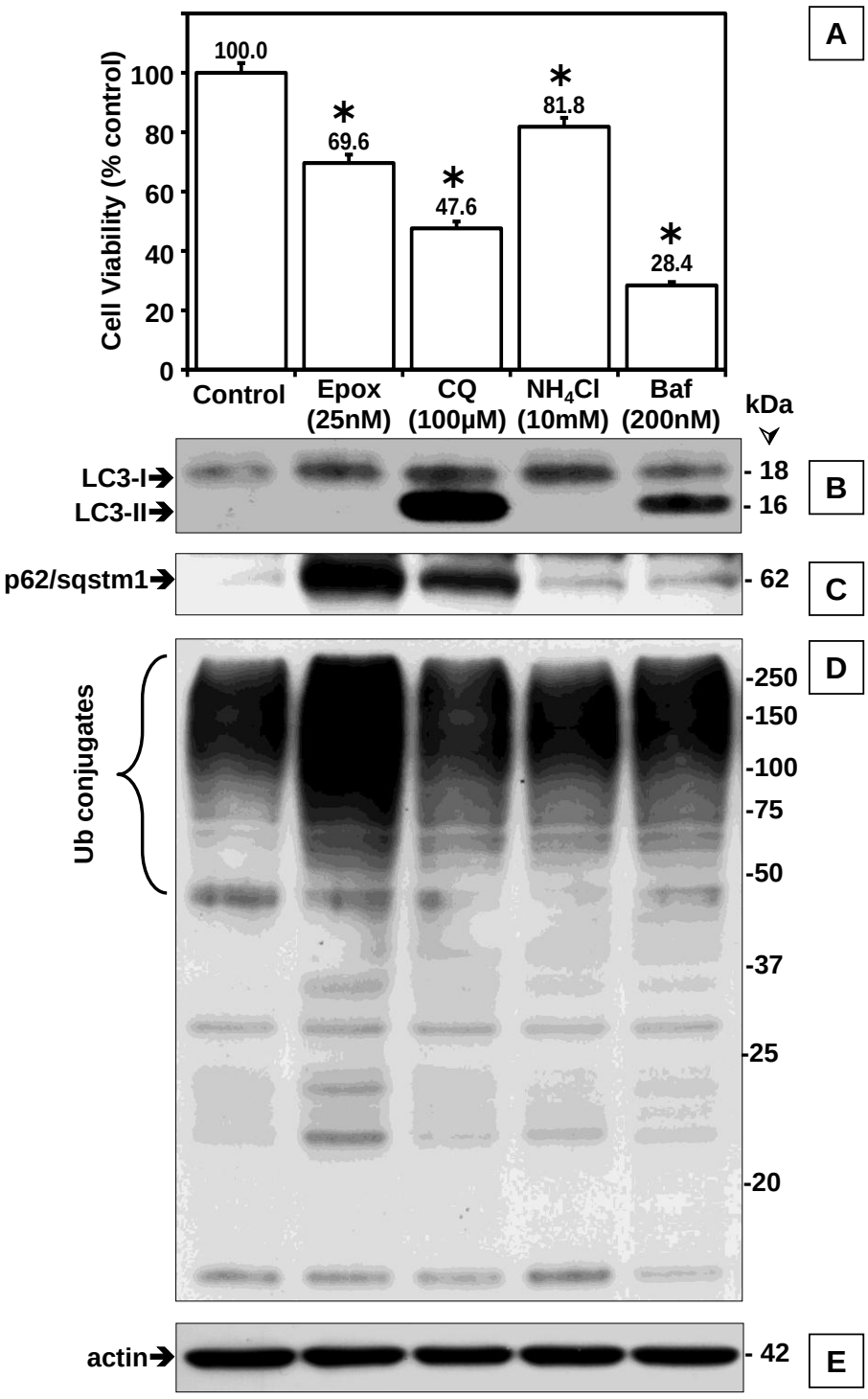
A
Cell Viability (% control)
100.0
69.6
47.6
81.8
28.4
Control
Epox (25nM)
CQ (100μM)
NH4Cl (10mM)
Baf (200nM)
kDa
LC3-I
LC3-II
- 18
- 16
B
p62/sqstm1
- 62
C
Ub conjugates
-250
-150
-100
-75
-50
-37
-25
-20
D
actin
- 42
E

Figure 1

Figure 2 (next two pages) – Comparison between the effects of epoxomicin (Epx or E, 25nM), chloroquine (CQ, 100μM) and the two combined (E+CQ) on p62/sqstm1, LC3-I and LC3-II, ubiquitinated proteins, protein aggregates and proteasome activity in SK-N-SH cells maintained under serum conditions. Western blot analyses to detect p62/sqstm1 **(A),** LC3-I and LC3-II **(B),** the proteasome subunit α4 **(C)** and ubiquitinated proteins as well as actin as loading control **(E)** in total extracts of human SK-N-SH neuroblastoma cells (40 μg of protein/lane). In vitro synthesized K63-only and K48-only polyubiquitinated substrates (5μg of protein/lane) were also loaded in the first two lanes in **(E)**. Molecular mass markers in kDa are shown on the right. Cells were treated with each inhibitor by itself or in combination for 24h. The levels of p62/sqstm1, LC3-I and LC3-II **(D),** and ubiquitinated proteins **(F)** were semi-quantified by densitometry. Data represent the relative intensity for all proteins. Values represent means and s.d. from at least duplicate experiments. The *asterisks* identify values that are significantly different (*p at least <0.05; **$p<0.01$) from control (Ct). The chymotrypsin-like activity of the proteasome **(G)** was measured in cleared supernatants obtained from total cell homogenates (25μg of protein/sample). The peptidase activity was assayed

colorimetrically after 24h incubations at 37°C with Suc-LLVY-AMC. Data represent the mean ± s.e. from three experiments. The *asterisks* identify values that are significantly different (*p at least <0.001) from control conditions. Aggregates of ubiquitinated proteins were assessed with the filter trap assay **(H)**.

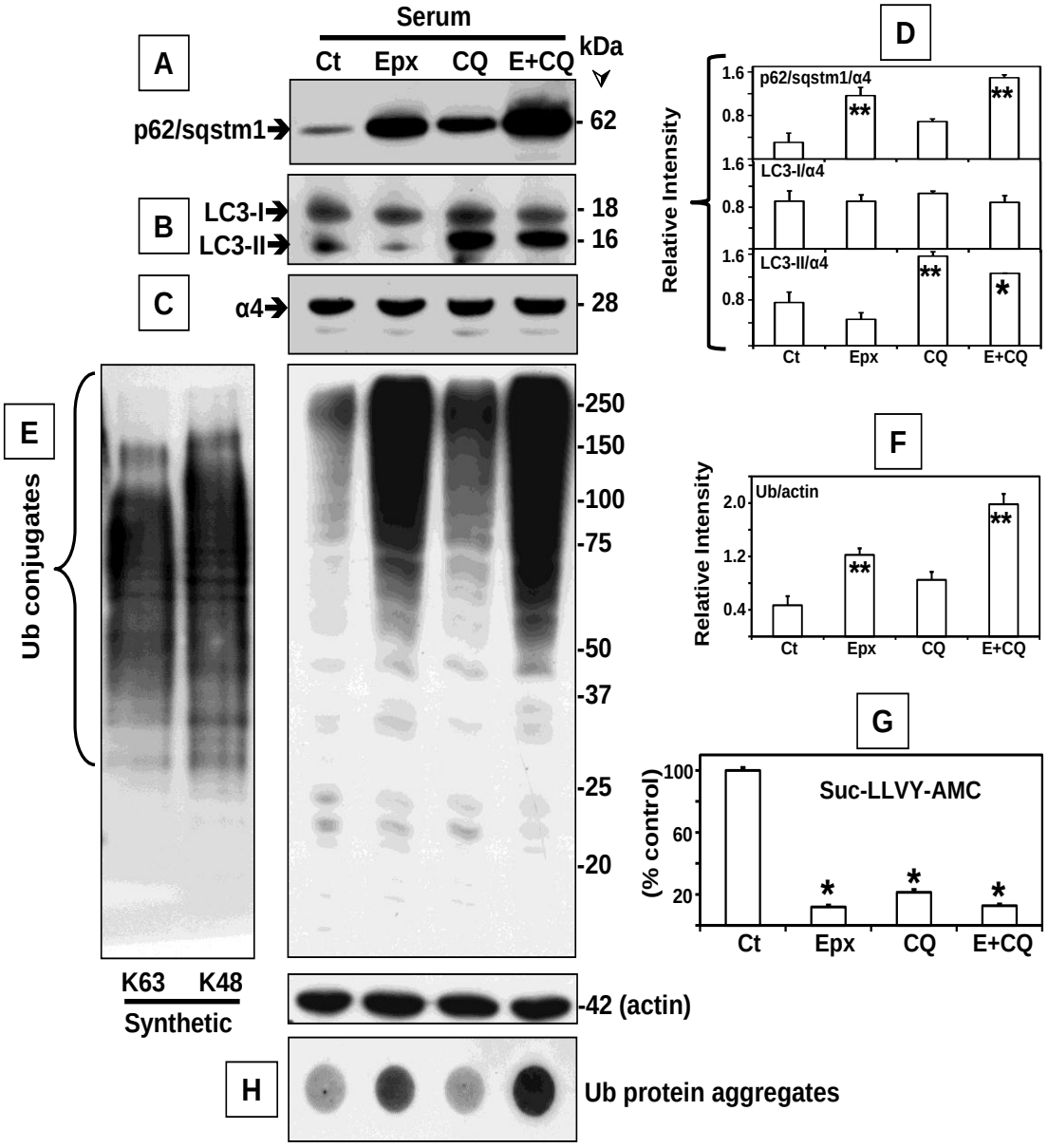
Serum
Ct
Epx
CQ
E+CQ
kDa
A
p62/sqstm1
62
B
LC3-I
LC3-II
18
16
C
α4
28
D
p62/sqstm1/α4
LC3-I/α4
LC3-II/α4
Relative Intensity
1.6
0.8
**
*
E
Ub conjugates
250
150
100
75
50
37
25
20
F
Ub/actin
2.0
1.2
0.4
G
Suc-LLVY-AMC
(% control)
100
60
20
K63
K48
Synthetic
42 (actin)
H
Ub protein aggregates

Figure 2

Figure 3 (next page) – Effects of epoxomicin (25nM) and chloroquine (100μM) on the sedimentation velocity of proteasomes and autophagosome-related proteins in SK-N-SH cells maintained in serum conditions. Total lysates (2mg protein/sample) were fractionated by glycerol density gradient centrifugation (10-40% glycerol corresponding to fractions 13 to 1). **(A)** - Aliquots (50μl) of each fraction obtained from control (Ct, *squares*), chloroquine (CQ, *circles*) and epoxomicin (Epx, *crosses*) treated cells under serum conditions were assayed for chymotrypsin-like activity with Suc-LLVY-AMC. Data represent the mean ± s.e. from three experiments. **(B to D)** - Immunoblot analyses of each fraction probed with antibodies that react with the proteasome (*α*4, core particle; Rpt6/S8, 19S regulatory particle), with autophagy-related proteins (Atg5, Atg16 and LC3) and with p62/sqstm1. Proteins were precipitated with acetone from 700μl of each fraction. The fractions were obtained from **(B)** control, **(C)** chloroquine and **(D)** epoxomicin-treated cells. Similar results were obtained in triplicate experiments and under serum and serum free conditions. The numbers on the right designate each row.

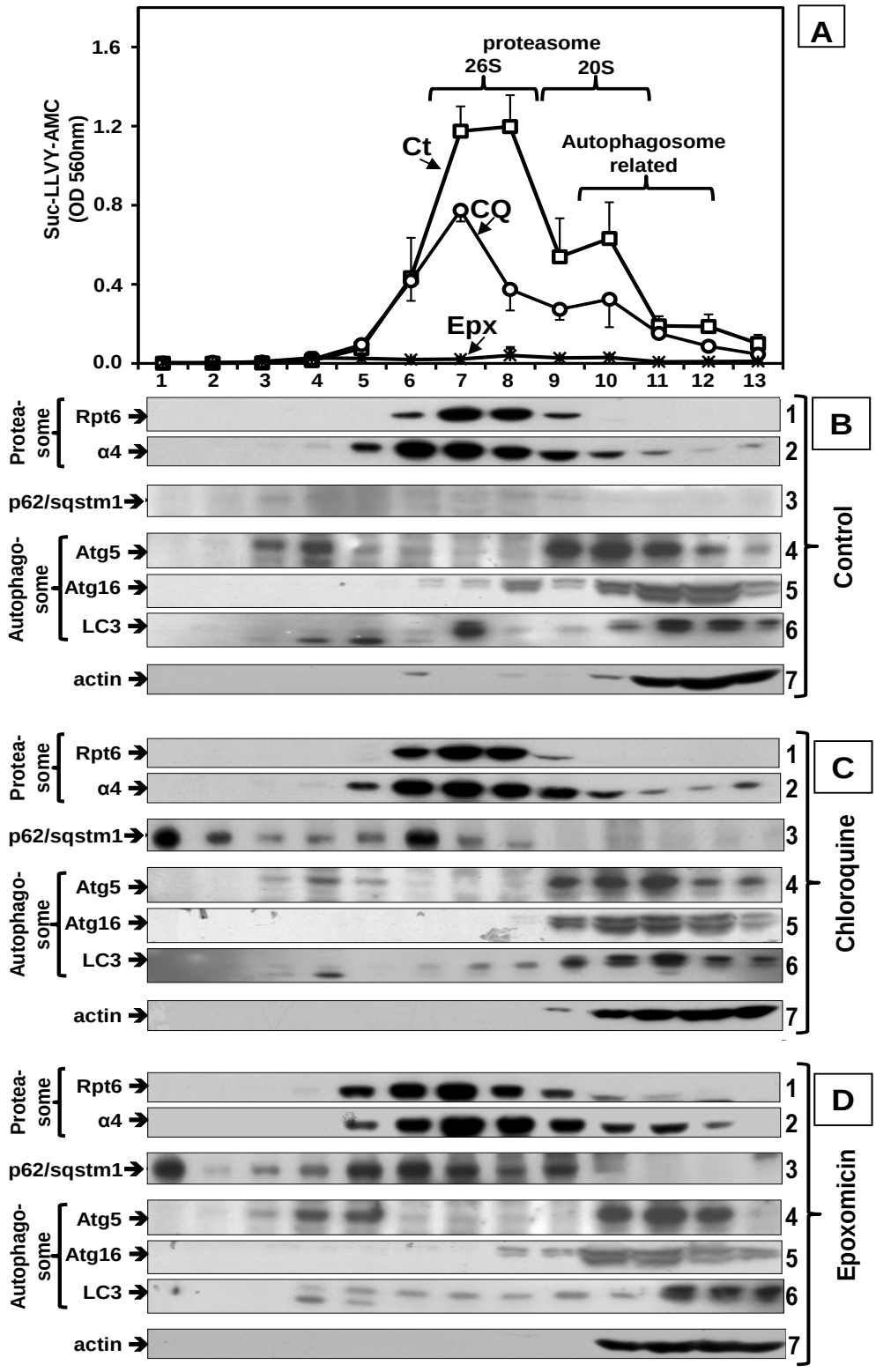
A
proteasome
26S
20S
Autophagosome
related
Ct
CQ
Epx
Suc-LLVY-AMC
(OD 560nm)
1.6
1.2
0.8
0.4
0.0
1 2 3 4 5 6 7 8 9 10 11 12 13
B
Control
C
Chloroquine
D
Epoxomicin
Protea-
some
Autophago-
some
Rpt6
α4
p62/sqstm1
Atg5
Atg16
LC3
actin
1
2
3
4
5
6
7

Figure 3

Figure 4 (next two pages) – Chloroquine inhibits the proteasome activity and affects its assembly. Crude extracts were prepared from control (0) SK-N-SH cells or cells treated with increasing chloroquine (CQ) concentrations for 24h. Cleared lysates (80µg/sample) were subjected to non-denaturing gel electrophoresis. **(A)** The proteasomal chymotrypsin-like activity was measured with Suc-LLVY-AMC by the in-gel assay (*left panel*). 26S and 20S proteasomes were detected by immunobloting with an anti-β5 antibody, a subunit of the core proteasome particle (20S) [*two middle panels (long and short exposures)*]. The 26S holoenzyme was further identified with an antibody that reacts with the Rpt6/S8 (ATPase) subunit of the 19S regulatory particle (*right panel*). Proteasomal 26S (two capped and one capped) and 20S forms are indicated by arrows on the left. Activity **(B)** and immunoblot **(C)** bands on the non-denaturing (native) gel were semi-quantified by densitometry. Data represent total pixels compared to control (no chloroquine) and means and s.e. from three experiments. In **(B)** the *asterisks* identify values that are significantly different (**p* at least*<0.05; **p<0.01*) from control (Ct). In parallel experiments **(D)**, cells were harvested for SDS-PAGE followed by western blot analyses (40 *µg* of protein/lane) to detect proteasome subunits β5

and Rpt6/S8, autophagy proteins LC3-I and LC3-II and actin (loading control) after treatment with increasing chloroquine concentrations for 24h. The level of each protein band was semi-quantified by densitometry (*graph*). Data represent total pixels and means and s.d. from duplicate experiments. Molecular mass markers in kDa are shown on the right. The small numbers within the immunoblots designate each row.

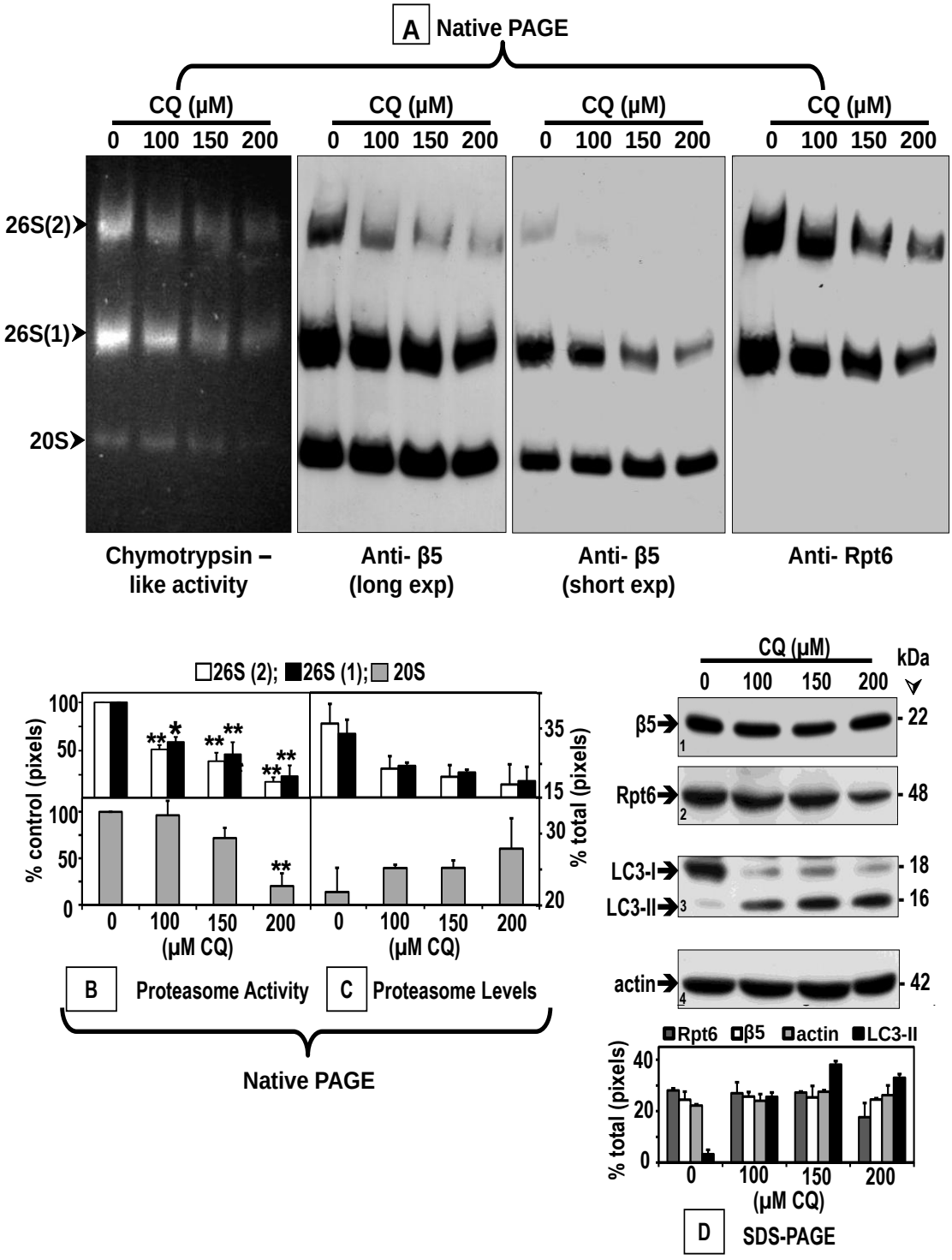
A Native PAGE
CQ (μM)
0 100 150 200
26S(2)
26S(1)
20S
Chymotrypsin – like activity
Anti- β5 (long exp)
Anti- β5 (short exp)
Anti- Rpt6
26S (2); 26S (1); 20S
% control (pixels)
% total (pixels)
(μM CQ)
B Proteasome Activity
C Proteasome Levels
Native PAGE
kDa
β5
Rpt6
LC3-I
LC3-II
actin
22
48
18
16
42
Rpt6 β5 actin LC3-II
D SDS-PAGE

Figure 4

Figure 5 (next two and three pages) – Comparison between the effects of epoxomicin (Epx, 25nM) and chloroquine (CQ, 100µM) on p62/sqstm1 and its association with proteasomes and LC3 in supernatant and pellet fractions. Crude extracts were prepared from SK-N-SH cells control (Ct) or treated with each inhibitor for 24h. Cleared lysates (80µg/sample) were subjected to non-denaturing gel electrophoresis.**(A and B)** The proteasomal chymotrypsin-like activity was measured with Suc-LLVY-AMC by the in-gel assay (*left panels*). In **(A)** 26S and 20S proteasomes were detected by immunobloting with an anti-β5 antibody, a subunit of the core proteasome particle (20S) (*middle panel*) and with the anti-Rpt6/S8 antibody, an ATPase subunit of the 19S regulatory particle (*right panel*). Proteasomal 26S (two capped and one capped) and 20S forms are indicated by arrows on the left. In **(B)** p62/sqstm1 (*middle panel*) and LC3 (*right panel*) were detected by immunobloting with the respective antibodies. In **(C)** aliquots of the supernatant (cleared lysate) and pellet fractions were run on SDS-PAGE followed by immunobloting with the anti-ubiquitinated proteins antibody as well as the same antibodies listed in **(A)** and **(B)**. Molecular mass markers in kDa are shown on the right. The small numbers next to the immunoblots designate each row. The level of the proteins in each immunoblot was semi-

quantified by densitometry **(D).** Data represent % of total pixels (total = supernatant+pellet). The pellet fractions were also subjected to the filter trap assay to detect protein aggregates **(E).**The chymotrypsin-like activity of the supernatant and pellet fractions was measured with Suc-LLVY-AMC **(F).** The *asterisks* identify values that are significantly different (*p at least <0.001) from the control supernatant.

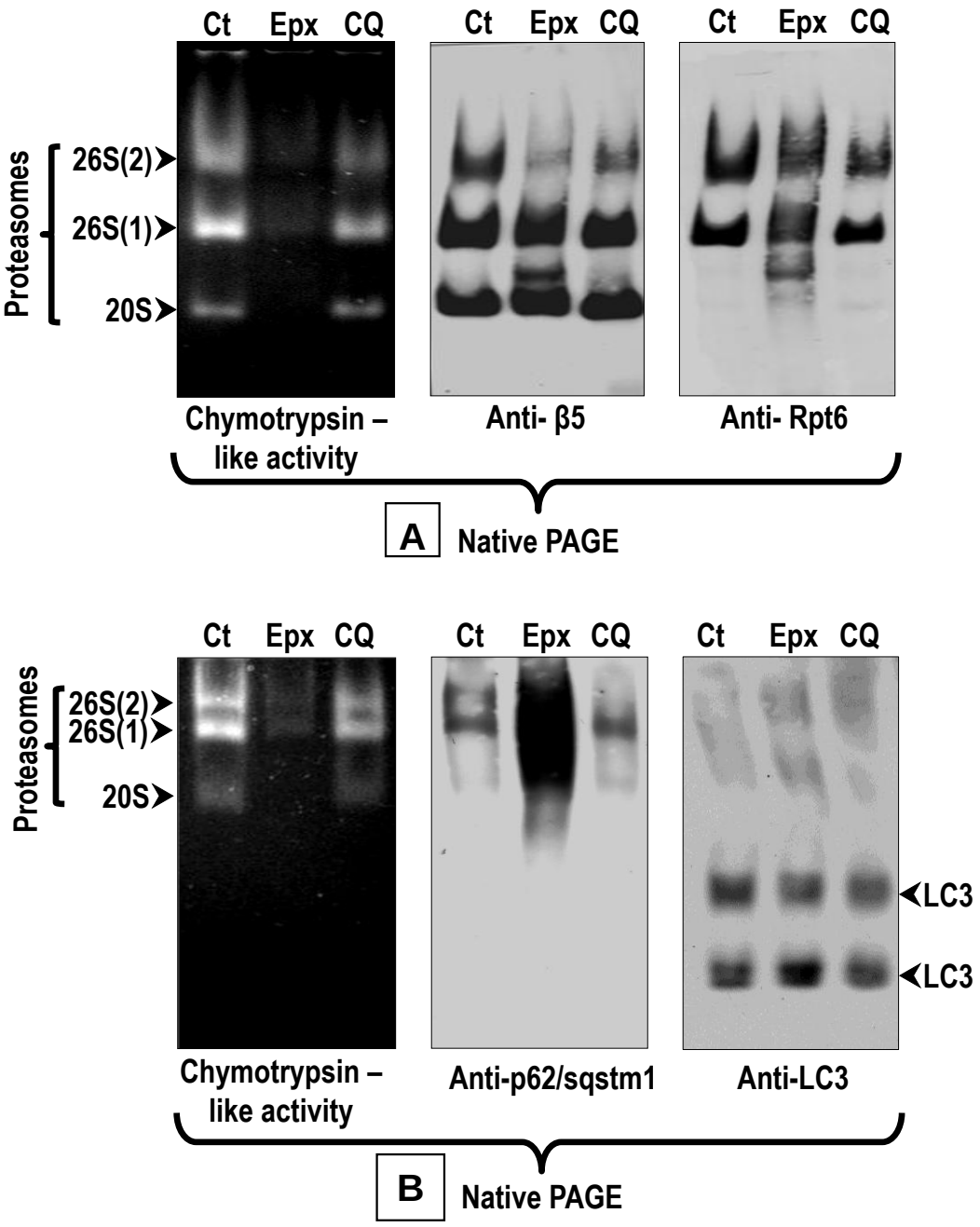
Ct
Epx
CQ
Proteasomes
26S(2)
26S(1)
20S
Chymotrypsin – like activity
Anti- β5
Anti- Rpt6
A
Native PAGE
Anti-p62/sqstm1
Anti-LC3
LC3
LC3
B

Figure 5

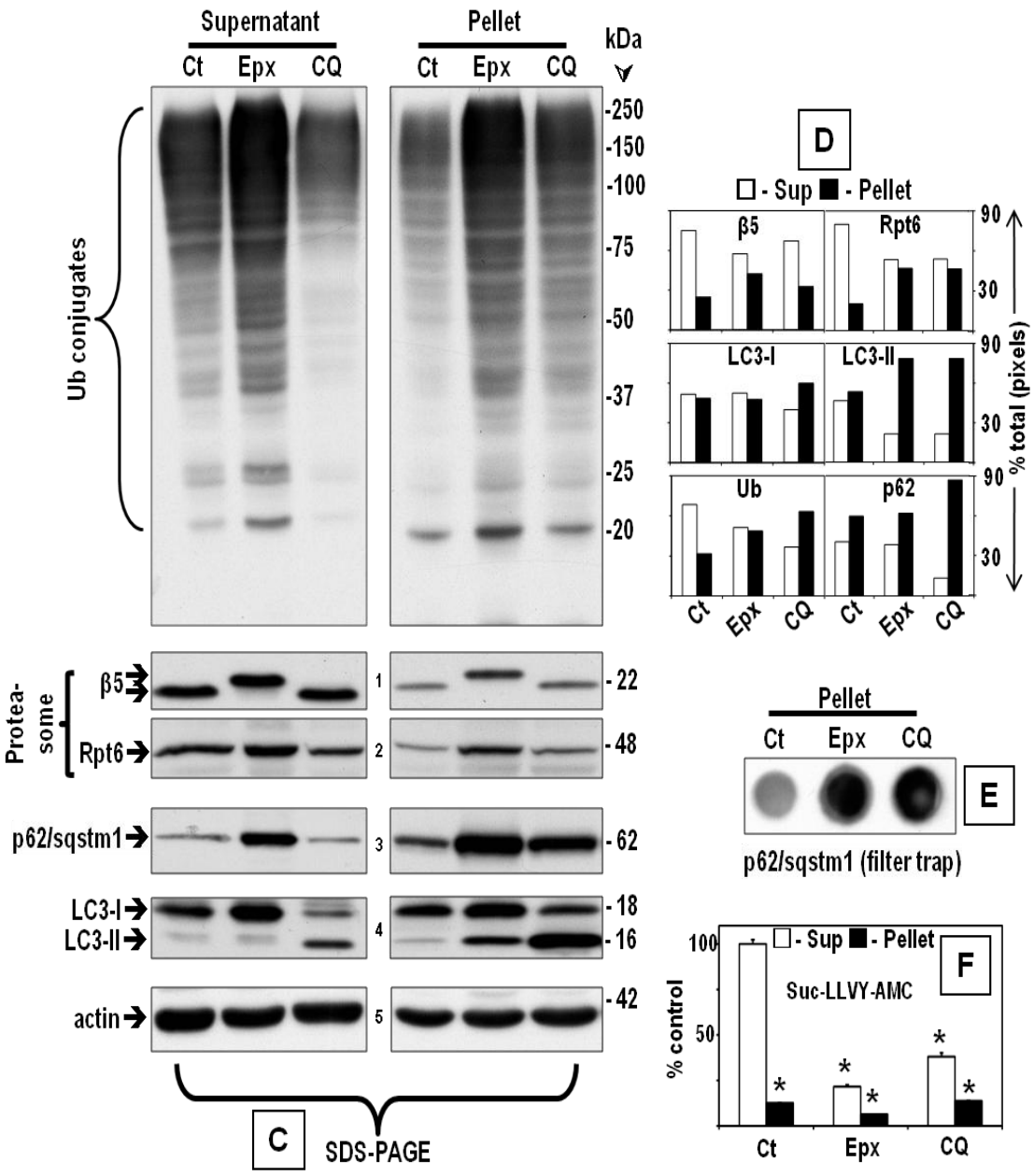

Figure 5 (continue)

Figure 6 – Protein interaction between p62/sqstm1 and proteasomes detected by the Proximity Ligation Assay (PLA). SK-N-SH cells control (**A**, Ct), or treated for 24h with 100µM chloroquine (**B**, CQ) or 25nM epoxomicin (**C**, Epx) were co-incubated with a proteasome antibody (Rpt6/S8) and a p62/sqstm1 antibody. Nuclear staining, DAPI and PLA signal, Texas Red. Scale bars = 7µm.

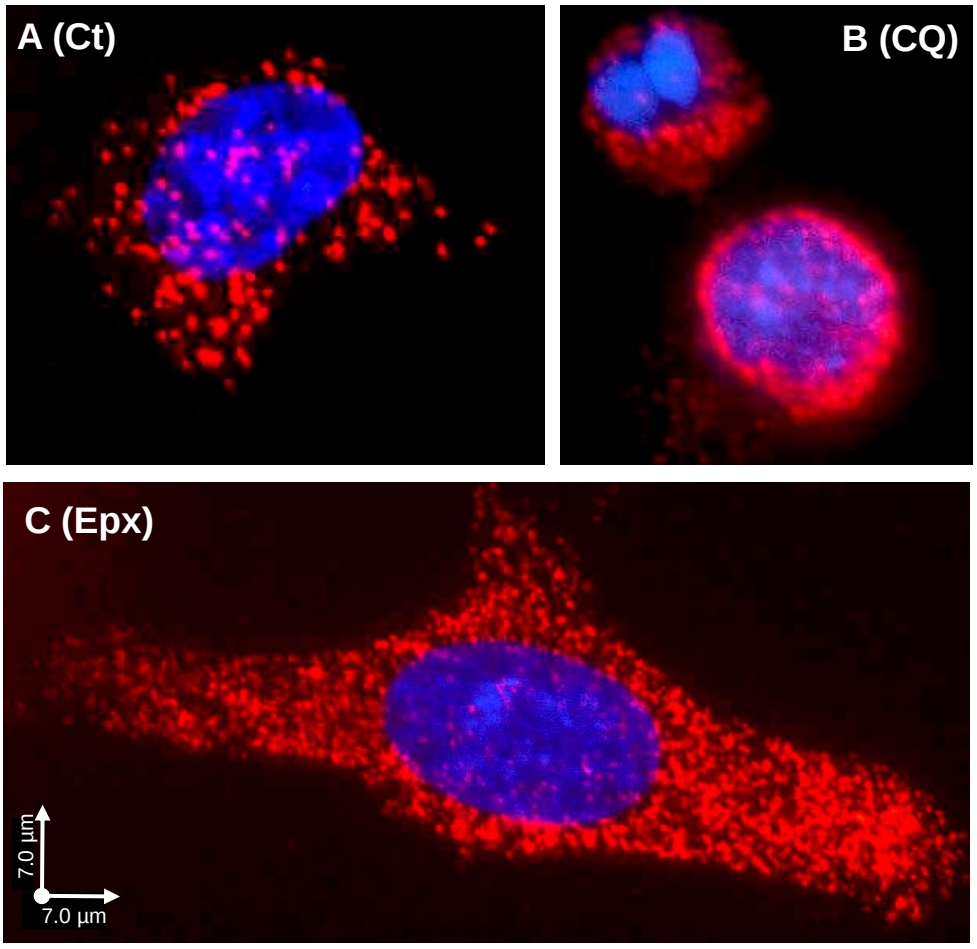

Figure 6

Figure 7 (next two pages) – Comparison between the effects of chloroquine (CQ) and epoxomicin (Epx) on proteasome activity in wild type (WT) and Atg5-/- mouse embryonic fibroblasts (MEF). (A) The chymotrypsin-like activity was measured in cleared supernatants obtained from total cell homogenates (25μg of protein/sample). The peptidase activity was assayed colorimetrically after 24h incubations at 37°C with Suc-LLVY-AMC. Data represent the mean ± s.e. from eight determinations. The *asterisks* identify values that are significantly different (*p at least <0.01) from control (0). **(B and C)** Crude extracts were prepared from WT and Atg5-/- MEFs control (0) or treated with increasing chloroquine (**B,** CQ) or epoxomicin (**C,** Epx) concentrations for 24h. Cleared lysates (80μg/sample) were subjected to non-denaturing gel electrophoresis. The proteasomal chymotrypsin-like activity was measured with Suc-LLVY-AMC by the in-gel assay (*left panels*). 26S and 20S proteasomes were detected by immunobloting with the anti-Rpt6/S8 antibody (for 26S, *middle panels*) and the anti-β5 antibody (for 26S and 20S, *right panels*). Proteasomal 26S (two capped and one capped) and 20S forms are indicated by arrows on the left. In parallel experiments **(D),** cells were harvested for SDS-PAGE followed by western blot analyses (40 μg of protein/lane) to detect the autophagy proteins

Atg5, LC3-I and LC3-II under control (0) and chloroquine (CQ) treatment for 24h. Molecular mass markers in kDa are shown on the right.

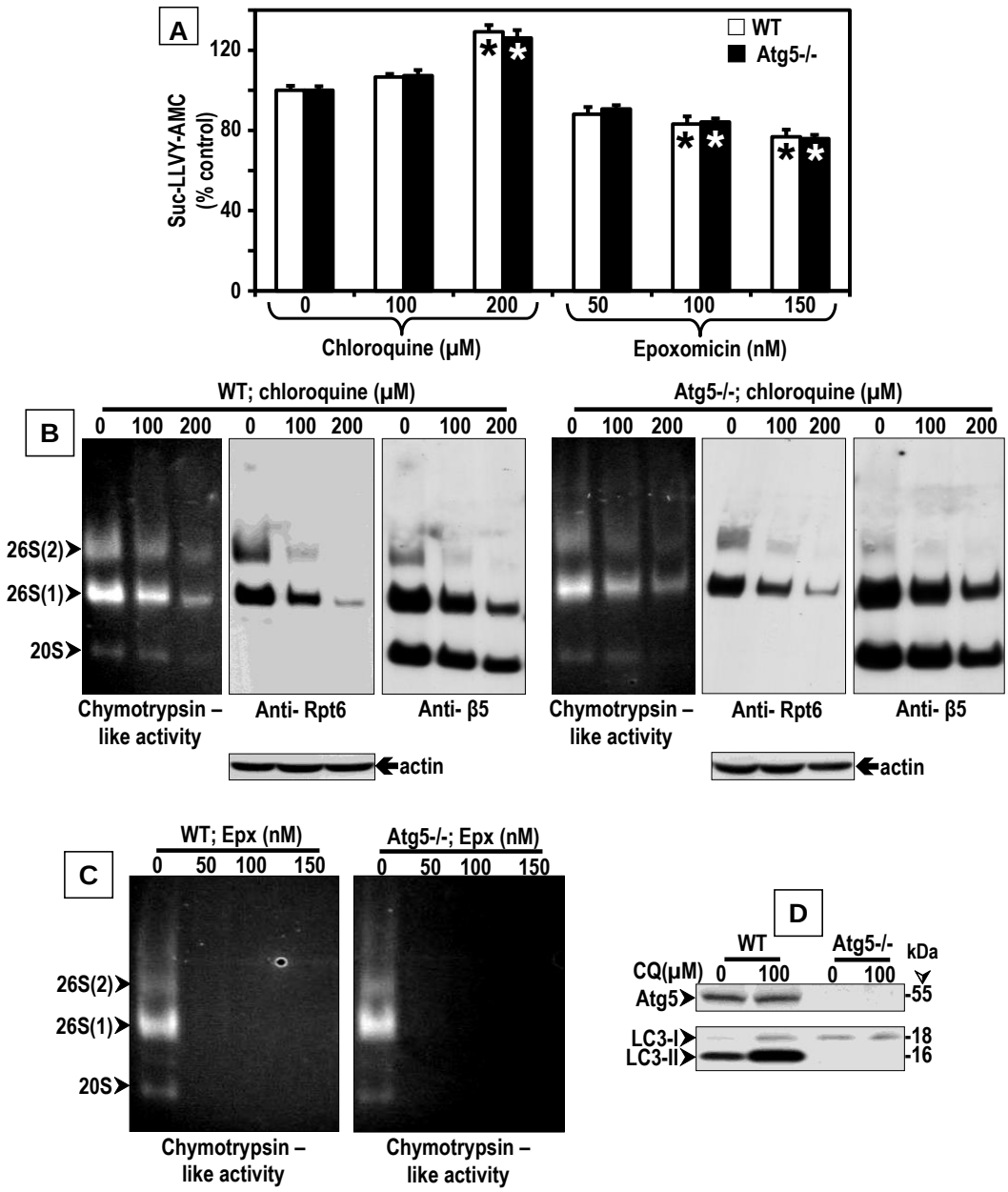
A
WT
Atg5-/-
Suc-LLVY-AMC (% control)
120
80
40
0
0
100
200
50
100
150
Chloroquine (μM)
Epoxomicin (nM)
B
WT; chloroquine (μM)
Atg5-/-; chloroquine (μM)
0 100 200 0 100 200 0 100 200
0 100 200 0 100 200 0 100 200
26S(2)
26S(1)
20S
Chymotrypsin – like activity
Anti- Rpt6
Anti- β5
actin
C
WT; Epx (nM)
Atg5-/-; Epx (nM)
0 50 100 150
0 50 100 150
26S(2)
26S(1)
20S
Chymotrypsin – like activity
Chymotrypsin – like activity
D
WT
Atg5-/-
kDa
CQ(μM) 0 100 0 100
Atg5
-55
LC3-I
LC3-II
-18
-16

Figure 7

Figure 8 (next page) – Effect of chloroquine (CQ) and epoxomicin (Epx) on ubiquitinated protein, p62/sqstm1, LC3-I and LC3-II levels in wild type (WT) and Atg5-/- mouse embryonic fibroblasts (MEF). Western blot analyses (8% or 10% gels) to detect ubiquitinated proteins (A), p62/sqstm1 (B), LC3-I and –II (C) and the proteasome α4 subunit (D, loading control) in total cell extracts (40µg of protein/lane) treated with each inhibitor for 24h. Molecular mass markers in kDa are shown on the left. The protein levels were semi-quantified by densitometry (E). Data represent the relative intensity and means and s.d. from duplicate experiments. The *asterisks* identify values that are significantly different (*p at least <0.05; **$p<0.01$) from control conditions (0).

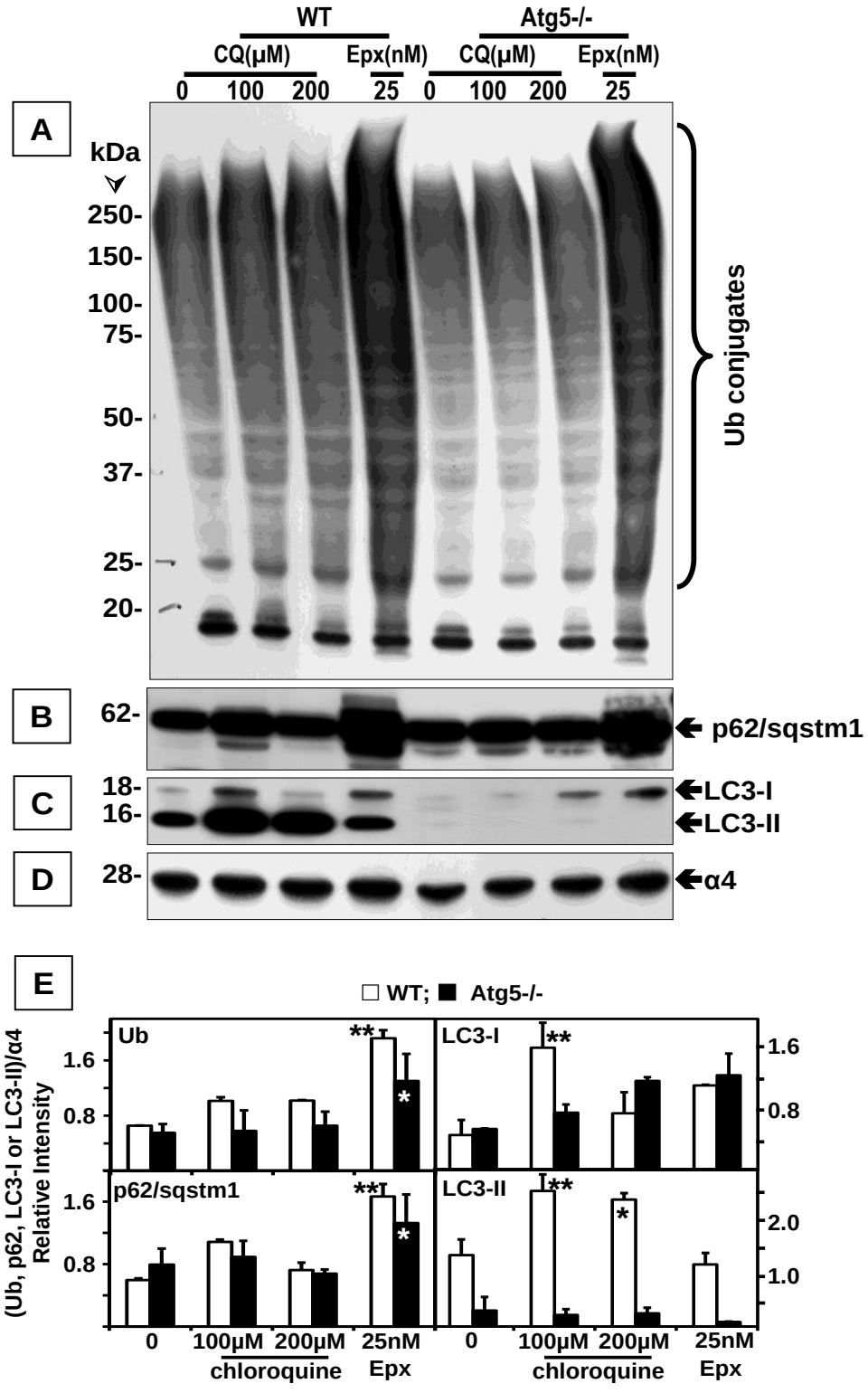
WT
Atg5-/-
CQ(μM)
Epx(nM)
0
100
200
25
A
kDa
250-
150-
100-
75-
50-
37-
25-
20-
Ub conjugates
B
62-
p62/sqstm1
C
18-
16-
LC3-I
LC3-II
D
28-
α4
E
□ WT; ■ Atg5-/-
(Ub, p62, LC3-I or LC3-II)/α4
Relative Intensity
Ub
LC3-I
p62/sqstm1
LC3-II
1.6
0.8
2.0
1.0
**
*
0
100μM
200μM
25nM
chloroquine
Epx

Figure 8

Figure 9 (next page) – Effect of chloroquine (CQ, 10µM) and epoxomicin (Epx, 5nM) on ubiquitinated protein, LC3-I and LC3-II levels in rat primary neuronal cortical cultures. Western blot analyses (10% gels) to detect ubiquitinated proteins **(A)**, LC3-I and –II **(B)** and β-tubulin (**C,** loading control) in total cell extracts (40µg of protein/lane) treated with each inhibitor for 24h, 48h, and 96h. Molecular mass markers in kDa are shown on the right. The protein levels were semi-quantified by densitometry **(D)**. Data represent relative intensity obtained from at least three cell culture dishes per condition.

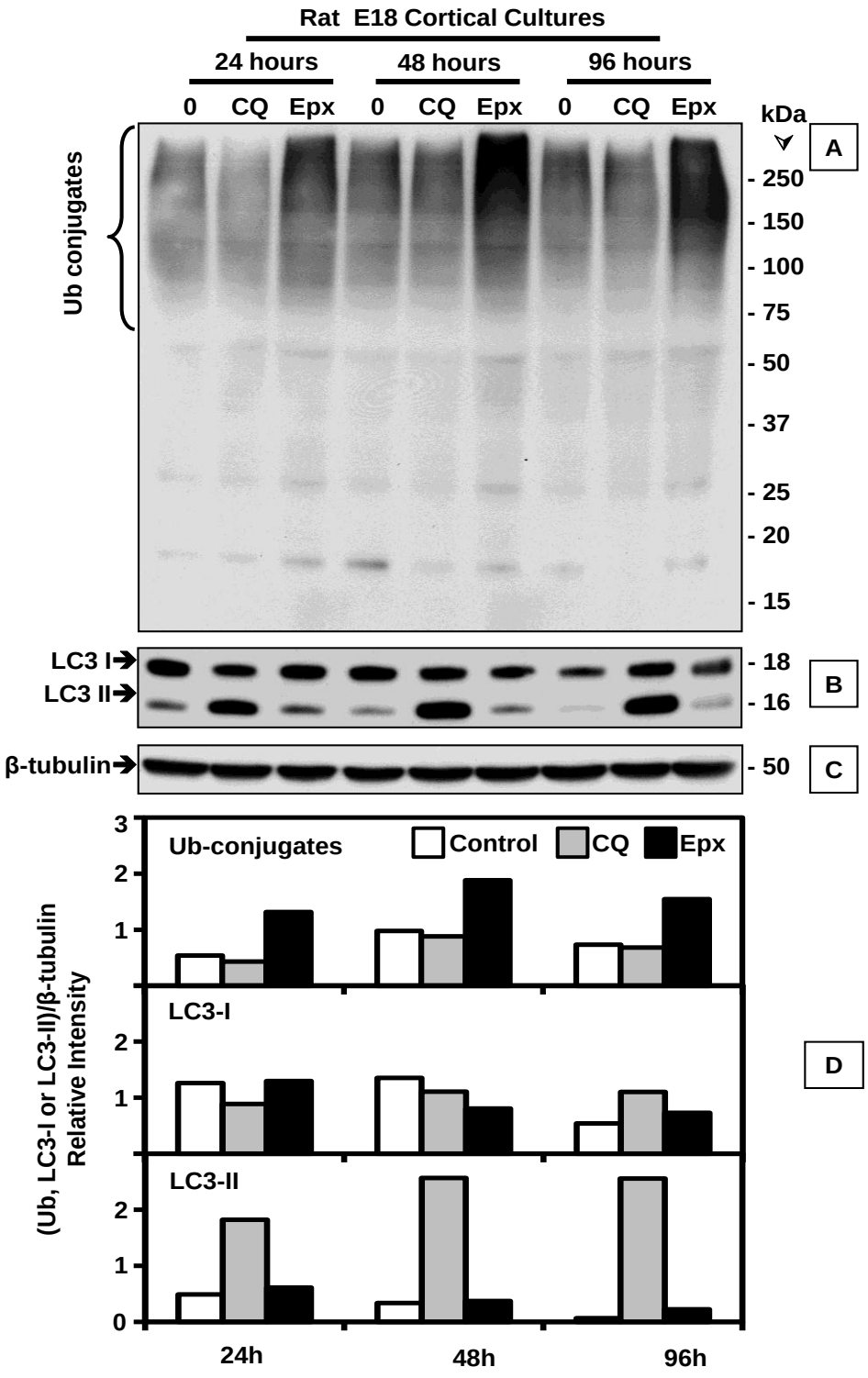
Rat E18 Cortical Cultures
24 hours
48 hours
96 hours
0 CQ Epx 0 CQ Epx 0 CQ Epx
kDa
A
Ub conjugates
- 250
- 150
- 100
- 75
- 50
- 37
- 25
- 20
- 15
LC3 I
LC3 II
- 18
- 16
B
β-tubulin
- 50
C
Ub-conjugates
Control
CQ
Epx
LC3-I
LC3-II
(Ub, LC3-I or LC3-II)/β-tubulin Relative Intensity
3
2
1
0
24h
48h
96h
D

Figure 9

Figure 10 (next page) – Db-cAMP enhances proteasome activity. Cell extracts were prepared from rat E18 spinal cord neuronal cultures treated with 0.5% DMSO (control), 1mM db-cAMP (db-cAMP) or 100μM forskolin and 10μM rolipram (Fk+Rp) for 24h. Clear lysates (80μg/sample) were subjected to non-denaturing gel electrophoresis as described under "Methods". (**A**) Proteasomal chymotrypsin-like activity was assessed with Suc-LLVY-AMC by the in-gel assay (*left panel*). 26S and 20S proteasomes (indicated on the left by *arrows*) were detected by immunoblotting with anti-Rpt6/S8 and anti-β5. Rpt6 is an ATPase subunit of the 19S regulatory particle of the proteasome, thus anti-Rpt6/S8 detects only 26S proteasomes (two caps and one cap, *middle panel*). β5 is a subunit of the 20S core particle of the proteasome, thus anti-β5 detects both 20S and 26S proteasomes (*right panel*). βIII-tubulin was detected as loading control (*bottom row*). Activity (**B**) and immunoblot (**C**) bands were semi-quantified by densitometry. Percentages represent the ratio between data for each condition and control (DMSO) considered to be 100%. Values indicate means and s.e. from four experiments (**B**) and means and s.d. from two experiments (**C**). The *asterisks* identify values that are significantly different from control (*$p < 0.05$; **$p < 0.01$; ***$p < 0.001$).

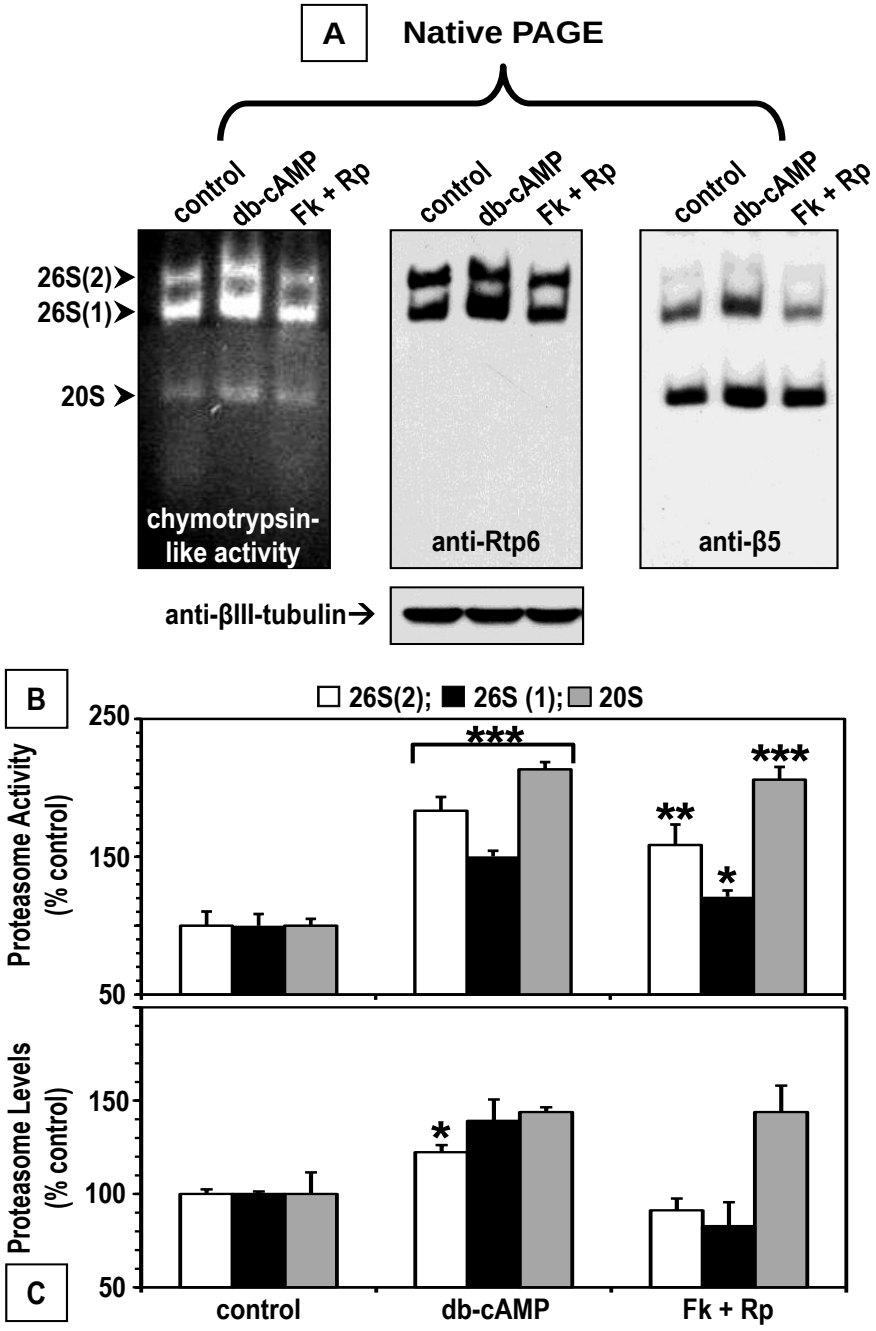
A
Native PAGE
control
db-cAMP
Fk + Rp
26S(2)
26S(1)
20S
chymotrypsin-like activity
anti-Rtp6
anti-β5
anti-βIII-tubulin
B
26S(2); 26S (1); 20S
Proteasome Activity (% control)
250
150
50
***
**
*
***
Proteasome Levels (% control)
150
100
50
*
C
control
db-cAMP
Fk + Rp

Figure 10

Figure 11 (next page) – Db-cAMP mitigates the inhibitory effect of PGJ2 on 26S proteasome activity. Cell extracts were prepared from rat E18 spinal cord neuronal cultures treated with 0.5% DMSO (control) or 20μM PGJ2 (J2) for 24h. Parallel cultures were pretreated for one hour with 1mM db-cAMP followed by 20μM PGJ2 for 24h (J2+db-cAMP) or with 100μM forskolin/10μM rolipram followed by 20μM PGJ2 for 24h (J2+Fk+Rp). Clear lysates (80μg/sample) were subjected to non-denaturing gel electrophoresis as described under "Methods". (**A**) Proteasomal chymotrypsin-like activity was assessed with Suc-LLVY-AMC by the in-gel assay (*left panel*). 26S and 20S proteasomes were detected by immunoblotting with anti-Rpt6 (*middle panel*) or anti-β5 (*right panel*) as described in Fig. 1. 26S and 20S proteasomes are indicated by *arrows* on the left. βIII-tubulin was detected as loading control (*bottom row*). Activity (**B**) and immunoblot (**C**) bands were semi-quantified by densitometry. Percentages represent the ratio between data for each condition and control (DMSO) considered to be 100%. Values indicate means and s.e. from four experiments (**B**) and means and s.d. from two experiments (**C**). The *asterisks* identify values that are significantly different from control (***p<0.01; ***p<0.001*).

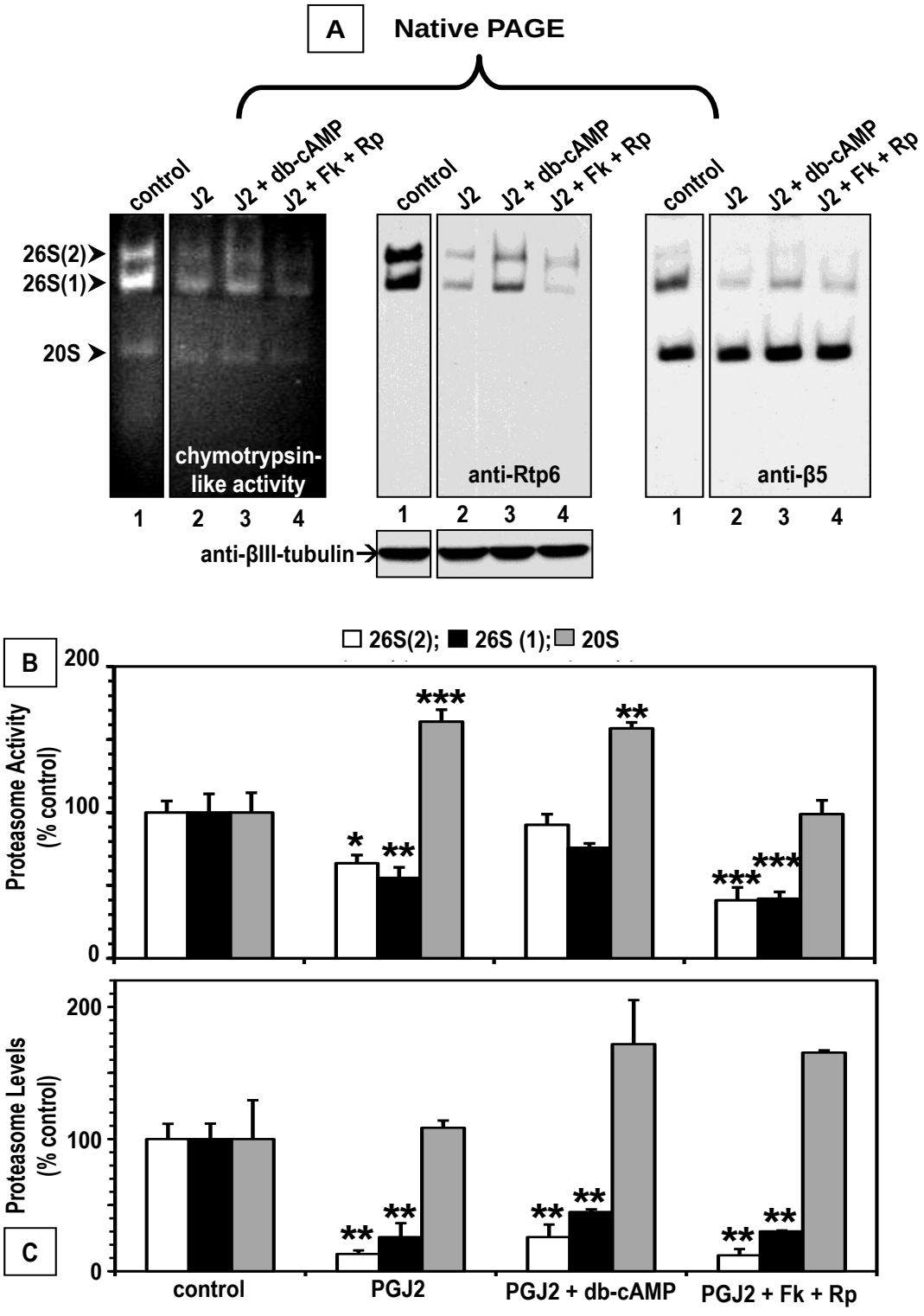
A
Native PAGE
control
J2
J2 + db-cAMP
J2 + Fk + Rp
26S(2)
26S(1)
20S
chymotrypsin-like activity
anti-Rtp6
anti-β5
anti-βIII-tubulin
1 2 3 4
B
26S(2); 26S (1); 20S
Proteasome Activity (% control)
200
100
0
C
Proteasome Levels (% control)
control
PGJ2
PGJ2 + db-cAMP
PGJ2 + Fk + Rp

Figure 11

Figure 12 (next page) – Effect of db-cAMP, forskolin/rolipram (Fk+Rp), or PGJ2 (J2) separately or combined on the protein levels of proteasome subunits (Rpt6 and β5), p62/sqstm1 and PKA (sub Cα). Cell extracts were prepared from rat E18 spinal cord neuronal cultures treated separately with 0.5% DMSO (control), 1mM db-cAMP (db-cAMP), 100µM forskolin/10µM rolipram (Fk+Rp) or 20µM PGJ2 (J2) for 24h. Parallel cultures were pretreated for one hour with 1mM db-cAMP followed by 20µM PGJ2 for 24h (J2+db-cAMP) or with 100µM forskolin/10µM rolipram followed by 20µM PGJ2 for 24h (J2+Fk+Rp). (**A**) Western blot analyses (40µg of protein/lane; 10% gels) detected proteasome subunits (Rpt6 and β5), p62/sqstm1, PKA catalytic subunit Cα (PKA sub Cα), and βIII-tubulin (loading control). Molecular mass markers in kDa are shown on the left. (**B**) Protein bands were semi-quantified by densitometry. Percentages represent the ratio between the relative intensities for each condition and control (DMSO) considered to be 100%. Values indicate means and s.e. from three experiments. The *asterisks* identify values that are significantly different (*$p<0.05$; **$p<0.01$; ***$p<0.001$).

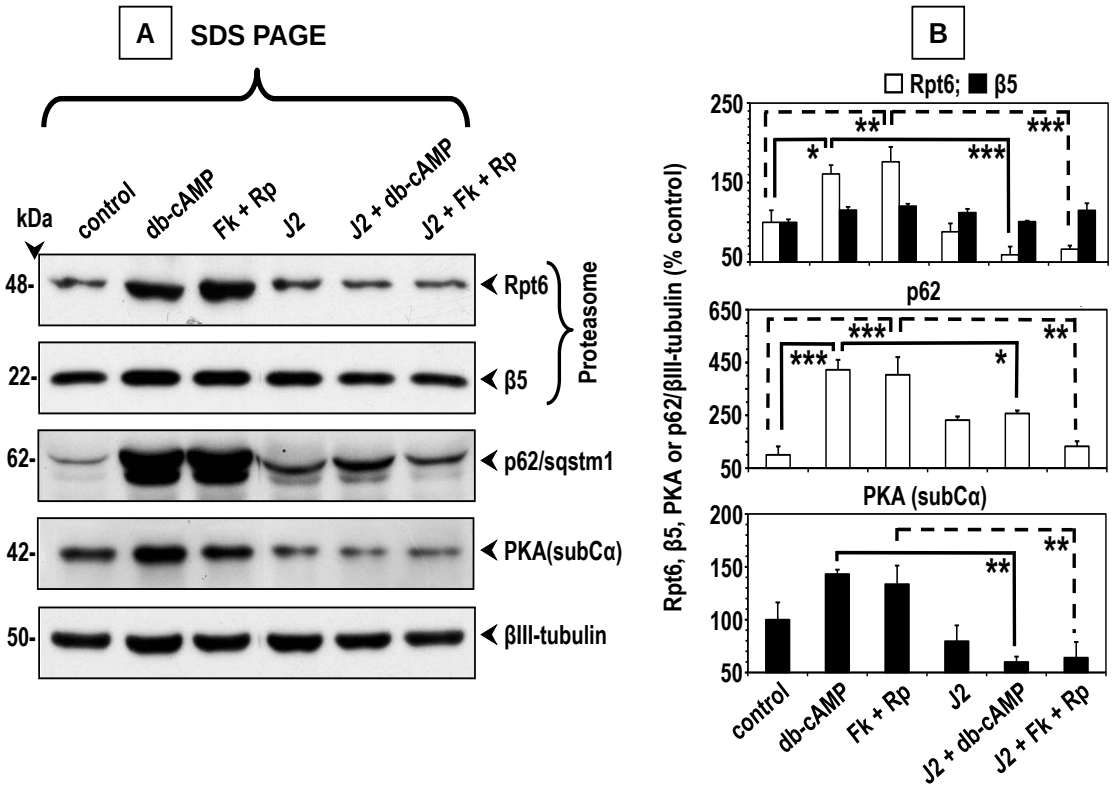
A
SDS PAGE
kDa
control
db-cAMP
Fk + Rp
J2
J2 + db-cAMP
J2 + Fk + Rp
48-
22-
62-
42-
50-
Rpt6
β5
Proteasome
p62/sqstm1
PKA(subCα)
βIII-tubulin
B
Rpt6; β5
p62
PKA (subCα)
Rpt6, β5, PKA or p62/βIII-tubulin (% control)
250
150
50
650
450
250
50
200
150
100
50
*
**
***
control
db-cAMP
Fk + Rp
J2
J2 + db-cAMP
J2 + Fk + Rp

Figure 12

Figure 13 (next page) – Effect of db-cAMP, forskolin/rolipram (Fk+Rp), or PGJ2 (J2) separately or combined on the expression of proteasome genes [*Rpt6 (psmc5*) and *β5* (*psmb5*)], p62/sqstm1 gene (*sqstm1*) and PKA subunit Cα gene (*prkaca*). Rat E18 spinal cord neuronal cultures were treated separately with 0.5% DMSO (control), 1mM db-cAMP, 100μM forskolin/10μM rolipram (Fk+Rp) or 20μM PGJ2 (J2) for 24h. Parallel cultures were pretreated for one hour with 1mM db-cAMP followed by 20μM PGJ2 for 24h (J2+db-cAMP) or with 100μM forskolin/10μM rolipram followed by 20μM PGJ2 for 24h (J2+Fk+Rp). Cell extracts were analyzed for expression of the listed genes by quantitative RT-PCR as described under "Methods". The mRNA level for each gene was normalized to *gapdh*. Percentages represent the ratio between data for each condition and control (DMSO) considered to be 100%. Values indicate mean and s.e. from two experiments each including triplicate determinations. The *asterisks* identify values that are significantly different *(*p <0.05; **p<0.01; ***p<0.001).*

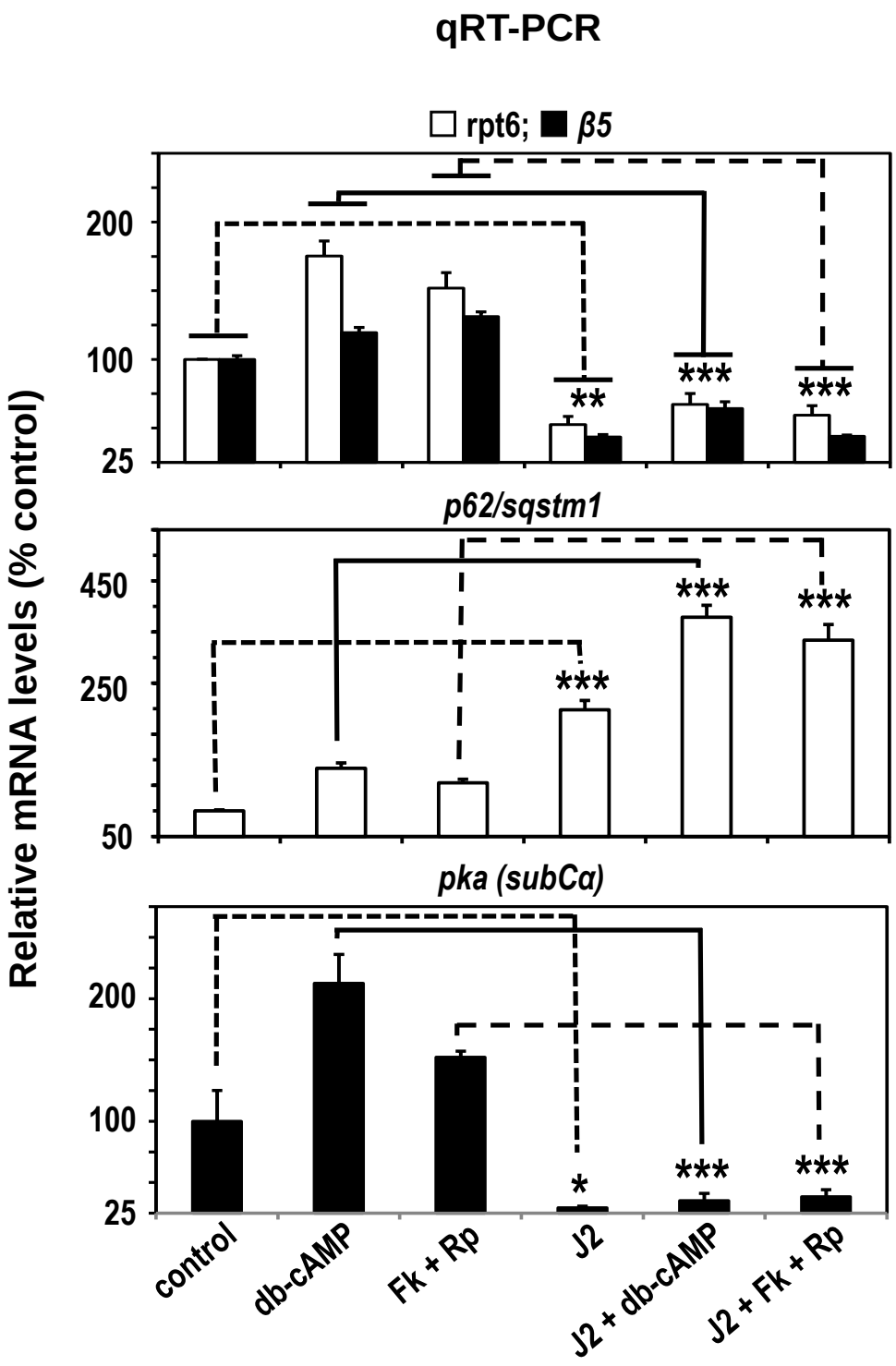
qRT-PCR
rpt6; β5
p62/sqstm1
pka (subCα)
Relative mRNA levels (% control)
200
100
25
450
250
50
**
***
*
control
db-cAMP
Fk + Rp
J2
J2 + db-cAMP
J2 + Fk + Rp

Figure 13

Figure 14 – (next page) PGJ2 reduces PKA stimulation by db-cAMP. Cell extracts were prepared from rat E18 spinal cord neuronal cultures treated separately with 0.5% DMSO (control), 1mM db-cAMP, 100µM forskolin/10µM rolipram (Fk+Rp) or 20µM PGJ2 (J2) for 24h. Parallel cultures were pretreated for one hour with 1mM db-cAMP followed by 20µM PGJ2 for 24h (J2+db-cAMP) or with 100µM forskolin/10µM rolipram followed by 20µM PGJ2 for 24h (J2+Fk+Rp). PKA activity was determined with a nonradioactive assay kit as described under "Methods". Percentages represent the ratio between data for each condition and control (DMSO) considered to be 100%. Values indicate mean and s.e. from three experiments. The *asterisks* identify values that are significantly different *(***p<0.001)*.

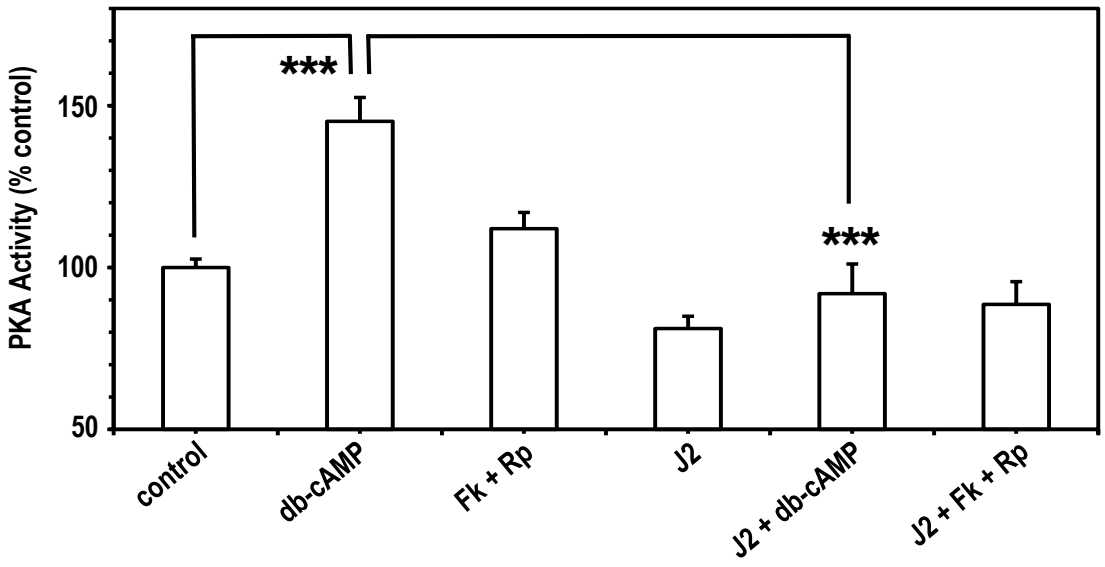
PKA Activity (% control)
150
100
50
***
***
control
db-cAMP
Fk + Rp
J2
J2 + db-cAMP
J2 + Fk + Rp

Figure 14

Figure 15 (next two pages) – Effect of db-cAMP, forskolin/rolipram (Fk+Rp), or PGJ2 (J2) separately or combined on ubiquitinated protein levels as well as on the expression of the ubiquitin genes *ubB* and *ubC*. Cell extracts were prepared from rat E18 spinal cord neuronal cultures treated separately with 0.5% DMSO (control), 1mM db-cAMP, 100µM forskolin/10µM rolipram (Fk+Rp) or 20µM PGJ2 (J2) for 24h. Parallel cultures were pretreated for one hour with 1mM db-cAMP followed by 20µM PGJ2 for 24h (J2+db-cAMP) or with 100µM forskolin/10µM rolipram followed by 20µM PGJ2 for 24h (J2+Fk+Rp). (**A**) Western blot analyses (40µg of protein/lane; 10% gels) detected ubiquitinated proteins (Ub-conjugates) and βIII-tubulin (loading control). Molecular mass markers in kDa are shown on the left. (**B**) Ub-conjugates were semi-quantified by densitometry. (**C**) *ubB and ubC* expression was analyzed by quantitative RT-PCR as described under "Methods". The mRNA level for each gene was normalized to *gapdh*. For (**B**) and (**C**) percentages represent the ratio between the data for each condition and control (DMSO) considered to be 100%. Data for (**B**) represent relative intensity. Values indicate means and s.e. from three experiments (**B**) and two experiments each including triplicate determinations (**C**).

The *asterisks* identify values that are significantly different (*$p<0.05$; **$p<0.01$; ***$p<0.001$

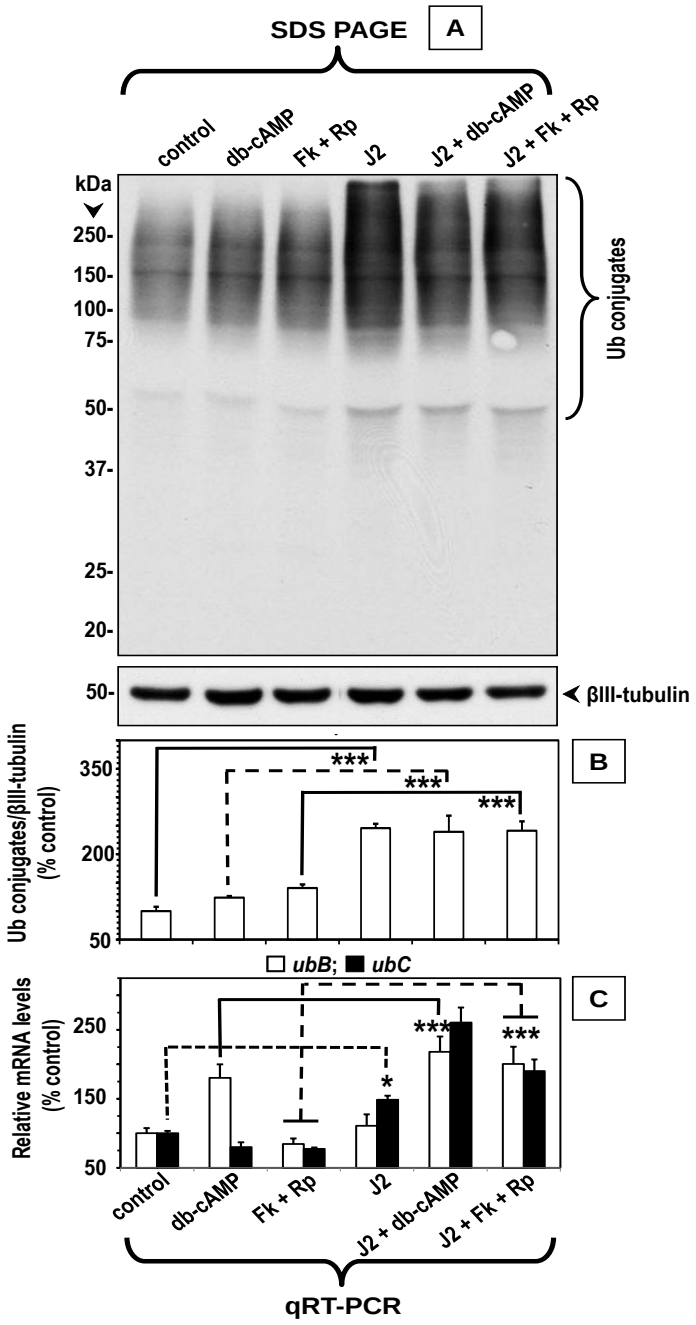
SDS PAGE
A
control
db-cAMP
Fk + Rp
J2
J2 + db-cAMP
J2 + Fk + Rp
kDa
250-
150-
100-
75-
50-
37-
25-
20-
Ub conjugates
50-
βIII-tubulin
B
Ub conjugates/βIII-tubulin (% control)
350
200
50
***
***
***
ubB; ubC
C
Relative mRNA levels (% control)
250
150
50
*
***
***
control
db-cAMP
Fk + Rp
J2
J2 + db-cAMP
J2 + Fk + Rp
qRT-PCR

Figure 15

Fig. 16 (next page) – Db-cAMP mitigates PGJ2 cytotoxicity and its reduction of cell viability. Rat E18 spinal cord neuronal cultures were treated separately with 0.5% DMSO (control), 1mM db-cAMP, 100µM forskolin/10µM rolipram (Fk+Rp) or 20µM PGJ2 for 24h. Parallel cultures were pretreated for one hour with 1mM db-cAMP followed by 20µM PGJ2 for 24h (J2+db-cAMP) or with 100µM forskolin/10µM rolipram followed by 20µM PGJ2 for 24h (J2+Fk+Rp). Cell toxicity was assessed with the bioluminescent cytotoxicity assay (**A**) and viability with the MTT assay (**B**) as described in "Methods". Percentages represent the ratio between the data for each condition and control (DMSO) considered to be 100%. Values indicate means and s.e. from three experiments. The *asterisks* identify values that are significantly different (*$p<0.05$; ***$p<0.001$)

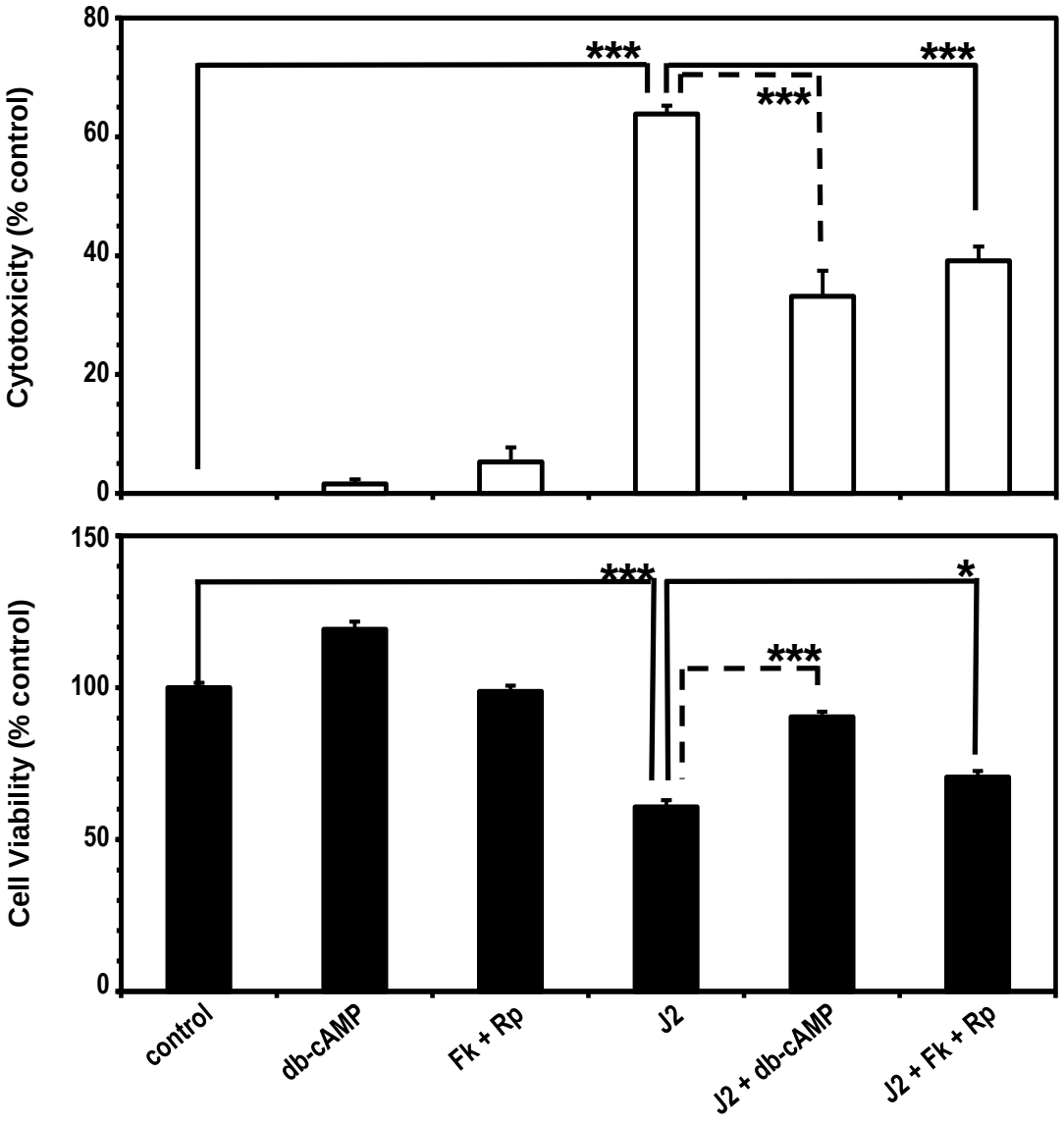
Cytotoxicity (% control)
80
60
40
20
0
***
***
***
Cell Viability (% control)
150
100
50
0
***
***
*
control
db-cAMP
Fk + Rp
J2
J2 + db-cAMP
J2 + Fk + Rp

Figure 16

Figure 17 (next page) – PGJ2 induces aggregation of ubiquitinated proteins and neurite fragmentation in spinal cord neuronal cultures. Double immunofluorescence staining of rat E18 spinal cord neuronal cultures treated separately with 0.5% DMSO (control, **A**), 1mM db-cAMP (**B**), and 20μM PGJ2 (**C**) for 24h or pre-treated with 1mM db-cAMP followed by 20μM PGJ2 for 24h (**D**). Neurofilament (heavy chain) was detected (*green*) with the SMI-32 antibody, ubiquitin aggregates (*red*) with the anti-ubiquitin antibody, and nuclei (*blue*) with DAPI. Merged images are shown for SMI-32/DAPI (*left panels*) and SMI-32/ubiquitin (*right panels*). The *arrows* point to fragmented neurites. Scale bar = 34μm. Similar results were obtained in duplicate experiments

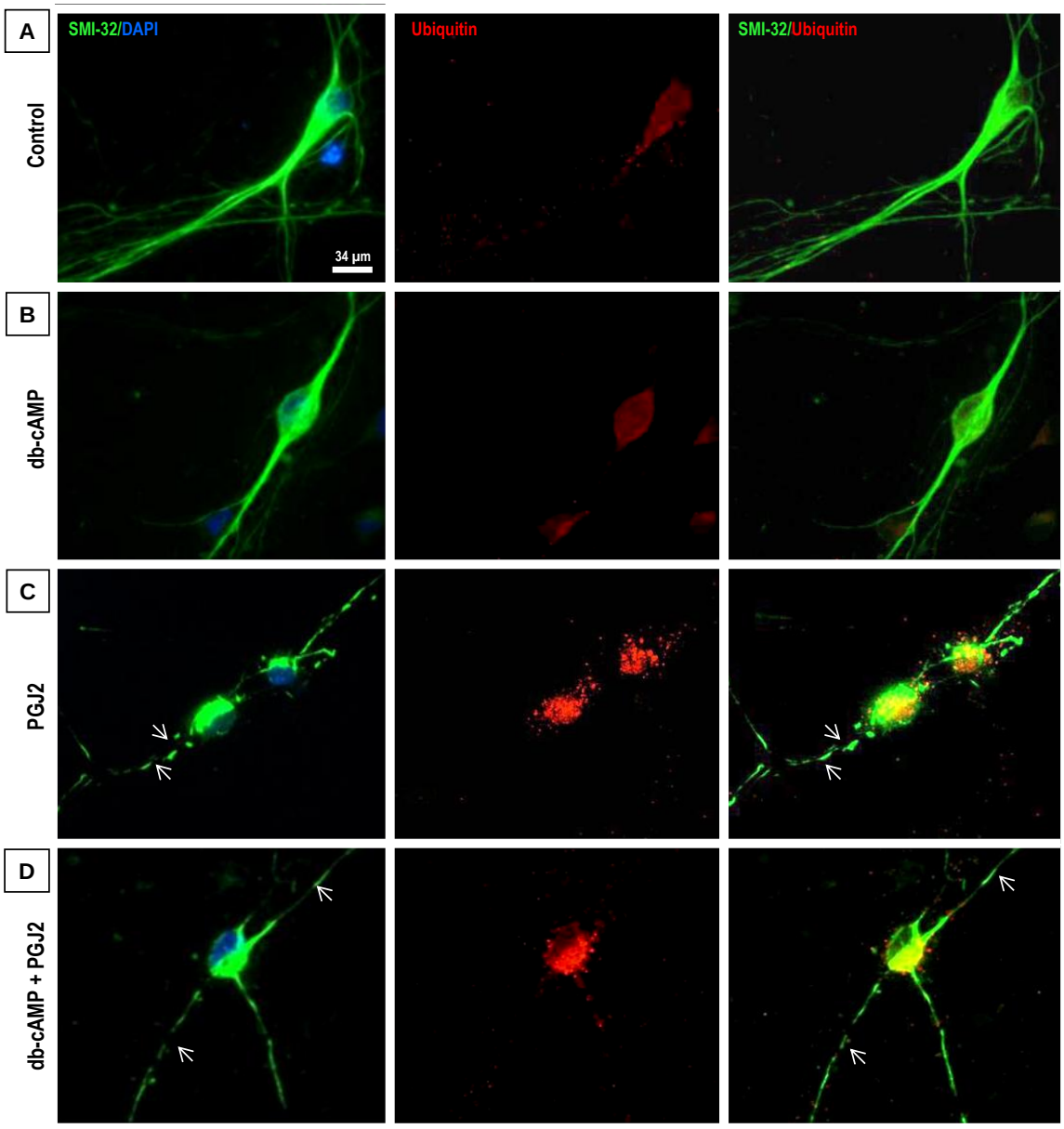
A
Control
SMI-32/DAPI
Ubiquitin
SMI-32/Ubiquitin
34 µm
B
db-cAMP
C
PGJ2
D
db-cAMP + PGJ2

Figure 17

Figure 18 (next page) – PGJ2 induces neurofilament (heavy chain) redistribution in ventral horn motor neurons of spinal cord (lumbar) organotypic slices. Neurofilament (heavy chain) immunofluorescence staining of rat E18 lumbar spinal cord organotypic slices treated separately with 0.5% DMSO (control, **A, E**), 1mM db-cAMP (**B, F**), and 20µM PGJ2 (**C, G**) for 24h or pre-treated with 1mM db-cAMP followed by 20µM PGJ2 for 24h (**D, H**). Neurofilament (heavy chain) was detected with the SMI-32 antibody. Scale bars = 200µm (***A-D***) and 20µm (***E-H***). Similar results were obtained in duplicate experiments.

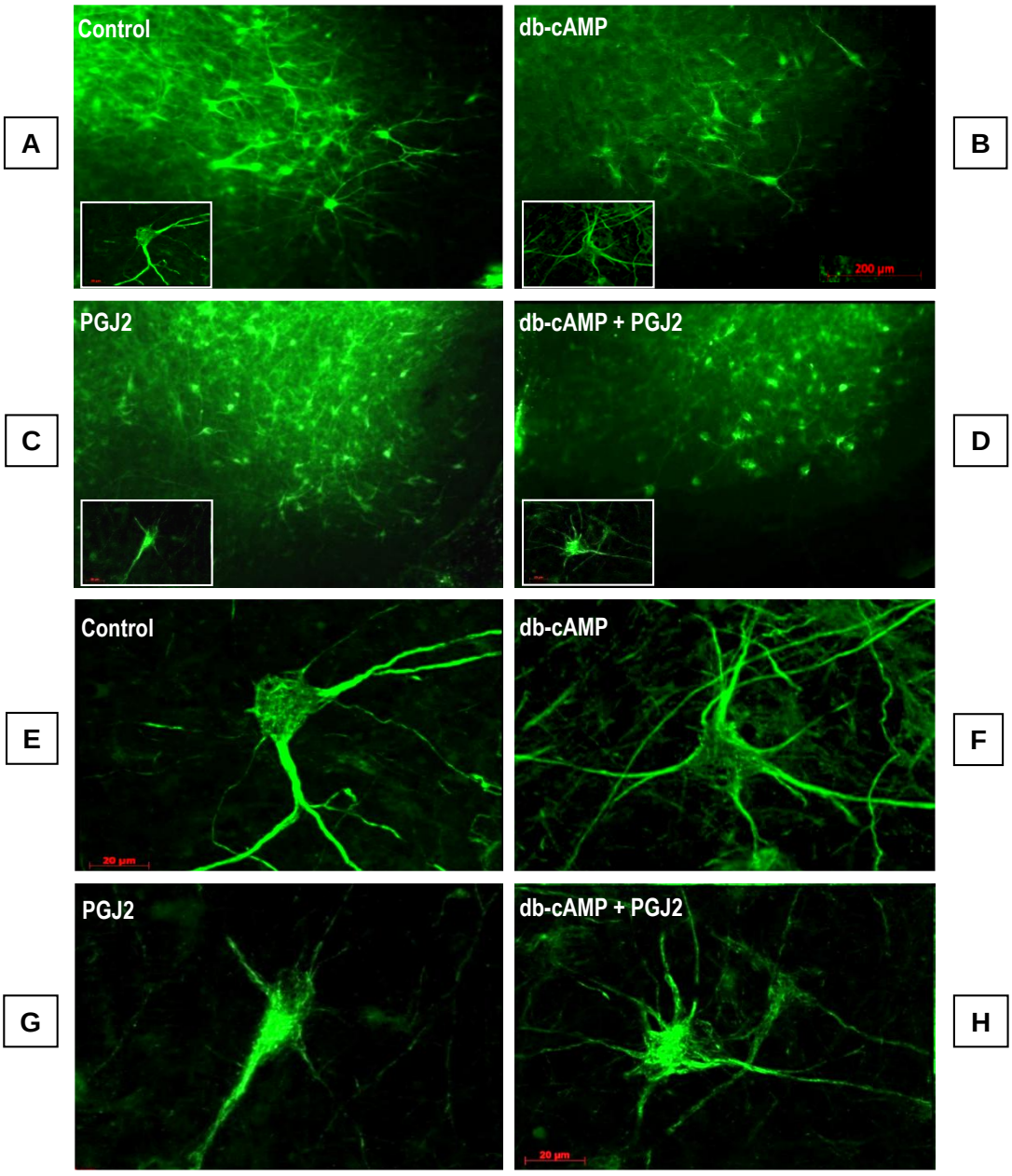
A
Control
B
db-cAMP
200 µm
C
PGJ2
D
db-cAMP + PGJ2
E
Control
20 µm
F
db-cAMP
G
PGJ2
H
db-cAMP + PGJ2
20 µm

Figure 18

Figure. 19 (next page). PGJ2-treatment increases caspase activity. (a) The activities of caspases 2, 3, 8 and 9 were determined in SK-N-SH cells treated with DMSO (vehicle, *black bars*) or with 20µM PGJ2 (*white bars*) for 16h. Relative caspase activities (RFU = relative fluorescent units) normalized for protein (200µg/assay) are shown. Results from two determinations are presented (mean ± SD). The *asterisk* (*) identifies the values that are significantly different ($p \leq 0.014$, t-test) from the controls. **(b)** Caspase 3 and **(c)** Caspase 2 activities were determined in SK-N-SH cells treated with DMSO (control, 2h and 20h, *black bars*) or with 20µM PGJ2 (*white bars*) for 2h, 4h, 8h, 16h, and 20h. Relative caspase activities (RFU or RCU = relative fluorescent or colorimetric units, respectively) normalized for protein (200µg/assay) are shown. Results from at least two determinations are presented [mean ± SEM **(b)** and SD **(c)**]. The *asterisk* (*) identifies the values that are significantly different (at least $p<0.01$, ANOVA, Tukey-Kramer multiple comparison test) from the control.

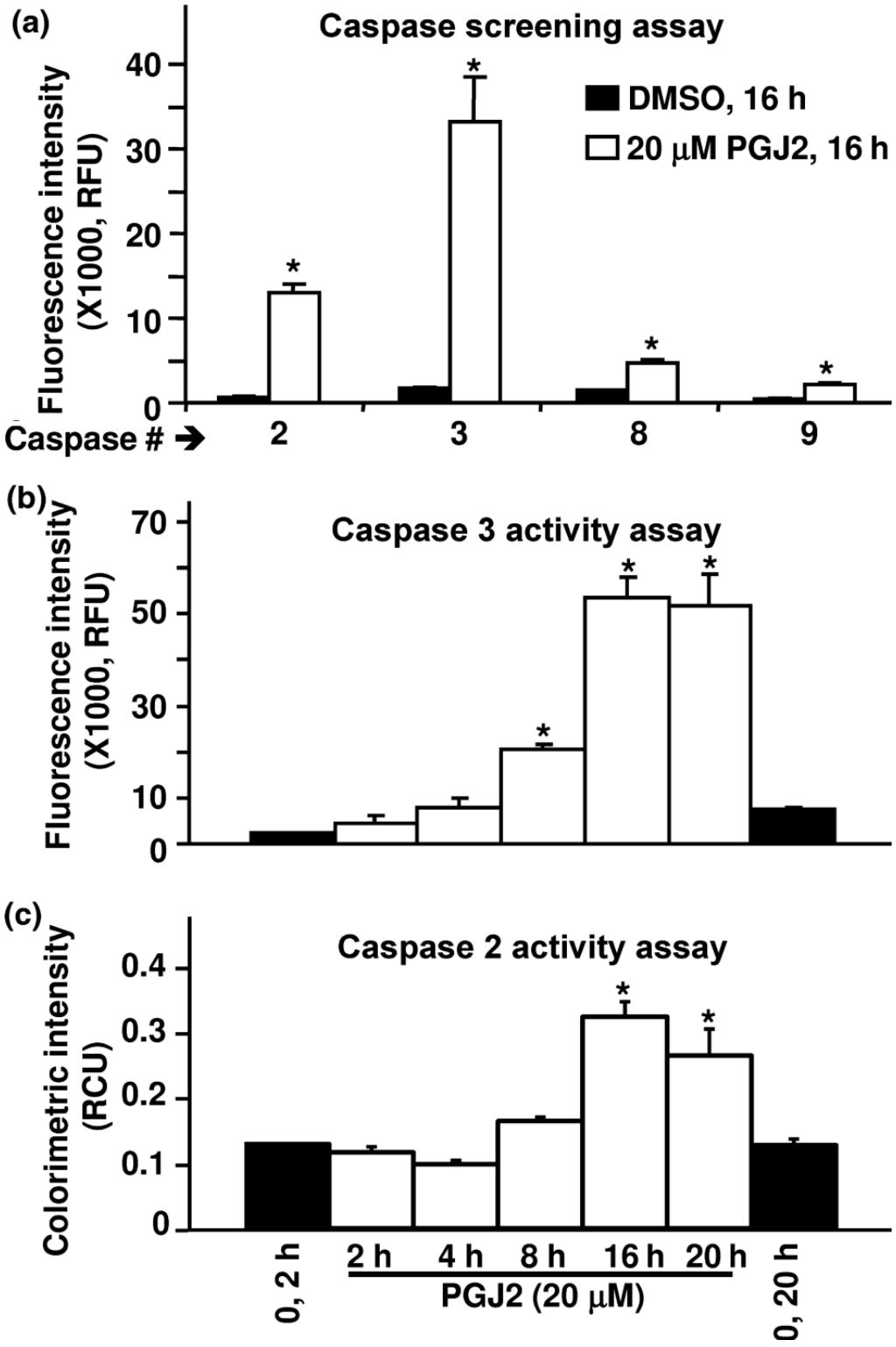
(a)
Caspase screening assay
DMSO, 16 h
20 μM PGJ2, 16 h
Fluorescence intensity (X1000, RFU)
40
30
20
10
0
Caspase # ➔
2
3
8
9
(b)
Caspase 3 activity assay
Fluorescence intensity (X1000, RFU)
70
50
30
10
0
(c)
Caspase 2 activity assay
Colorimetric intensity (RCU)
0.4
0.3
0.2
0.1
0
0, 2 h
2 h
4 h
8 h
16 h
20 h
PGJ2 (20 μM)
0, 20 h

Figure 19

Fig. 20. (next page). Caspase 3 knockdown by siRNA decreases the levels of PGJ2-induced tau cleavage at Asp421 in rat (E18) primary cortical neuronal cultures. Neuronal cultures were treated with Caspase 3 (Casp3) siRNA at 80nM and total lysates were analyzed by western blotting (18µg of protein/lane) to detect in **(a)** full length (FL) and cleaved (Δ) tau as well as pro-caspase 3, in **(b)** Δtau, in **(c)** cleaved (Δ) caspase 3 and in **(d)** β tubulin, as loading control. Following siRNA incubations (6h) the cortical cultures were treated with DMSO (vehicle, control, C) or 20µM PGJ2 (J2) for 16h. The same blot was probed sequentially with the TauC3, caspase 3, pan TauC5 and β tubulin antibodies. The levels of tauFL, Δtau, pro-caspase3 (*pro-Casp3*) and cleaved caspase3 (Δ*Casp3*) were semi-quantified by densitometry **(e and f)**. The graphs correspond to control **(e)** and PGJ2-treated **(f)** cultures. Within each graph, the *white bars* represent untreated cultures (*no Casp3 siRNA*) and *black bars* represent cultures treated with Casp3 siRNA. The numbers above the *black bars* correspond to the percent decrease in expression because of the Casp3 siRNA treatment. As a control, cells were treated with a scrambled siRNA instead of the Casp 3 siRNA and probed for Δtau **(h)** and procaspase 3 **(g)**. Molecular mass markers in

kDa are shown in the middle. ΔTAU, tau cleaved at Asp421; TAU FL, full length tau.

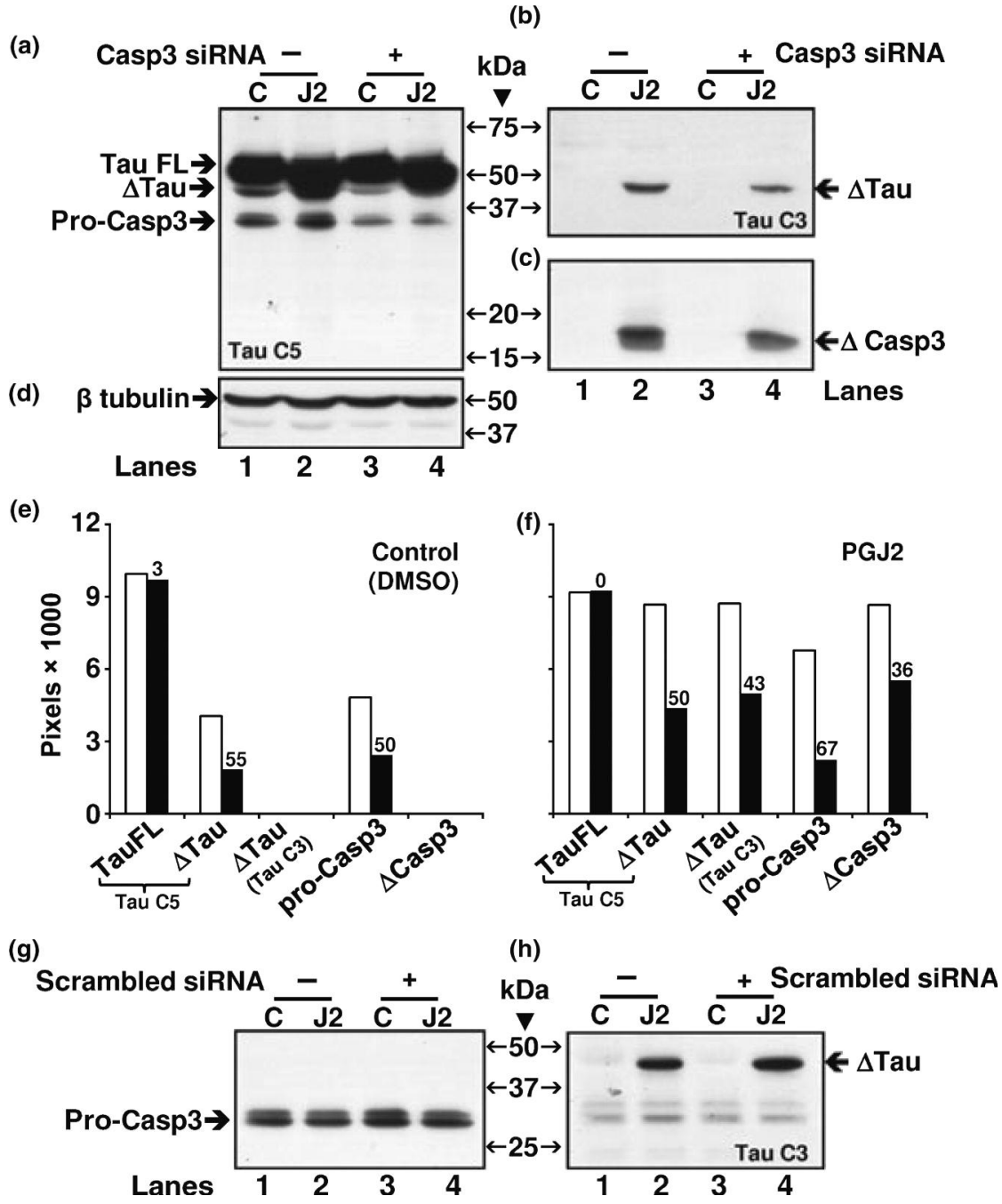

Figure 20

CHAPTER VIII

REFERENCES

Reference List

1. **Abdel-Halim MS, Hamberg M, Sjoquist B and Anggard E.** Identification of prostaglandin D2 as a major prostaglandin in homogenates of rat brain. *Prostaglandins* 14: 633-643, 1977.

2. **Abeliovich H and Klionsky DJ.** Autophagy in yeast: mechanistic insights and physiological function. *Microbiol Mol Biol Rev* 65: 463-79, table, 2001.

3. **Allen S, Heath PR, Kirby J, Wharton SB, Cookson MR, Menzies FM, Banks RE and Shaw PJ.** Analysis of the cytosolic proteome in a cell culture model of familial amyotrophic lateral sclerosis reveals alterations to the proteasome, antioxidant defenses, and nitric oxide synthetic pathways. *J Biol Chem* 278: 6371-6383, 2003.

4. **Almer G, Guegan C, Teismann P, Naini A, Rosoklija G, Hays AP, Chen C and Przedborski S.** Increased expression of the pro-inflammatory enzyme cyclooxygenase-2 in amyotrophic lateral sclerosis. *Ann Neurol* 49: 176-185, 2001.

5. **Almer G, Kikuchi H, Teismann P and Przedborski S.** Is prostaglandin E(2) a pathogenic factor in amyotrophic lateral sclerosis? *Ann Neurol* 59: 980-983, 2006.

6. **Alves-Rodrigues A, Gregori L and Figueiredo-Pereira ME.** Ubiquitin, cellular inclusions and their role in neurodegeneration. *Trends Neurosci* 21: 516-520, 1998.

7. **Alves-Rodrigues A, Gregori L and Figueiredo-Pereira ME.** Ubiquitin, cellular inclusions and their role in neurodegeneration. *Trends Neurosci* 21: 516-520, 1998.

8. **Asai M, Tsukamoto O, Minamino T, Asanuma H, Fujita M, Asano Y, Takahama H, Sasaki H, Higo S, Asakura M, Takashima S, Hori M and Kitakaze M.** PKA rapidly

enhances proteasome assembly and activity in in vivo canine hearts. *J Mol Cell Cardiol* 46: 452-462, 2009.

9. **Asai M, Tsukamoto O, Minamino T, Asanuma H, Fujita M, Asano Y, Takahama H, Sasaki H, Higo S, Asakura M, Takashima S, Hori M and Kitakaze M.** PKA rapidly enhances proteasome assembly and activity in in vivo canine hearts. *J Mol Cell Cardiol* 46: 452-462, 2009.

10. **Asai M, Tsukamoto O, Minamino T, Asanuma H, Fujita M, Asano Y, Takahama H, Sasaki H, Higo S, Asakura M, Takashima S, Hori M and Kitakaze M.** PKA rapidly enhances proteasome assembly and activity in in vivo canine hearts. *J Mol Cell Cardiol* 46: 452-462, 2009.

11. **Asai M, Tsukamoto O, Minamino T, Asanuma H, Fujita M, Asano Y, Takahama H, Sasaki H, Higo S, Asakura M, Takashima S, Hori M and Kitakaze M.** PKA rapidly enhances proteasome assembly and activity in in vivo canine hearts. *J Mol Cell Cardiol* 46: 452-462, 2009.

12. **Babbitt SE, Kiss A, Deffenbaugh AE, Chang YH, Bailly E, Erdjument-Bromage H, Tempst P, Buranda T, Sklar LA, Baumler J, Gogol E and Skowyra D.** ATP hydrolysis-dependent disassembly of the 26S proteasome is part of the catalytic cycle. *Cell* 121: 553-565, 2005.

13. **Bader N, Jung T and Grune T.** The proteasome and its role in nuclear protein maintenance. *Exp Gerontol* 2007.

14. **Bartolini M and Andrisano V.** Strategies for the inhibition of protein aggregation in human diseases. *Chembiochem* 11: 1018-1035, 2010.

15. **Bartolini M and Andrisano V.** Strategies for the inhibition of protein aggregation in human diseases. *Chembiochem* 11: 1018-1035, 2010.

16. **Bedford L, Hay D, Paine S, Rezvani N, Mee M, Lowe J and Mayer RJ.** Is malfunction of the ubiquitin

proteasome system the primary cause of alpha-synucleinopathies and other chronic human neurodegenerative disease? *Biochim Biophys Acta* 1782: 683-690, 2008.

17. **Benaroudj N, Zwickl P, Seemuller E, Baumeister W and Goldberg AL.** ATP hydrolysis by the proteasome regulatory complex PAN serves multiple functions in protein degradation. *Mol Cell* 11: 69-78, 2003.

18. **Biederer T and Scheiffele P.** Mixed-culture assays for analyzing neuronal synapse formation. *Nat Protoc* 2: 670-676, 2007.

19. **Biedler JL, Roffler-Tarlov S, Schachner M and Freedman LS.** Multiple neurotransmitter synthesis by human neuroblastoma cell lines and clones. *Cancer Res* 38: 3751-3757, 1978.

20. **Bjorkoy G, Lamark T, Brech A, Outzen H, Perander M, Overvatn A, Stenmark H and Johansen T.** p62/SQSTM1 forms protein aggregates degraded by autophagy and has a protective effect on huntingtin-induced cell death. *J Cell Biol* 171: 603-614, 2005.

21. **Boland B and Nixon RA.** Neuronal macroautophagy: from development to degeneration. *Mol Aspects Med* 27: 503-519, 2006.

22. **Boland B and Nixon RA.** Neuronal macroautophagy: from development to degeneration. *Mol Aspects Med* 27: 503-519, 2006.

23. **Brooks P, Fuertes G, Murray RZ, Bose S, Knecht E, Rechsteiner MC, Hendil KB, Tanaka K, Dyson J and Rivett J.** Subcellular localization of proteasomes and their regulatory complexes in mammalian cells. *Biochem J* 346 Pt 1: 155-161, 2000.

24. **Bruijn LI, Miller TM and Cleveland DW.** Unraveling the mechanisms involved in motor neuron degeneration in ALS. *Annu Rev Neurosci* 27: 723-749, 2004.

25. **Chain DG, Hegde AN, Yamamoto N, Liu-Marsh B and Schwartz JH.** Persistent activation of cAMP-dependent protein kinase by regulated proteolysis suggests a neuron-specific function of the ubiquitin system in Aplysia. *J Neurosci* 15: 7592-7603, 1995.

26. **Chen P and Hochstrasser M.** Autocatalytic subunit processing couples active site formation in the 20S proteasome to completion of assembly. *Cell* 86: 961-972, 1996.

27. **Cheroni C, Marino M, Tortarolo M, Veglianese P, De BS, Fontana E, Zuccarello LV, Maynard CJ, Dantuma NP and Bendotti C.** Functional alterations of the ubiquitin-proteasome system in motor neurons of a mouse model of familial amyotrophic lateral sclerosis. *Hum Mol Genet* 18: 82-96, 2009.

28. **Ciechanover A.** Intracellular protein degradation: from a vague idea thru the lysosome and the ubiquitin-proteasome system and onto human diseases and drug targeting. *Cell Death Differ* 12: 1178-1190, 2005.

29. **Costa J, Gomes C and de CM.** Diagnosis, pathogenesis and therapeutic targets in amyotrophic lateral sclerosis. *CNS Neurol Disord Drug Targets* 9: 764-778, 2010.

30. **Costes S, Vandewalle B, Tourrel-Cuzin C, Broca C, Linck N, Bertrand G, Kerr-Conte J, Portha B, Pattou F, Bockaert J and Dalle S.** Degradation of cAMP-responsive element-binding protein by the ubiquitin-proteasome pathway contributes to glucotoxicity in beta-cells and human pancreatic islets. *Diabetes* 58: 1105-1115, 2009.

31. **Coux O, Tanaka K and Goldberg AL.** Structure and functions of the 20S and 26S proteasomes. *Annu Rev Biochem* 65: 801-847, 1996.

32. **Dasuri K, Ebenezer PJ, Zhang L, Fernandez-Kim SO, Uranga RM, Gavilan E, Di BA and Keller JN.** Selective vulnerability of neurons to acute toxicity after proteasome inhibitor treatment: implications for oxidative stress and insolubility of newly synthesized proteins. *Free Radic Biol Med* 49: 1290-1297, 2010.

33. **Davidson TJ, Harel S, Arboleda VA, Prunell GF, Shelanski ML, Greene LA and Troy CM.** Highly efficient small interfering RNA delivery to primary mammalian neurons induces MicroRNA-like effects before mRNA degradation. *J Neurosci* 24: 10040-10046, 2004.

34. **DeMartino GN and Slaughter CA.** The proteasome, a novel protease regulated by multiple mechanisms. *J Biol Chem* 274: 22123-22126, 1999.

35. **Dirig DM and Yaksh TL.** In vitro prostanoid release from spinal cord following peripheral inflammation: effects of substance P, NMDA and capsaicin. *Br J Pharmacol* 126: 1333-1340, 1999.

36. **Drachman DB, Frank K, Dykes-Hoberg M, Teismann P, Almer G, Przedborski S and Rothstein JD.** Cyclooxygenase 2 inhibition protects motor neurons and prolongs survival in a transgenic mouse model of ALS. *Ann Neurol* 52: 771-778, 2002.

37. **Drews O, Tsukamoto O, Liem D, Streicher J, Wang Y and Ping P.** Differential regulation of proteasome function in isoproterenol-induced cardiac hypertrophy. *Circ Res* 107: 1094-1101, 2010.

38. **Drews O, Tsukamoto O, Liem D, Streicher J, Wang Y and Ping P.** Differential regulation of proteasome function in isoproterenol-induced cardiac hypertrophy. *Circ Res* 107: 1094-1101, 2010.

39. **Du J, Mitch WE, Wang X and Price SR.** Glucocorticoids induce proteasome C3 subunit expression in L6 muscle cells by opposing the suppression of its transcription by NF-kappa B. *J Biol Chem* 275: 19661-19666, 2000.

40. **Du Y, Wooten MC and Wooten MW.** Oxidative damage to the promoter region of SQSTM1/p62 is common to neurodegenerative disease. *Neurobiol Dis* 35: 302-310, 2009.

41. **Du Y, Wooten MC and Wooten MW.** Oxidative damage to the promoter region of SQSTM1/p62 is common to neurodegenerative disease. *Neurobiol Dis* 35: 302-310, 2009.

42. **Elsasser S, Schmidt M and Finley D.** Characterization of the proteasome using native gel electrophoresis. *Methods Enzymol* 398: 353-363, 2005.

43. **Fredriksson S, Gullberg M, Jarvius J, Olsson C, Pietras K, Gustafsdottir SM, Ostman A and Landegren U.** Protein detection using proximity-dependent DNA ligation assays. *Nat Biotechnol* 20: 473-477, 2002.

44. **Fuentes JJ, Pritchard MA, Planas AM, Bosch A, Ferrer I and Estivill X.** A new human gene from the Down syndrome critical region encodes a proline-rich protein highly expressed in fetal brain and heart. *Hum Mol Genet* 4: 1935-1944, 1995.

45. **Fukushima M.** Prostaglandin J2--anti-tumour and anti-viral activities and the mechanisms involved. *Eicosanoids* 3: 189-199, 1990.

46. **Gao Z, Gammoh N, Wong PM, Erdjument-Bromage H, Tempst P and Jiang X.** Processing of autophagic protein LC3 by the 20S proteasome. *Autophagy* 6: 126-137, 2010.

47. **Gilroy DW, Colville-Nash PR, Willis D, Chivers J, Paul-Clark MJ and Willoughby DA.** Inducible cyclooxygenase may have anti-inflammatory properties [see comments]. *Nat Med* 5: 698-701, 1999.

48. **Glass CK, Saijo K, Winner B, Marchetto MC and Gage FH.** Mechanisms underlying inflammation in neurodegeneration. *Cell* 140: 918-934, 2010.

49. **Glass CK, Saijo K, Winner B, Marchetto MC and Gage FH.** Mechanisms underlying inflammation in neurodegeneration. *Cell* 140: 918-934, 2010.

50. **Goldberg AL.** Functions of the proteasome: from protein degradation and immune surveillance to cancer therapy. *Biochem Soc Trans* 35: 12-17, 2007.

51. **Groll M, Bajorek M, Kohler A, Moroder L, Rubin DM, Huber R, Glickman MH and Finley D.** A gated channel into the proteasome core particle. *Nat Struct Biol* 7: 1062-1067, 2000.

52. **Groll M, Ditzel L, Lowe J, Stock D, Bochtler M, Bartunik HD and Huber R.** Structure of 20S proteasome from yeast at 2.4 A resolution [see comments]. *Nature* 386: 463-471, 1997.

53. **Gronostajski RM, Pardee AB and Goldberg AL.** The ATP dependence of the degradation of short- and long-lived proteins in growing fibroblasts. *J Biol Chem* 260: 3344-3349, 1985.

54. **Guillozet-Bongaarts AL, Garcia-Sierra F, Reynolds MR, Horowitz PM, Fu Y, Wang T, Cahill ME, Bigio EH, Berry RW and Binder LI.** Tau truncation during neurofibrillary tangle evolution in Alzheimer's disease. *Neurobiol Aging* 26: 1015-1022, 2005.

55. **Haas AL and Bright PM.** The dynamics of ubiquitin pools within cultured human lung fibroblasts. *J Biol Chem* 262: 345-351, 1987.

56. **Halliwell B.** Hypothesis: proteasomal dysfunction: a primary event in neurogeneration that leads to nitrative and oxidative stress and subsequent cell death. *Ann N Y Acad Sci* 962: 182-194, 2002.

57. **Hanna J and Finley D.** A proteasome for all occasions. *FEBS Lett* 581: 2854-2861, 2007.

58. **Hanna J, Meides A, Zhang DP and Finley D.** A ubiquitin stress response induces altered proteasome composition. *Cell* 129: 747-759, 2007.

59. **Hara T, Nakamura K, Matsui M, Yamamoto A, Nakahara Y, Suzuki-Migishima R, Yokoyama M, Mishima K, Saito I, Okano H and Mizushima N.** Suppression of basal autophagy in neural cells causes neurodegenerative disease in mice. *Nature* 441: 885-889, 2006.

60. **Hara T, Nakamura K, Matsui M, Yamamoto A, Nakahara Y, Suzuki-Migishima R, Yokoyama M, Mishima K, Saito I, Okano H and Mizushima N.** Suppression of basal autophagy in neural cells causes neurodegenerative disease in mice. *Nature* 441: 885-889, 2006.

61. **Hara T, Nakamura K, Matsui M, Yamamoto A, Nakahara Y, Suzuki-Migishima R, Yokoyama M, Mishima K, Saito I, Okano H and Mizushima N.** Suppression of basal autophagy in neural cells causes neurodegenerative disease in mice. *Nature* 441: 885-889, 2006.

62. **Hara T, Nakamura K, Matsui M, Yamamoto A, Nakahara Y, Suzuki-Migishima R, Yokoyama M, Mishima K, Saito I, Okano H and Mizushima N.** Suppression of basal autophagy in neural cells causes neurodegenerative disease in mice. *Nature* 441: 885-889, 2006.

63. **Hara T, Nakamura K, Matsui M, Yamamoto A, Nakahara Y, Suzuki-Migishima R, Yokoyama M, Mishima K, Saito I, Okano H and Mizushima N.** Suppression of basal autophagy in neural cells causes neurodegenerative disease in mice. *Nature* 441: 885-889, 2006.

64. **Hara T, Nakamura K, Matsui M, Yamamoto A, Nakahara Y, Suzuki-Migishima R, Yokoyama M, Mishima K, Saito I, Okano H and Mizushima N.** Suppression of basal autophagy in neural cells causes neurodegenerative disease in mice. *Nature* 441: 885-889, 2006.

65. **Harris SG, Padilla J, Koumas L, Ray D and Phipps RP.** Prostaglandins as modulators of immunity. *Trends Immunol* 23: 144-150, 2002.

66. **Harris SG, Padilla J, Koumas L, Ray D and Phipps RP.** Prostaglandins as modulators of immunity. *Trends Immunol* 23: 144-150, 2002.

67. **Hartmann-Petersen R, Semple CA, Ponting CP, Hendil KB and Gordon C.** UBA domain containing proteins in fission yeast. *Int J Biochem Cell Biol* 35: 629-636, 2003.

68. **Heggie P, Burdon T, Lowe J, Landon M, Lennox G, Jefferson D and Mayer RJ.** Ubiquitin gene expression in brain and spinal cord in motor neurone disease. *Neurosci Lett* 102: 343-348, 1989.

69. **Heinen C, Garner TP, Long J, Bottcher C, Ralston SH, Cavey JR, Searle MS, Layfield R and Dantuma NP.** Mutant p62/SQSTM1 UBA domains linked to Paget's disease of bone differ in their abilities to function as stabilization signals. *FEBS Lett* 584: 1585-1590, 2010.

70. **Heink S, Ludwig D, Kloetzel PM and Kruger E.** IFN-gamma-induced immune adaptation of the proteasome system is an accelerated and transient response. *Proc Natl Acad Sci U S A* 102: 9241-9246, 2005.

71. **Heink S, Ludwig D, Kloetzel PM and Kruger E.** IFN-gamma-induced immune adaptation of the proteasome system is an accelerated and transient response. *Proc Natl Acad Sci U S A* 102: 9241-9246, 2005.

72. **Henderson CE, Bloch-Gallego E and Camu W.** Purified embryonic motoneurons. In: Neural Cell culture, edited by Cohen J and Wilkin GP. Oxford: Oxford University Press, 2002, p. 69-81.

73. **Herschman HR, Reddy ST and Xie W.** Function and regulation of prostaglandin synthase-2. *Adv Exp Med Biol* 407: 61-66, 1997.

74. **Hershko A and Ciechanover A.** The ubiquitin system [In Process Citation]. *Annu Rev Biochem* 67: 425-479, 1998.

75. **Hirai H, Tanaka K, Yoshie O, Ogawa K, Kenmotsu K, Takamori Y, Ichimasa M, Sugamura K, Nakamura M, Takano S and Nagata K.** Prostaglandin D2 selectively induces chemotaxis in T helper type 2 cells, eosinophils, and basophils via seven-transmembrane receptor CRTH2. *J Exp Med* 193: 255-261, 2001.

76. **Huang Q and Figueiredo-Pereira ME.** Ubiquitin/proteasome pathway impairment in neurodegeneration: therapeutic implications. *Apoptosis* 15: 1292-1311, 2010.

77. **Huang Q and Figueiredo-Pereira ME.** Ubiquitin/proteasome pathway impairment in neurodegeneration: therapeutic implications. *Apoptosis* 15: 1292-1311, 2010.

78. **Ishii T, Sakurai T, Usami H and Uchida K.** Oxidative modification of proteasome: identification of an oxidation-sensitive subunit in 26 s proteasome. *Biochemistry* 44: 13893-13901, 2005.

79. **Iwamoto N, Kobayashi K and Kosaka K.** The formation of prostaglandins in the postmortem cerebral cortex of Alzheimer-type dementia patients. *J Neurol* 236: 80-84, 1989.

80. **Jackson M, Ganel R and Rothstein JD.** Models of amyotrophic lateral sclerosis. *Curr Protoc Neurosci* Chapter 9: Unit, 2002.

81. **Jenner P.** Oxidative stress in Parkinson's disease. *Ann Neurol* 53 Suppl 3: S26-S36, 2003.

82. **Kabashi E, Agar JN, Taylor DM, Minotti S and Durham HD.** Focal dysfunction of the proteasome: a pathogenic factor in a mouse model of amyotrophic lateral sclerosis. *J Neurochem* 89: 1325-1335, 2004.

83. **Kanekiyo T, Ban T, Aritake K, Huang ZL, Qu WM, Okazaki I, Mohri I, Murayama S, Ozono K, Taniike M, Goto Y and Urade Y.** Lipocalin-type prostaglandin D synthase/beta-trace is a major amyloid beta-chaperone in human cerebrospinal fluid. *Proc Natl Acad Sci U S A* 104: 6412-6417, 2007.

84. **Kanekiyo T, Ban T, Aritake K, Huang ZL, Qu WM, Okazaki I, Mohri I, Murayama S, Ozono K, Taniike M, Goto Y and Urade Y.** Lipocalin-type prostaglandin D synthase/beta-trace is a major amyloid beta-chaperone in human cerebrospinal fluid. *Proc Natl Acad Sci U S A* 104: 6412-6417, 2007.

85. **Keller JN, Gee J and Ding Q.** The proteasome in brain aging. *Ageing Res Rev* 1: 279-293, 2002.

86. **Keller JN, Hanni KB and Markesbery WR.** Impaired proteasome function in Alzheimer's disease. *J Neurochem* 75: 436-439, 2000.

87. **Kiaei M, Kipiani K, Petri S, Choi DK, Chen J, Calingasan NY and Beal MF.** Integrative role of cPLA with COX-2 and the effect of non-steriodal anti-inflammatory drugs in a transgenic mouse model of amyotrophic lateral sclerosis. *J Neurochem* 93: 403-411, 2005.

88. **Kiaei M, Kipiani K, Petri S, Choi DK, Chen J, Calingasan NY and Beal MF.** Integrative role of cPLA with COX-2 and the effect of non-steriodal anti-inflammatory drugs in a transgenic mouse model of amyotrophic lateral sclerosis. *J Neurochem* 93: 403-411, 2005.

89. **Kim HM, Yu Y and Cheng Y.** Structure characterization of the 26S proteasome. *Biochim Biophys Acta* 2010.

90. **Kim JY and Ozato K.** The sequestosome 1/p62 attenuates cytokine gene expression in activated macrophages by inhibiting IFN regulatory factor 8 and TNF receptor-associated factor 6/NF-kappaB activity. *J Immunol* 182: 2131-2140, 2009.

91. **Kirkegaard K, Taylor MP and Jackson WT.** Cellular autophagy: surrender, avoidance and subversion by microorganisms. *Nat Rev Microbiol* 2: 301-314, 2004.

92. **Kirkegaard K, Taylor MP and Jackson WT.** Cellular autophagy: surrender, avoidance and subversion by microorganisms. *Nat Rev Microbiol* 2: 301-314, 2004.

93. **Klionsky DJ.** The molecular machinery of autophagy: unanswered questions. *J Cell Sci* 118: 7-18, 2005.

94. **Klionsky DJ.** Neurodegeneration: good riddance to bad rubbish. *Nature* 441: 819-820, 2006.

95. **Koga H, Kaushik S and Cuervo AM.** Protein homeostasis and aging: The importance of exquisite quality control. *Ageing Res Rev* 2010.

96. **Komatsu M, Waguri S, Chiba T, Murata S, Iwata J, Tanida I, Ueno T, Koike M, Uchiyama Y, Kominami E and Tanaka K.** Loss of autophagy in the central nervous system causes neurodegeneration in mice. *Nature* 441: 880-884, 2006.

97. **Komatsu M, Waguri S, Chiba T, Murata S, Iwata J, Tanida I, Ueno T, Koike M, Uchiyama Y, Kominami E and Tanaka K.** Loss of autophagy in the central nervous system causes neurodegeneration in mice. *Nature* 441: 880-884, 2006.

98. **Komatsu M, Waguri S, Chiba T, Murata S, Iwata J, Tanida I, Ueno T, Koike M, Uchiyama Y, Kominami E and Tanaka K.** Loss of autophagy in the central nervous system causes neurodegeneration in mice. *Nature* 441: 880-884, 2006.

99. **Komatsu M, Waguri S, Chiba T, Murata S, Iwata J, Tanida I, Ueno T, Koike M, Uchiyama Y, Kominami E and Tanaka K.** Loss of autophagy in the central nervous system causes neurodegeneration in mice. *Nature* 441: 880-884, 2006.

100. **Komatsu M, Waguri S, Chiba T, Murata S, Iwata J, Tanida I, Ueno T, Koike M, Uchiyama Y, Kominami E and Tanaka K.** Loss of autophagy in the central nervous system causes neurodegeneration in mice. *Nature* 441: 880-884, 2006.

101. **Komatsu M, Waguri S, Koike M, Sou YS, Ueno T, Hara T, Mizushima N, Iwata J, Ezaki J, Murata S, Hamazaki J, Nishito Y, Iemura S, Natsume T, Yanagawa T, Uwayama J, Warabi E, Yoshida H, Ishii T, Kobayashi A, Yamamoto M, Yue Z, Uchiyama Y, Kominami E and Tanaka K.** Homeostatic levels of p62 control cytoplasmic inclusion body formation in autophagy-deficient mice. *Cell* 131: 1149-1163, 2007.

102. **Kondo M, Oya-Ito T, Kumagai T, Osawa T and Uchida K.** Cyclopentenone prostaglandins as potential inducers of intracellular oxidative stress. *J Biol Chem* 276: 12076-12083, 2001.

103. **Kondo M, Shibata T, Kumagai T, Osawa T, Shibata N, Kobayashi M, Sasaki S, Iwata M, Noguchi N and Uchida K.** 15-Deoxy-Delta(12,14)-prostaglandin J(2): the endogenous electrophile that induces neuronal apoptosis. *Proc Natl Acad Sci U S A* 99: 7367-7372, 2002.

104. **Kuma A, Hatano M, Matsui M, Yamamoto A, Nakaya H, Yoshimori T, Ohsumi Y, Tokuhisa T and Mizushima N.** The role of autophagy during the early neonatal starvation period. *Nature* 432: 1032-1036, 2004.

105. **Kuma A, Hatano M, Matsui M, Yamamoto A, Nakaya H, Yoshimori T, Ohsumi Y, Tokuhisa T and Mizushima N.** The role of autophagy during the early neonatal starvation period. *Nature* 432: 1032-1036, 2004.

106. **Kwak MK, Wakabayashi N, Greenlaw JL, Yamamoto M and Kensler TW.** Antioxidants enhance mammalian proteasome expression through the Keap1-Nrf2 signaling pathway. *Mol Cell Biol* 23: 8786-8794, 2003.

107. **Larsen KE and Sulzer D.** Autophagy in neurons: a review. *Histol Histopathol* 17: 897-908, 2002.

108. **Laurin N, Brown JP, Morissette J and Raymond V.** Recurrent mutation of the gene encoding sequestosome 1 (SQSTM1/p62) in Paget disease of bone. *Am J Hum Genet* 70: 1582-1588, 2002.

109. **Lee DH and Goldberg AL.** Proteasome inhibitors: valuable new tools for cell biologists [In Process Citation]. *Trends Cell Biol* 8: 397-403, 1998.

110. **Li Z, Melandri F, Berdo I, Jansen M, Hunter L, Wright S, Valbrun D and Figueiredo-Pereira ME.** delta12-Prostaglandin J2 inhibits the ubiquitin hydrolase UCH-L1 and elicits ubiquitin-protein aggregation without proteasome inhibition. *Biochem Biophys Res Commun* 319: 1171-1180, 2004.

111. **Li Z, Melandri F, Berdo I, Jansen M, Hunter L, Wright S, Valbrun D and Figueiredo-Pereira ME.** delta12-Prostaglandin J2 inhibits the ubiquitin hydrolase UCH-L1 and elicits ubiquitin-protein aggregation without proteasome inhibition. *Biochem Biophys Res Commun* 319: 1171-1180, 2004.

112. **Li Z, Melandri F, Berdo I, Jansen M, Hunter L, Wright S, Valbrun D and Figueiredo-Pereira ME.** delta12-Prostaglandin J2 inhibits the ubiquitin hydrolase UCH-L1 and elicits ubiquitin-protein aggregation without proteasome inhibition. *Biochem Biophys Res Commun* 319: 1171-1180, 2004.

113. **Li Z, Melandri F, Berdo I, Jansen M, Hunter L, Wright S, Valbrun D and Figueiredo-Pereira ME.** delta12-Prostaglandin J2 inhibits the ubiquitin hydrolase UCH-L1 and elicits ubiquitin-protein aggregation without

proteasome inhibition. *Biochem Biophys Res Commun* 319: 1171-1180, 2004.

114. **Liang X, Wu L, Hand T and Andreasson K.** Prostaglandin D2 mediates neuronal protection via the DP1 receptor. *J Neurochem* 92: 477-486, 2005.

115. **Liang X, Wu L, Hand T and Andreasson K.** Prostaglandin D2 mediates neuronal protection via the DP1 receptor. *J Neurochem* 92: 477-486, 2005.

116. **Liang X, Wu L, Hand T and Andreasson K.** Prostaglandin D2 mediates neuronal protection via the DP1 receptor. *J Neurochem* 92: 477-486, 2005.

117. **Liu CW, Corboy MJ, DeMartino GN and Thomas PJ.** Endoproteolytic activity of the proteasome. *Science* 299: 408-411, 2003.

118. **Lowe J, Blanchard A, Morrell K, Lennox G, Reynolds L, Billett M, Landon M and Mayer RJ.** Ubiquitin is a common factor in intermediate filament inclusion bodies of diverse type in man, including those of Parkinson's disease, Pick's disease, and Alzheimer's disease, as well as Rosenthal fibres in cerebellar astrocytomas, cytoplasmic bodies in muscle, and mallory bodies in alcoholic liver disease. *J Pathol* 155: 9-15, 1988.

119. **Lu H, Zong C, Wang Y, Young GW, Deng N, Souda P, Li X, Whitelegge J, Drews O, Yang PY and Ping P.** Revealing the dynamics of the 20 S proteasome phosphoproteome: a combined CID and electron transfer dissociation approach. *Mol Cell Proteomics* 7: 2073-2089, 2008.

120. **Madura K.** Rad23 and Rpn10: perennial wallflowers join the melee. *Trends Biochem Sci* 29: 637-640, 2004.

121. **Manabe Y, Anrather J, Kawano T, Niwa K, Zhou P, Ross ME and Iadecola C.** Prostanoids, not reactive oxygen

species, mediate COX-2-dependent neurotoxicity. *Ann Neurol* 55: 668-675, 2004.

122. **Mao X, Stewart AK, Hurren R, Datti A, Zhu X, Zhu Y, Shi C, Lee K, Tiedemann R, Eberhard Y, Trudel S, Liang S, Corey SJ, Gillis LC, Barber DL, Wrana JL, Ezzat S and Schimmer AD.** A chemical biology screen identifies glucocorticoids that regulate c-maf expression by increasing its proteasomal degradation through up-regulation of ubiquitin. *Blood* 110: 4047-4054, 2007.

123. **Massey AC, Zhang C and Cuervo AM.** Chaperone-mediated autophagy in aging and disease. *Curr Top Dev Biol* 73: 205-235, 2006.

124. **Matsumoto S, Goto S, Kusaka H, Imai T, Murakami N, Hashizume Y, Okazaki H and Hirano A.** Ubiquitin-positive inclusion in anterior horn cells in subgroups of motor neuron diseases: a comparative study of adult-onset amyotrophic lateral sclerosis, juvenile amyotrophic lateral sclerosis and Werdnig-Hoffmann disease. *J Neurol Sci* 115: 208-213, 1993.

125. **Mayer RJ.** From neurodegeneration to neurohomeostasis: the role of ubiquitin. *Drug News Perspect* 16: 103-108, 2003.

126. **McGeer EG and McGeer PL.** The role of anti-inflammatory agents in Parkinson's disease. *CNS Drugs* 21: 789-797, 2007.

127. **McGrath ME.** The lysosomal cysteine proteases. *Annu Rev Biophys Biomol Struct* 28: 181-204, 1999.

128. **McNaught KS, Belizaire R, Isacson O, Jenner P and Olanow CW.** Altered proteasomal function in sporadic Parkinson's disease. *Exp Neurol* 179: 38-46, 2003.

129. **Meiners S, Heyken D, Weller A, Ludwig A, Stangl K, Kloetzel PM and Kruger E.** Inhibition of proteasome activity induces concerted expression of proteasome

genes and de novo formation of Mammalian proteasomes. *J Biol Chem* 278: 21517-21525, 2003.

130. **Meiners S, Heyken D, Weller A, Ludwig A, Stangl K, Kloetzel PM and Kruger E.** Inhibition of proteasome activity induces concerted expression of proteasome genes and de novo formation of Mammalian proteasomes. *J Biol Chem* 278: 21517-21525, 2003.

131. **Miller JP, Shuman DA, Scholten MB, Dimmitt MK, Stewart CM, Khwaja TA, Robins RK and Simon LN.** Synthesis and biological activity of some 2' derivatives of adenosine 3',5'-cyclic phosphate. *Biochemistry* 12: 1010-1016, 1973.

132. **Minghetti L.** Role of inflammation in neurodegenerative diseases. *Curr Opin Neurol* 18: 315-321, 2005.

133. **Mizushima N and Klionsky DJ.** Protein Turnover Via Autophagy: Implications for Metabolism. *Annu Rev Nutr* 2007.

134. **Mizushima N and Klionsky DJ.** Protein Turnover Via Autophagy: Implications for Metabolism (*). *Annu Rev Nutr* 27: 19-40, 2007.

135. **Mizushima N, Ohsumi Y and Yoshimori T.** Autophagosome formation in mammalian cells. *Cell Struct Funct* 27: 421-429, 2002.

136. **Mizushima N, Ohsumi Y and Yoshimori T.** Autophagosome formation in mammalian cells. *Cell Struct Funct* 27: 421-429, 2002.

137. **Mohri I, Kadoyama K, Kanekiyo T, Sato Y, Kagitani-Shimono K, Saito Y, Suzuki K, Kudo T, Takeda M, Urade Y, Murayama S and Taniike M.** Hematopoietic prostaglandin D synthase and DP1 receptor are selectively upregulated in microglia and astrocytes within senile plaques from human patients and in a

mouse model of Alzheimer disease. *J Neuropathol Exp Neurol* 66: 469-480, 2007.

138. **Mohri I, Kadoyama K, Kanekiyo T, Sato Y, Kagitani-Shimono K, Saito Y, Suzuki K, Kudo T, Takeda M, Urade Y, Murayama S and Taniike M.** Hematopoietic prostaglandin D synthase and DP1 receptor are selectively upregulated in microglia and astrocytes within senile plaques from human patients and in a mouse model of Alzheimer disease. *J Neuropathol Exp Neurol* 66: 469-480, 2007.

139. **Moore DJ, Dawson VL and Dawson TM.** Role for the ubiquitin-proteasome system in Parkinson's disease and other neurodegenerative brain amyloidoses. *Neuromolecular Med* 4: 95-108, 2003.

140. **Moscat J, az-Meco MT and Wooten MW.** Signal integration and diversification through the p62 scaffold protein. *Trends Biochem Sci* 32: 95-100, 2007.

141. **Mosmann T.** Rapid colorimetric assay for cellular growth and survival: application to proliferation and cytotoxicity assays. *J Immunol Methods* 65: 55-63, 1983.

142. **Mullally JE, Moos PJ, Edes K and Fitzpatrick FA.** Cyclopentenone prostaglandins of the J series inhibit the ubiquitin isopeptidase activity of the proteasome pathway. *J Biol Chem* 276: 30366-30373, 2001.

143. **Murad F.** Nitric oxide signaling: would you believe that a simple free radical could be a second messenger, autacoid, paracrine substance, neurotransmitter, and hormone? *Recent Prog Horm Res* 53: 43-59, 1998.

144. **Musiek ES, Milne GL, McLaughlin B and Morrow JD.** Cyclopentenone eicosanoids as mediators of neurodegeneration: a pathogenic mechanism of oxidative stress-mediated and cyclooxygenase-mediated neurotoxicity. *Brain Pathol* 15: 149-158, 2005.

145. **Nakaso K, Yoshimoto Y, Nakano T, Takeshima T, Fukuhara Y, Yasui K, Araga S, Yanagawa T, Ishii T and Nakashima K.** Transcriptional activation of p62/A170/ZIP during the formation of the aggregates: possible mechanisms and the role in Lewy body formation in Parkinson's disease. *Brain Res* 1012: 42-51, 2004.

146. **Narumiya S, Ogorochi T, Nakao K and Hayaishi O.** Prostaglandin D2 in rat brain, spinal cord and pituitary: basal level and regional distribution. *Life Sci* 31: 2093-2103, 1982.

147. **Navon A and Ciechanover A.** The 26 S proteasome: from basic mechanisms to drug targeting. *J Biol Chem* 284: 33713-33718, 2009.

148. **Ogburn KD and Figueiredo-Pereira ME.** Cytoskeleton/endoplasmic reticulum collapse induced by prostaglandin J2 parallels centrosomal deposition of ubiquitinated protein aggregates. *J Biol Chem* 281: 23274-23284, 2006.

149. **Ogburn KD and Figueiredo-Pereira ME.** Cytoskeleton/endoplasmic reticulum collapse induced by prostaglandin J2 parallels centrosomal deposition of ubiquitinated protein aggregates. *J Biol Chem* 281: 23274-23284, 2006.

150. **Ogburn KD and Figueiredo-Pereira ME.** Cytoskeleton/endoplasmic reticulum collapse induced by prostaglandin J2 parallels centrosomal deposition of ubiquitinated protein aggregates. *J Biol Chem* 281: 23274-23284, 2006.

151. **Ogburn KD and Figueiredo-Pereira ME.** Cytoskeleton/endoplasmic reticulum collapse induced by prostaglandin J2 parallels centrosomal deposition of ubiquitinated protein aggregates. *J Biol Chem* 281: 23274-23284, 2006.

152. **Ogorochi T, Narumiya S, Mizuno N, Yamashita K, Miyazaki H and Hayaishi O.** Regional distribution of prostaglandins D2, E2, and F2 alpha and related enzymes in postmortem human brain. *J Neurochem* 43: 71-82, 1984.

153. **Ogorochi T, Narumiya S, Mizuno N, Yamashita K, Miyazaki H and Hayaishi O.** Regional distribution of prostaglandins D2, E2, and F2 alpha and related enzymes in postmortem human brain. *J Neurochem* 43: 71-82, 1984.

154. **Ogorochi T, Narumiya S, Mizuno N, Yamashita K, Miyazaki H and Hayaishi O.** Regional distribution of prostaglandins D2, E2, and F2 alpha and related enzymes in postmortem human brain. *J Neurochem* 43: 71-82, 1984.

155. **Ohsumi Y.** Molecular dissection of autophagy: two ubiquitin-like systems. *Nat Rev Mol Cell Biol* 2: 211-216, 2001.

156. **Ohsumi Y.** Molecular dissection of autophagy: two ubiquitin-like systems. *Nat Rev Mol Cell Biol* 2: 211-216, 2001.

157. **Ohsumi Y.** Molecular dissection of autophagy: two ubiquitin-like systems. *Nat Rev Mol Cell Biol* 2: 211-216, 2001.

158. **Pandey UB, Batlevi Y, Baehrecke EH and Taylor JP.** HDAC6 at the Intersection of Autophagy, the Ubiquitin-Proteasome System and Neurodegeneration. *Autophagy* 3: 2007.

159. **Pandey UB, Batlevi Y, Baehrecke EH and Taylor JP.** HDAC6 at the Intersection of Autophagy, the Ubiquitin-Proteasome System and Neurodegeneration. *Autophagy* 3: 2007.

160. **Pankiv S, Clausen TH, Lamark T, Brech A, Bruun JA, Outzen H, Overvatn A, Bjorkoy G and Johansen T.** p62/SQSTM1 binds directly to Atg8/LC3 to facilitate degradation of ubiquitinated protein aggregates by autophagy. *J Biol Chem* 282: 24131-24145, 2007.

161. **Pankiv S, Clausen TH, Lamark T, Brech A, Bruun JA, Outzen H, Overvatn A, Bjorkoy G and Johansen T.** p62/SQSTM1 binds directly to Atg8/LC3 to facilitate degradation of ubiquitinated protein aggregates by autophagy. *J Biol Chem* 282: 24131-24145, 2007.

162. **Pankiv S, Clausen TH, Lamark T, Brech A, Bruun JA, Outzen H, Overvatn A, Bjorkoy G and Johansen T.** p62/SQSTM1 binds directly to Atg8/LC3 to facilitate degradation of ubiquitinated protein aggregates by autophagy. *J Biol Chem* 282: 24131-24145, 2007.

163. **Pankiv S, Clausen TH, Lamark T, Brech A, Bruun JA, Outzen H, Overvatn A, Bjorkoy G and Johansen T.** p62/SQSTM1 binds directly to Atg8/LC3 to facilitate degradation of ubiquitinated protein aggregates by autophagy. *J Biol Chem* 282: 24131-24145, 2007.

164. **Pankiv S, Hoyvarde CT, Lamark T, Brech A, Bruun JA, Outzen H, Overvatn A, Bjorkoy G and Johansen T.** p62/SQSTM1 binds directly to Atg8/LC3 to facilitate degradation of Ubiquitinated protein aggregates by autophagy. *J Biol Chem* 2007.

165. **Park I, Chung J, Walsh CT, Yun Y, Strominger JL and Shin J.** Phosphotyrosine-independent binding of a 62-kDa protein to the src homology 2 (SH2) domain of p56lck and its regulation by phosphorylation of Ser-59 in the lck unique N-terminal region. *Proc Natl Acad Sci U S A* 92: 12338-12342, 1995.

166. **Park I, Chung J, Walsh CT, Yun Y, Strominger JL and Shin J.** Phosphotyrosine-independent binding of a 62-kDa protein to the src homology 2 (SH2) domain of p56lck and its regulation by phosphorylation of Ser-59 in the lck unique N-terminal region. *Proc Natl Acad Sci U S A* 92: 12338-12342, 1995.

167. **Pereira ME and Wilk S.** Phosphorylation of the multicatalytic proteinase complex from bovine pituitaries by a copurifying cAMP-dependent protein kinase. *Arch Biochem Biophys* 283: 68-74, 1990.

168. **Pettipher R, Hansel TT and Armer R.** Antagonism of the prostaglandin D2 receptors DP1 and CRTH2 as an approach to treat allergic diseases. *Nat Rev Drug Discov* 6: 313-325, 2007.

169. **Pompl PN, Ho L, Bianchi M, McManus T, Qin W and Pasinetti GM.** A therapeutic role for cyclooxygenase-2 inhibitors in a transgenic mouse model of amyotrophic lateral sclerosis. *FASEB J* 17: 725-727, 2003.

170. **Prudencio M, Hart PJ, Borchelt DR and Andersen PM.** Variation in aggregation propensities among ALS-associated variants of SOD1: correlation to human disease. *Hum Mol Genet* 18: 3217-3226, 2009.

171. **Prudencio M, Hart PJ, Borchelt DR and Andersen PM.** Variation in aggregation propensities among ALS-associated variants of SOD1: correlation to human disease. *Hum Mol Genet* 18: 3217-3226, 2009.

172. **Qiao L and Zhang J.** Inhibition of lysosomal functions reduces proteasomal activity. *Neurosci Lett* 456: 15-19, 2009.

173. **Qu WM, Huang ZL, Xu XH, Aritake K, Eguchi N, Nambu F, Narumiya S, Urade Y and Hayaishi O.** Lipocalin-type prostaglandin D synthase produces prostaglandin D2 involved in regulation of physiological sleep. *Proc Natl Acad Sci U S A* 103: 17949-17954, 2006.

174. **Raasi S, Orlov I, Fleming KG and Pickart CM.** Binding of polyubiquitin chains to ubiquitin-associated (UBA) domains of HHR23A. *J Mol Biol* 341: 1367-1379, 2004.

175. **Ramesh BJ, Lamar SM, Peng J, Strom AL, Kemppainen R, Cox N, Zhu H, Wooten MC, az-Meco MT, Moscat J and**

Wooten MW. Genetic inactivation of p62 leads to accumulation of hyperphosphorylated tau and neurodegeneration. *J Neurochem* 106: 107-120, 2008.

176. **Rape M and Jentsch S**. Productive RUPture: activation of transcription factors by proteasomal processing. *Biochim Biophys Acta* 1695: 209-213, 2004.

177. **Reggiori F and Klionsky DJ**. Autophagosomes: biogenesis from scratch? *Curr Opin Cell Biol* 17: 415-422, 2005.

178. **Reggiori F and Klionsky DJ**. Autophagosomes: biogenesis from scratch? *Curr Opin Cell Biol* 17: 415-422, 2005.

179. **Rissman RA, Poon WW, Blurton-Jones M, Oddo S, Torp R, Vitek MP, LaFerla FM, Rohn TT and Cotman CW**. Caspase-cleavage of tau is an early event in Alzheimer disease tangle pathology. *J Clin Invest* 114: 121-130, 2004.

180. **Rubinsztein DC**. The roles of intracellular protein-degradation pathways in neurodegeneration. *Nature* 443: 780-786, 2006.

181. **Ryu KY, Garza JC, Lu XY, Barsh GS and Kopito RR**. Hypothalamic neurodegeneration and adult-onset obesity in mice lacking the Ubb polyubiquitin gene. *Proc Natl Acad Sci U S A* 105: 4016-4021, 2008.

182. **Ryu KY, Maehr R, Gilchrist CA, Long MA, Bouley DM, Mueller B, Ploegh HL and Kopito RR**. The mouse polyubiquitin gene UbC is essential for fetal liver development, cell-cycle progression and stress tolerance. *EMBO J* 26: 2693-2706, 2007.

183. **Sasaki T, Kikuchi T, Yumoto N, Yoshimura N and Murachi T**. Comparative specificity and kinetic studies on porcine calpain I and calpain II with naturally occurring peptides and synthetic fluorogenic substrates. *J Biol Chem* 259: 12489-12494, 1984.

184. **Satoh T and Lipton SA.** Redox regulation of neuronal survival mediated by electrophilic compounds. *Trends Neurosci* 30: 37-45, 2007.

185. **Satoh T and Lipton SA.** Redox regulation of neuronal survival mediated by electrophilic compounds. *Trends Neurosci* 30: 37-45, 2007.

186. **Scher JU and Pillinger MH.** 15d-PGJ2: the anti-inflammatory prostaglandin? *Clin Immunol* 114: 100-109, 2005.

187. **Schmidtke G, Kraft R, Kostka S, Henklein P, Frommel C, Lowe J, Huber R, Kloetzel PM and Schmidt M.** Analysis of mammalian 20S proteasome biogenesis: the maturation of beta- subunits is an ordered two-step mechanism involving autocatalysis. *EMBO J* 15: 6887-6898, 1996.

188. **Schotte P, Declercq W, Van HS, Vandenabeele P and Beyaert R.** Non-specific effects of methyl ketone peptide inhibitors of caspases. *FEBS Lett* 442: 117-121, 1999.

189. **Seibenhener ML, Babu JR, Geetha T, Wong HC, Krishna NR and Wooten MW.** Sequestosome 1/p62 is a polyubiquitin chain binding protein involved in ubiquitin proteasome degradation. *Mol Cell Biol* 24: 8055-8068, 2004.

190. **Seibenhener ML, Babu JR, Geetha T, Wong HC, Krishna NR and Wooten MW.** Sequestosome 1/p62 is a polyubiquitin chain binding protein involved in ubiquitin proteasome degradation. *Mol Cell Biol* 24: 8055-8068, 2004.

191. **Seibenhener ML, Geetha T and Wooten MW.** Sequestosome 1/p62--more than just a scaffold. *FEBS Lett* 581: 175-179, 2007.

192. **Seibenhener ML, Geetha T and Wooten MW.** Sequestosome 1/p62--more than just a scaffold. *FEBS Lett* 581: 175-179, 2007.

193. **Seibenhener ML, Geetha T and Wooten MW.** Sequestosome 1/p62--more than just a scaffold. *FEBS Lett* 581: 175-179, 2007.

194. **Seo H, Sonntag KC and Isacson O.** Generalized brain and skin proteasome inhibition in Huntington's disease. *Ann Neurol* 56: 319-328, 2004.

195. **Seo SR and Chung KC.** CREB activates proteasomal degradation of DSCR1/RCAN1. *FEBS Lett* 582: 1889-1893, 2008.

196. **Sharon M, Witt S, Felderer K, Rockel B, Baumeister W and Robinson CV.** 20S proteasomes have the potential to keep substrates in store for continual degradation. *J Biol Chem* 281: 9569-9575, 2006.

197. **Shibata T, Kondo M, Osawa T, Shibata N, Kobayashi M and Uchida K.** 15-deoxy-delta 12,14-prostaglandin J2. A prostaglandin D2 metabolite generated during inflammatory processes. *J Biol Chem* 277: 10459-10466, 2002.

198. **Shibata T, Kondo M, Osawa T, Shibata N, Kobayashi M and Uchida K.** 15-deoxy-delta 12,14-prostaglandin J2. A prostaglandin D2 metabolite generated during inflammatory processes. *J Biol Chem* 277: 10459-10466, 2002.

199. **Shin J.** P62 and the sequestosome, a novel mechanism for protein metabolism. *Arch Pharm Res* 21: 629-633, 1998.

200. **Silveira MS and Linden R.** Neuroprotection by cAMP: Another brick in the wall. *Adv Exp Med Biol* 557: 164-176, 2006.

201. **Soderberg O, Gullberg M, Jarvius M, Ridderstrale K, Leuchowius KJ, Jarvius J, Wester K, Hydbring P, Bahram F, Larsson LG and Landegren U.** Direct observation of individual endogenous protein complexes in situ by proximity ligation. *Nat Methods* 3: 995-1000, 2006.

202. **Soderberg O, Gullberg M, Jarvius M, Ridderstrale K, Leuchowius KJ, Jarvius J, Wester K, Hydbring P, Bahram F, Larsson LG and Landegren U.** Direct observation of individual endogenous protein complexes in situ by proximity ligation. *Nat Methods* 3: 995-1000, 2006.

203. **Stanhill A, Haynes CM, Zhang Y, Min G, Steele MC, Kalinina J, Martinez E, Pickart CM, Kong XP and Ron D.** An arsenite-inducible 19S regulatory particle-associated protein adapts proteasomes to proteotoxicity. *Mol Cell* 23: 875-885, 2006.

204. **Stanhill A, Haynes CM, Zhang Y, Min G, Steele MC, Kalinina J, Martinez E, Pickart CM, Kong XP and Ron D.** An arsenite-inducible 19S regulatory particle-associated protein adapts proteasomes to proteotoxicity. *Mol Cell* 23: 875-885, 2006.

205. **Stein RL, Melandri F and Dick L.** Kinetic characterization of the chymotryptic activity of the 20S proteasome. *Biochemistry* 35: 3899-3908, 1996.

206. **Straus DS and Glass CK.** Cyclopentenone prostaglandins: new insights on biological activities and cellular targets. *Med Res Rev* 21: 185-210, 2001.

207. **Straus DS and Glass CK.** Cyclopentenone prostaglandins: new insights on biological activities and cellular targets. *Med Res Rev* 21: 185-210, 2001.

208. **Tabuchi K, Oikawa K, Hoshino T, Nishimura B, Hayashi K, Yanagawa T, Warabi E, Ishii T, Tanaka S and Hara A.** Cochlear protection from acoustic injury by inhibitors of p38 mitogen-activated protein kinase and sequestosome 1 stress protein. *Neuroscience* 166: 665-670, 2010.

209. **Tan JM, Wong ES, Kirkpatrick DS, Pletnikova O, Ko HS, Tay SP, Ho MW, Troncoso J, Gygi SP, Lee MK, Dawson VL, Dawson TM and Lim KL.** Lysine 63-linked ubiquitination promotes the formation and autophagic clearance of protein inclusions associated with neurodegenerative diseases. *Hum Mol Genet* 17: 431-439, 2008.

210. **Taylor CT, Furuta GT, Synnestvedt K and Colgan SP.** Phosphorylation-dependent targeting of cAMP response element binding protein to the ubiquitin/proteasome pathway in hypoxia. *Proc Natl Acad Sci U S A* 97: 12091-12096, 2000.

211. **Thrower JS, Hoffman L, Rechsteiner M and Pickart CM.** Recognition of the polyubiquitin proteolytic signal. *EMBO J* 19: 94-102, 2000.

212. **Thrower JS, Hoffman L, Rechsteiner M and Pickart CM.** Recognition of the polyubiquitin proteolytic signal. *EMBO J* 19: 94-102, 2000.

213. **Thrower JS, Hoffman L, Rechsteiner M and Pickart CM.** Recognition of the polyubiquitin proteolytic signal. *EMBO J* 19: 94-102, 2000.

214. **Thrower JS, Hoffman L, Rechsteiner M and Pickart CM.** Recognition of the polyubiquitin proteolytic signal. *EMBO J* 19: 94-102, 2000.

215. **Tsukamoto O, Minamino T and Kitakaze M.** Functional alterations of cardiac proteasomes under physiological and pathological conditions. *Cardiovasc Res* 85: 339-346, 2010.

216. **Uchida K and Shibata T.** 15-Deoxy-Delta(12,14)-prostaglandin J2: an electrophilic trigger of cellular responses. *Chem Res Toxicol* 21: 138-144, 2008.

217. **Uchida K and Shibata T.** 15-Deoxy-Delta(12,14)-prostaglandin J2: an electrophilic trigger of cellular responses. *Chem Res Toxicol* 21: 138-144, 2008.

218. **Urade Y and Eguchi N.** Lipocalin-type and hematopoietic prostaglandin D synthases as a novel example of functional convergence. *Prostaglandins Other Lipid Mediat* 68-69: 375-382, 2002.

219. **Urade Y and Eguchi N.** Lipocalin-type and hematopoietic prostaglandin D synthases as a novel example of functional convergence. *Prostaglandins Other Lipid Mediat* 68-69: 375-382, 2002.

220. **Urade Y and Hayaishi O.** Prostaglandin D synthase: structure and function. *Vitam Horm* 58: 89-120, 2000.

221. **Vernace VA, Schmidt-Glenewinkel T and Figueiredo-Pereira ME.** Aging and regulated protein degradation: who has the UPPer hand? *Aging Cell* 6: 599-606, 2007.

222. **Wang CW and Klionsky DJ.** The molecular mechanism of autophagy. *Mol Med* 9: 65-76, 2003.

223. **Wang Q, Johnson JL, Agar NY and Agar JN.** Protein aggregation and protein instability govern familial amyotrophic lateral sclerosis patient survival. *PLoS Biol* 6: e170, 2008.

224. **Wang Q, Johnson JL, Agar NY and Agar JN.** Protein aggregation and protein instability govern familial amyotrophic lateral sclerosis patient survival. *PLoS Biol* 6: e170, 2008.

225. **Wang X, Xu H, Ha SW, Ju D and Xie Y.** Proteasomal degradation of Rpn4 in Saccharomyces cerevisiae is critical for cell viability under stressed conditions. *Genetics* 184: 335-342, 2010.

226. **Wang Z, Aris VM, Ogburn KD, Soteropoulos P and Figueiredo-Pereira ME.** Prostaglandin J2 alters pro-survival and pro-death gene expression patterns and 26 S proteasome assembly in human neuroblastoma cells. *J Biol Chem* 281: 21377-21386, 2006.

227. **Wang Z, Aris VM, Ogburn KD, Soteropoulos P and Figueiredo-Pereira ME.** Prostaglandin J2 alters pro-survival and pro-death gene expression patterns and 26 S proteasome assembly in human neuroblastoma cells. *J Biol Chem* 281: 21377-21386, 2006.

228. **Wang Z and Figueiredo-Pereira ME.** Inhibition of sequestosome 1/p62 up-regulation prevents aggregation of ubiquitinated proteins induced by prostaglandin J2 without reducing its neurotoxicity. *Mol Cell Neurosci* 29: 222-231, 2005.

229. **Wanker EE, Scherzinger E, Heiser V, Sittler A, Eickhoff H and Lehrach H.** Membrane filter assay for detection of amyloid-like polyglutamine-containing protein aggregates. *Methods Enzymol* 309: 375-386, 1999.

230. **Weibrecht I, Leuchowius KJ, Clausson CM, Conze T, Jarvius M, Howell WM, Kamali-Moghaddam M and Soderberg O.** Proximity ligation assays: a recent addition to the proteomics toolbox. *Expert Rev Proteomics* 7: 401-409, 2010.

231. **Wilk S and Orlowski M.** Evidence that pituitary cation-sensitive neutral endopeptidase is a multicatalytic protease complex. *J Neurochem* 40: 842-849, 1983.

232. **Wilk S and Orlowski M.** Evidence that pituitary cation-sensitive neutral endopeptidase is a multicatalytic protease complex. *J Neurochem* 40: 842-849, 1983.

233. **Wilkinson CR, Seeger M, Hartmann-Petersen R, Stone M, Wallace M, Semple C and Gordon C.** Proteins containing the UBA domain are able to bind to multi-ubiquitin chains. *Nat Cell Biol* 3: 939-943, 2001.

234. **Wilkinson KD.** Ubiquitin-dependent signaling: the role of ubiquitination in the response of cells to their environment. *J Nutr* 129: 1933-1936, 1999.

235. **Wojcik C and DeMartino GN.** Intracellular localization of proteasomes. *Int J Biochem Cell Biol* 35: 579-589, 2003.

236. **Wooten MW, Hu X, Babu JR, Seibenhener ML, Geetha T, Paine MG and Wooten MC.** Signaling, Polyubiquitination, Trafficking, and Inclusions: Sequestosome 1/p62's Role in Neurodegenerative Disease. *J Biomed Biotechnol* 2006: 62079, 2006.

237. **Wooten MW, Hu X, Babu JR, Seibenhener ML, Geetha T, Paine MG and Wooten MC.** Signaling, Polyubiquitination, Trafficking, and Inclusions: Sequestosome 1/p62's Role in Neurodegenerative Disease. *J Biomed Biotechnol* 2006: 62079, 2006.

238. **Yoshiyama Y, Higuchi M, Zhang B, Huang SM, Iwata N, Saido TC, Maeda J, Suhara T, Trojanowski JQ and Lee VM.** Synapse loss and microglial activation precede tangles in a P301S tauopathy mouse model. *Neuron* 53: 337-351, 2007.

239. **Yoshiyama Y, Higuchi M, Zhang B, Huang SM, Iwata N, Saido TC, Maeda J, Suhara T, Trojanowski JQ and Lee VM.** Synapse loss and microglial activation precede tangles in a P301S tauopathy mouse model. *Neuron* 53: 337-351, 2007.

240. **Young P, Deveraux Q, Beal RE, Pickart CM and Rechsteiner M.** Characterization of two polyubiquitin binding sites in the 26 S protease subunit 5a. *J Biol Chem* 273: 5461-5467, 1998.

241. **Young P, Deveraux Q, Beal RE, Pickart CM and Rechsteiner M.** Characterization of two polyubiquitin binding sites in the 26 S protease subunit 5a. *J Biol Chem* 273: 5461-5467, 1998.

242. **Zhang F, Hu Y, Huang P, Toleman CA, Paterson AJ and Kudlow JE.** Proteasome function is regulated by cyclic AMP-dependent protein kinase through phosphorylation of Rpt6. *J Biol Chem* 282: 22460-22471, 2007.

243. **Zhang F, Hu Y, Huang P, Toleman CA, Paterson AJ and Kudlow JE.** Proteasome function is regulated by cyclic AMP-dependent protein kinase through phosphorylation of Rpt6. *J Biol Chem* 282: 22460-22471, 2007.

244. **Zhang F, Hu Y, Huang P, Toleman CA, Paterson AJ and Kudlow JE.** Proteasome function is regulated by cyclic AMP-dependent protein kinase through phosphorylation of Rpt6. *J Biol Chem* 282: 22460-22471, 2007.

245. **Zhang F, Hu Y, Huang P, Toleman CA, Paterson AJ and Kudlow JE.** Proteasome function is regulated by cyclic AMP-dependent protein kinase through phosphorylation of Rpt6. *J Biol Chem* 282: 22460-22471, 2007.

246. **Zhang HX, Tanji K, Yoshida H, Hayakari M, Shibata T, Mori F, Uchida K and Wakabayashi K.** Alteration of biochemical and pathological properties of TDP-43 protein by a lipid mediator, 15-deoxy-Delta(12,14)-prostaglandin J(2). *Exp Neurol* 222: 296-303, 2010.

247. **Zong C, Gomes AV, Drews O, Li X, Young GW, Berhane B, Qiao X, French SW, Bardag-Gorce F and Ping P.** Regulation of murine cardiac 20S proteasomes: role of associating partners. *Circ Res* 99: 372-380, 2006.

248. **Zong C, Gomes AV, Drews O, Li X, Young GW, Berhane B, Qiao X, French SW, Bardag-Gorce F and Ping P.** Regulation of murine cardiac 20S proteasomes: role of associating partners. *Circ Res* 99: 372-380, 2006.